

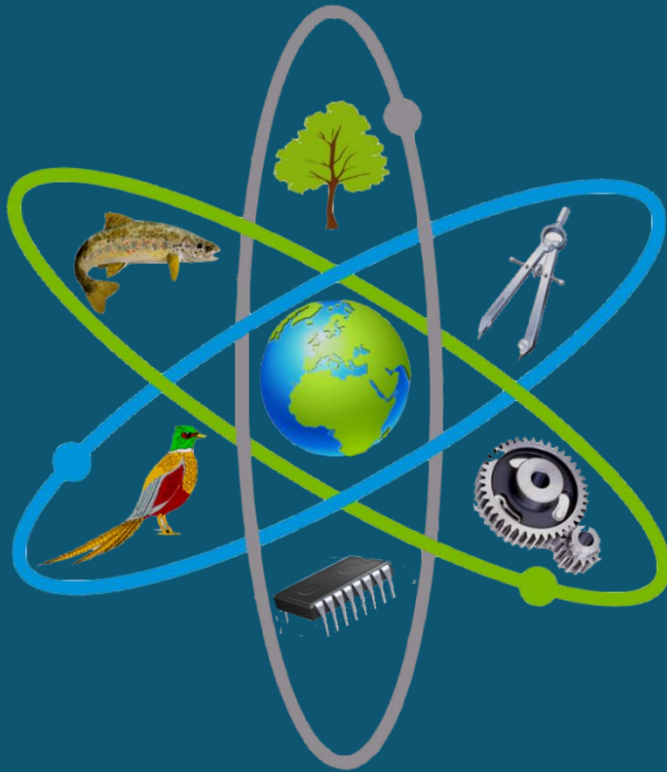
Volume: 8 Issue: 3 December - 2023

ISSN 2458-8989

NEsciences

Natural and Engineering Sciences

an International Journal



www.nesciences.com

Editor-in-Chief

Dr. Cemal Turan
Iskenderun Technical University
cemal.turan@iste.edu.tr

Managing Editor

Dr. Yakup Kutlu
Iskenderun Technical University
yakup.kutlu@iste.edu.tr

Editor of Natural Sciences

Dr. Servet Ahmet Dođdu
Iskenderun Technical University
servet.dogdu@iste.edu.tr
Turkey

Editor of Engineering Sciences

Dr. Tolga Depçi
Iskenderun Technical University
tolga.depci@iste.edu.tr
Turkey

Editorial Board

Dr. Adriana Vella
University of Malta
adriana.vella@um.edu.mt
Malta

Dr. Alen Soldo
University of Split
soldo@unist.hr
Croatia

Dr. Antonia Khanaychenko
Institute of Marine Biological Research,
Sevastopol
a.khanaychenko@gmail.com
Russia

Dr. Athanasios Exadactylos
University of Thessaly
exadact@uth.gr
Greece

Dr. Azza El-Ganainy
Egypt National Institute of
Oceanography and Fisheries
azzaelgan@yahoo.com
Egypt

Dr. Bujar Krasniqi
University of Prishtina
bujar.krasniqi@uni-pr.edu
Kosovo

Dr. Christian Capape
Universite de Montpellier
capape@univ-montp2.fr
France

Dr. Deniz Yađlıođlu
Duzce University
denizyagliglu@duze.edu.tr
Turkey

Dr. Joana Robalo
SPA-IU, MARE-Instituto Universitários
m-nayfeh@illinois.edu

Dr. Lovrenc Lipej
National Institute of Biology
lovrenc.lipej@nib.si
Slovenia

Dr. Munir H. Nayfeh
University of Illinois
m-nayfeh@illinois.edu
USA

Dr. Petya Ivanova
Institute of Oceanology
Bulgarian Academy of Science
pavl_petya@yahoo.com
Bulgaria

Dr. Sabina De Innocentiis
Istituti Prevenzione Ambiente ISPRA
sabina.deinnocentiis@isprambiente.it
Italy

Dr. Violin Raykov
Institute of Oceanology
Bulgarian Academy of Science
vio_raykov@abv.bg
Bulgaria

Dr. Quratulan Ahmed
University of Karachi
quratulanahmed_ku@yahoo.com
Pakistan

Publication Ethics Consultant

Nature and Science Society

Natural and Engineering Sciences

Volume 8, No: 3, December 2023




ISSN: 2458-8989

Contents

No	Article Title and Author(s)	Page Number
1	First Morphological and Genetic Record and Confirmation of Korean Rockfish <i>Sebastes schlegelii</i> Hilgendorf, 1880 in the Black Sea Coast of Türkiye Deniz Yağlıoğlu*, Servet Ahmet Dođdu, Cemal Turan	140-150
2	The Relationships of Otolith Dimensions (Length-Breadth) with Weight and Total Length of Greater Forkbeard (<i>Phycis blennoides</i> (Brünnich, 1768)) Captured from northeastern Mediterranean Sea Hülya Girgin, Nuri Başusta*	151-158
3	Occurrence of <i>Homola barbata</i> (Fabricius, 1793) (Decapoda, Brachyura) in Finike Bay (Türkiye, Eastern Mediterranean Sea) Cengiz Koçak* , Coşkun Menderes Aydın, Aydın Ünlüođlu	159-167
4	Two New Records of Eunicidae (Annelida, Errantia) Along the Makran Coast of Pakistan, Northern Arabian Sea Qadeer Mohammad Ali, Quratulan Ahmed*, Shumaila Mubarak, Ateeqa Baloch, Levent Bat, Hafsa Qazi, Iqra Shaikh	168-182
5	The Confirmed Stranding of an Adult Female Risso's Dolphin, <i>Grampus griseus</i> (G. Cuvier, 1812), in the northeastern Mediterranean Sea Deniz Ayas*, Nuray Çiftçi, Yekta Taniş	183-194
6	DNA Damage in Fish Due to Pesticide Pollution Ayşegül Ergenler*, Funda Turan	195-201
7	Glucose-Sensitive Biosensor Design by Zinc Ferrite (ZnFe₂O₄) Nanoparticle-Modified Poly (o-toluidine) Film Ali Tuncay Ozyilmaz*, Esiye Irem Bayram	202-213
8	Leaf Image Classification Based on Pre-trained Convolutional Neural Network Models Yunus Camgözlü*, Yakup Kutlu	214-232



First Morphological and Genetic Record and Confirmation of Korean Rockfish *Sebastes schlegelii* Hilgendorf, 1880 in the Black Sea Coast of Türkiye

Deniz Yağlıoğlu ^{1*} , Servet Ahmet Dođdu ^{2,3} , Cemal Turan ² 

¹ Department of Biology, Faculty of Arts and Sciences, Duzce University, 81620 Duzce, Türkiye.

² Molecular Ecology and Fisheries Genetics Laboratory, Marine Science Department, Faculty of Marine Science and Technology, Iskenderun Technical University, 31220 Iskenderun, Hatay, Türkiye.

³ Iskenderun Technical University, Maritime Vocational School of Higher Education, Underwater Technologies, 31220 Iskenderun, Hatay, Türkiye.

Abstract

One specimen of Korean rockfish *Sebastes schlegelii* Hilgendorf, 1880 was caught by using a fish net at a depth of 7 m on 14 May 2022 from Akçakoca, Düzce in the Black Sea. In this study, the Korean rockfish *Sebastes schlegelii* from the Black Sea coast of Türkiye is reported for the first time with both morphologic and genetic evidence. *S. schlegelii* is characterised by 5 spines on the preoperculum and 2 spines on the operculum. Genetic analyses using mtDNA COI gene region also confirmed the species as *Sebastes schlegelii*. This species is thought to have been transported to the Black Sea from other seas of the world, probably via ballast waters or aquarium escape. The most important reason for this is that the species has not been detected in the Mediterranean.

Keywords:

Sebastes schlegelii, rockfish, first record, Black Sea, genetic evidence

Article history:

Received 28 January 2023, Accepted 10 August 2023, Available online 20 September 2023

Introduction

The introduction of new species to the Black Sea can significantly disrupt ecosystem stability and functioning, posing a major threat to biodiversity. Mediterranean species have been increasingly

*Corresponding Author: Deniz YAĞLIOĞLU, E-mail: denizyaglioglu@duzce.edu.tr

recorded in the Black Sea since the 1920s, leading to the expansion of Black Sea ichthyofauna diversity, a phenomenon known as "Mediterranization" (Pusanov, 1967; Turan et al., 2009; Yağlıoğlu & Turan, 2021).

The Korean rockfish *Sebastes schlegelii* belongs to the Sebastinae subfamily and represents the Scorpaenidae family. The Sebastinae subfamily comprises about 124 valid species in 4 valid genera (Fricke et al., 2023). They are generally known as rockfishes. Its natural distribution area is the Pacific (North) Ocean (Hyde & Vetter, 2007; Kai & Soes, 2009; Kai et al., 2013;). Only six species are found in the Atlantic Ocean: *S. capensis* and *S. oculatus* on the southern Atlantic coast, and *S. fasciatus*, *S. mentella*, *S. norvegicus* and *S. viviparus* on the north coast of the Atlantic Ocean. Recently, *Sebastes schlegelii* has been reported on the Crimean coast of the Black Sea (Karpova et al., 2021). On the other hand, this genus has not been recorded in the Mediterranean, but in the Black Sea.

In this study, we first reported the Korean rockfish *Sebastes schlegelii* from the Black Sea coast of Türkiye is given for the first time with both morphologic and genetic evidence.

Materials and Methods

One specimen of the Korean rockfish *Sebastes schlegelii* from Akçakoca, Düzce, Türkiye, South Black Sea coast 41.086195, 31.090505, (41° 5' 10.302" N - 31° 5' 25.818" E) (Figure 1) on 14 May 2022 at a depth of about 7 m was captured by fisherman (Hüseyin Demircioğlu) using fish net. Captured species were immediately frozen and transported to the laboratory for detailed measurements in the laboratory. Each body length (± 0.1 mm) and total body weight (W) (± 0.01 g) were measured. The sample of *S. schlegelii* (Figure 2) was carefully examined and identified using previous records from the Black Sea by Karpova et al., (2021) and from Dutch coastal waters by Kai & Soes (2009). After that, the specimen was preserved in 98% Ethanol solution and deposited at the Duzce University, Faculty of Arts and Sciences, Department of Biology (catalogue number: DUFC/2022-001).

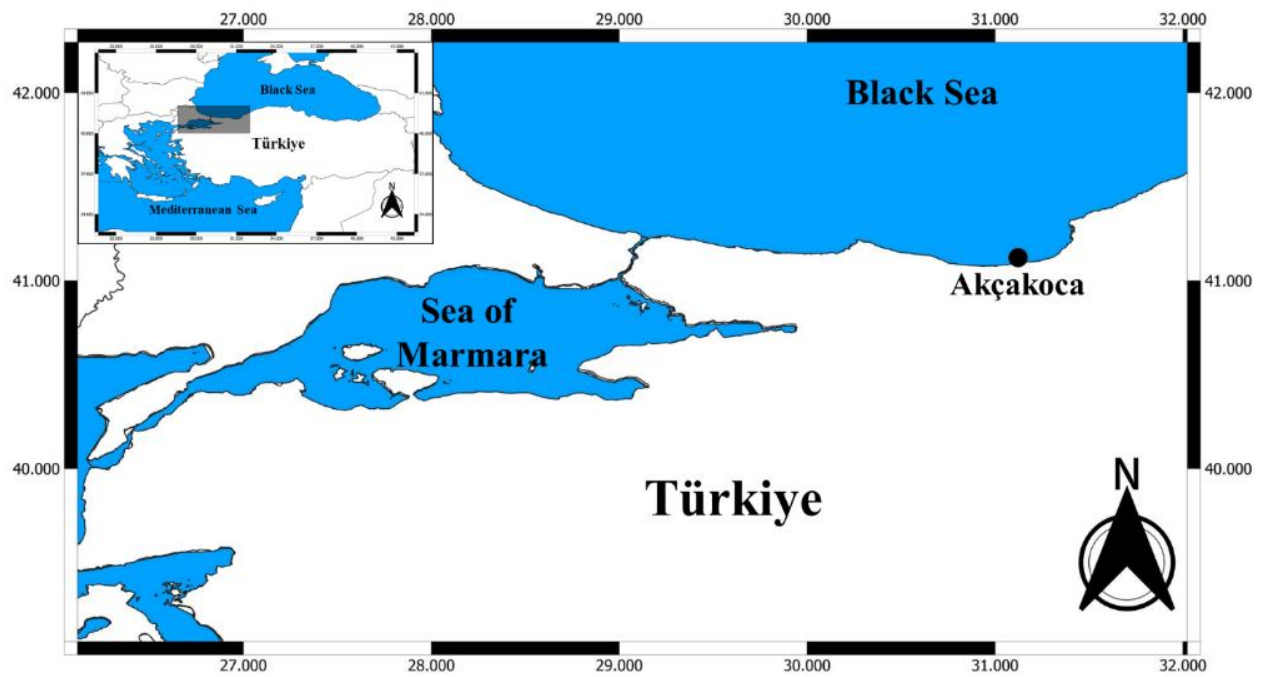


Figure 1. Sampling location of *S. schlegelii* from the Black Sea Coast of Türkiye.



Figure 2. *S. schlegelii* was captured in the southwestern Black Sea, Turkey.

Molecular Analysis

The specimen was delivered to the laboratory and stored in a deep freeze at -30 °C until DNA extraction. Total genomic DNA was extracted from the muscle sample using the DNeasy Blood and Tissue Kit (Qiagen, USA). The manufacturer's protocols were used during all steps. The mtDNA COI gene region was amplified through PCR with selective primers especially designed for groupers (Doğdu & Turan 2016). Fish_F: 5'-TCA ACC AAC CAC AAA GAC ATT GGC AC-3' -Fish_R: 5'-ACT TCA GGG TGA CCG AAG AAT CAG AA-3'.

The PCRs were conducted in a 50 µl total volume with 0.4 µM of each primer, 0.2 mM of dNTP and 1.25U of Taq DNA polymerase in a PCR buffer that included 20 mM of Tris-HCl (pH 8.0), 1.5 mM of MgCl₂, 15 mM of KCl and 1-2 µl template DNA. The denaturation step was at 94 °C for 30 s, 50 °C for 30 s, and 72 °C for 45 s for 30 cycles followed by a final extension for 7 min at 72 °C. The PCR products were visualized using electrophoresis on 1.5 % agarose gel. DNA sequencing was attempted to determine the order of the nucleotides of the mtDNA COI gene region. The chain termination method by Sanger et al. (1977) was applied with Bigdye Cycle Sequencing Kit V3.1 and ABI 3130 XL genetic analyzer. The initial alignments of partial COI sequences were performed with the BioEdit (Hall et al., 2011). The intraspecific and interspecific genetic analyses were performed with maximum likelihood (ML), and Neighbor-Joining analyses. The best-fit substitution model (TN93) was provided by the MEGAX software (Kumar et al., 2018). After sequence alignment, MEGA X was used to determine the genetic diversity and sequence divergences and to construct the phylogenetic tree (Kumar et al., 2018). Sequences of other Sebastinae species were obtained from Genbank.

Results

Diagnosis and Description

Taxonomic identification of the captured specimen (Figure 3) was classified as *Sebastes schlegelii* which can be distinguished from other Sebastinae species by the following characteristics: dorsal-fin rays XIII, 13; anal-fin rays III, 7; pectoral-fin rays 18; lateral-line scales 47; caudal fin rays 16 and convex; anal fin rounded. While it may be difficult to make a precise and definitive description regarding color and body patterns, it can be said that they are seen with a light coloration on the ventral region. Sebastinae species can exhibit variations in colour and patterns due to different age groups, gender differences, and their living environment. Therefore, it is not possible to state that this species is entirely of a specific colour or pattern. The presence of five distinct, sharp, bony, tooth-like structures on the preoperculum and two on the operculum. Moreover, the first spine of the opercular margin long arch being hook-shaped enables a definite distinction of the species.

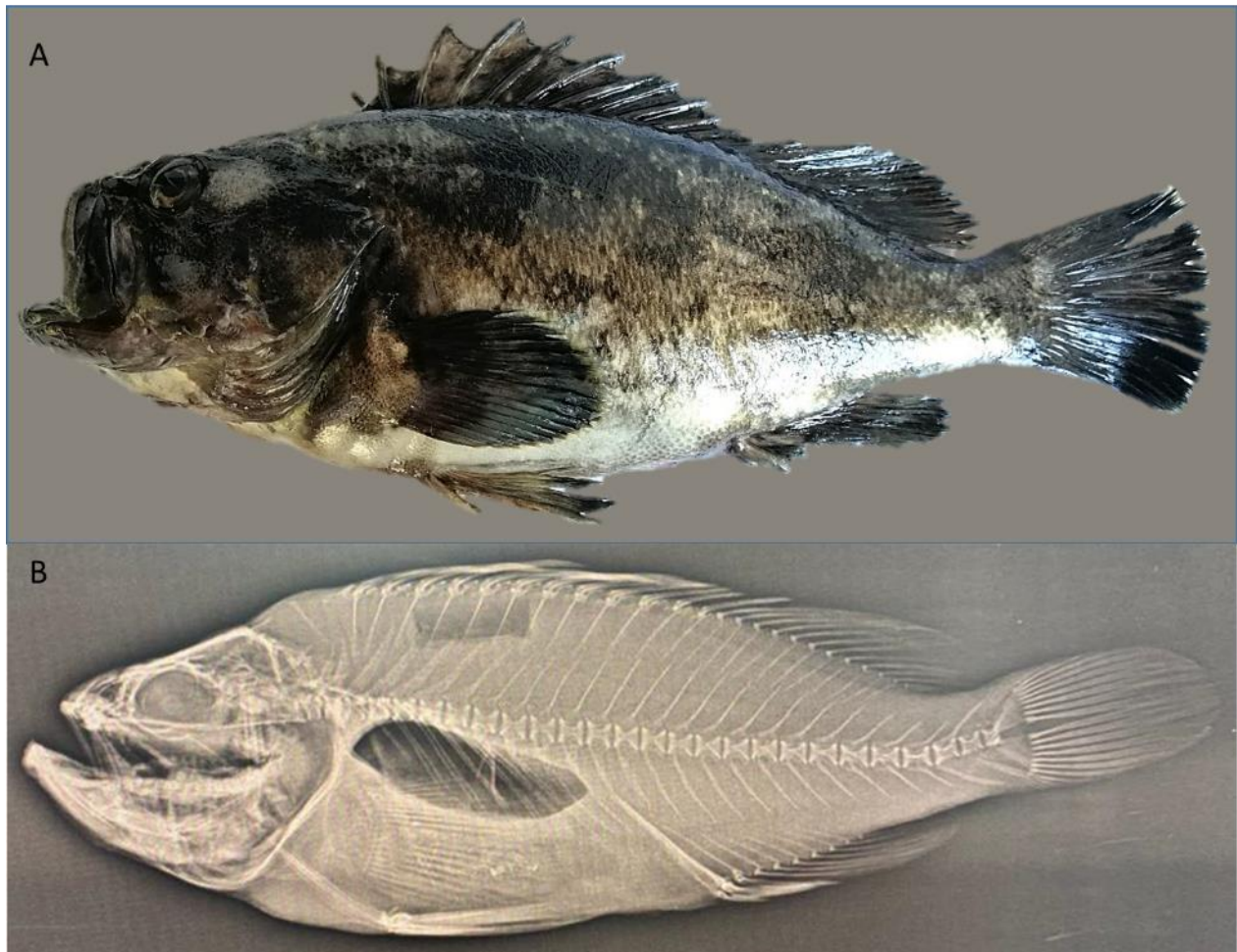


Figure 1. A) General view of *S. schlegelii* B) Radiograph of *S. schlegelii* DUFC/2022-001, 34.96 mm TL.

S. schlegelii is a fish with a wide mouth, protruding lower jaw, and a robust body relative to its size, featuring a large head covered in tough, tight scales. Its color can vary from light tones to black, with noticeable differences. It stands out with its lighter color on the ventral area. The tail fin, or caudal fin, is characterized by its upward structure and is not forked. Generally, its fins have a rounded shape. The dorsal fin consists of 13 spines and 13 soft rays. All the morphometric measurements and meristic characters of *S. schlegelii* are given in Table 1 with previously recorded.

Table 1. Morphometric measurements and meristic characters of the *S. schlegelii* captured in the Black Sea.

Morphometric Measurements	This Study	Karpova et al. (2021)	Kai & Soes (2009)
Total Length	34.96	35.07	20
Standard Length	29.93	29.75	-
Head Length	9.12	-	-
Snout Length	2.79	-	-
Body Depth	10.19	-	-
Body Width	5.95	-	-
Orbit Diameter	1.72	-	-
Interorbital Width	2.82	-	-
Length of Pelvic-Fin	10.19	-	-
Lengths of The Dorsal	4.72	-	-
Lengths of The Anal	5.32	-	-
Lengths of The Pectoral	6.03	-	-
Lengths of The Caudal Fins	5.08	-	-
Caudal-Peduncle Depth	3.04	-	-
Predorsal Length	9.3	-	-
Prepelvic Length	10.17	-	-
Longest Hard Dorsal Spine	4.26	-	-
Longest Soft Dorsal Rays	4.72	-	-
Meristic characters			
Gill Rakers	24	-	-
Lateral-Line Scales	47	47-49	-
Pectoral-Fin Rays	18	18	18
Anal-Fin Rays	III-7	III-7	III-7
Dorsal-Fin Rays	XIII-13	XIII-13	XIII-12/13
Pelvic-Fin Rays	I-5	I-5	I-5
Caudal-Fin Rays	16	-	-

Genetic analyses

The mtDNA COI gene region sequence of *S. schlegelii* was obtained at 612 bp and deposited to the Genbank with accession number: OR577041. The Genbank database was used to compare with sequences of other Sebastinae species distributed all over the world. Neighbor-Joining (NJ) and

Maximum Parsimony (MP) trees of the captured and other species from Genbank are given in Figure 4 and Figure 5.

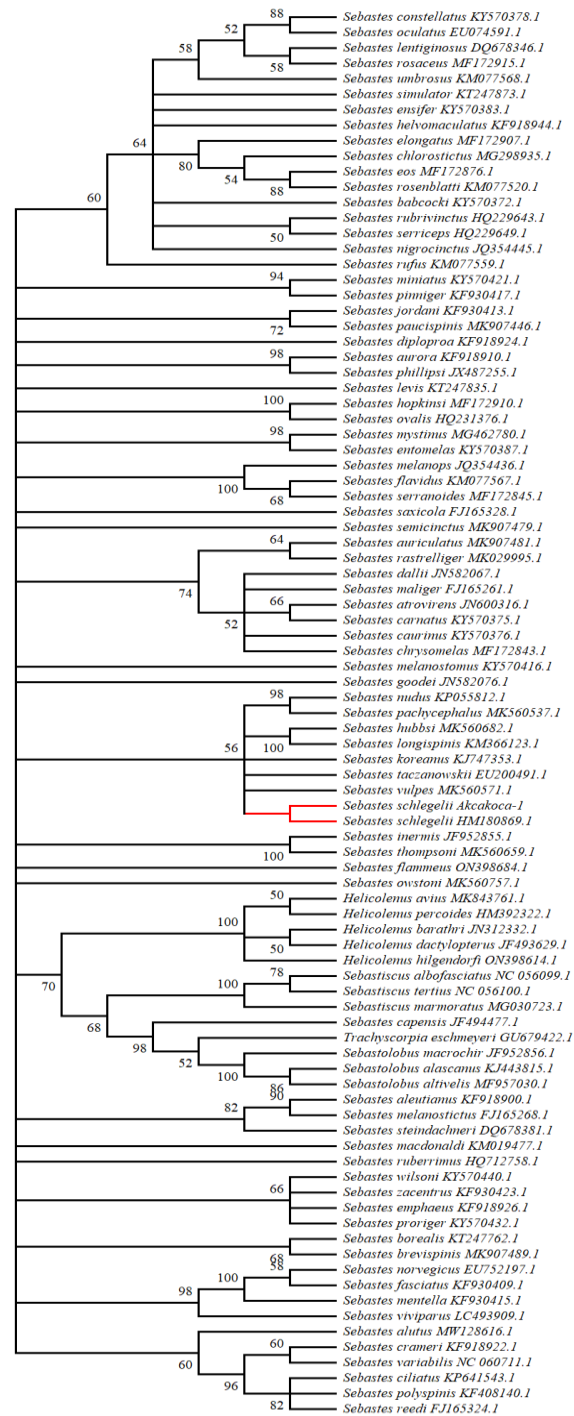


Figure 4. Neighbour-Joining tree analyses of *S. schlegelii* and other Sebastinae species distributed in the World. The red branch of the tree shows that the species we captured matches the record in the GenBank database.

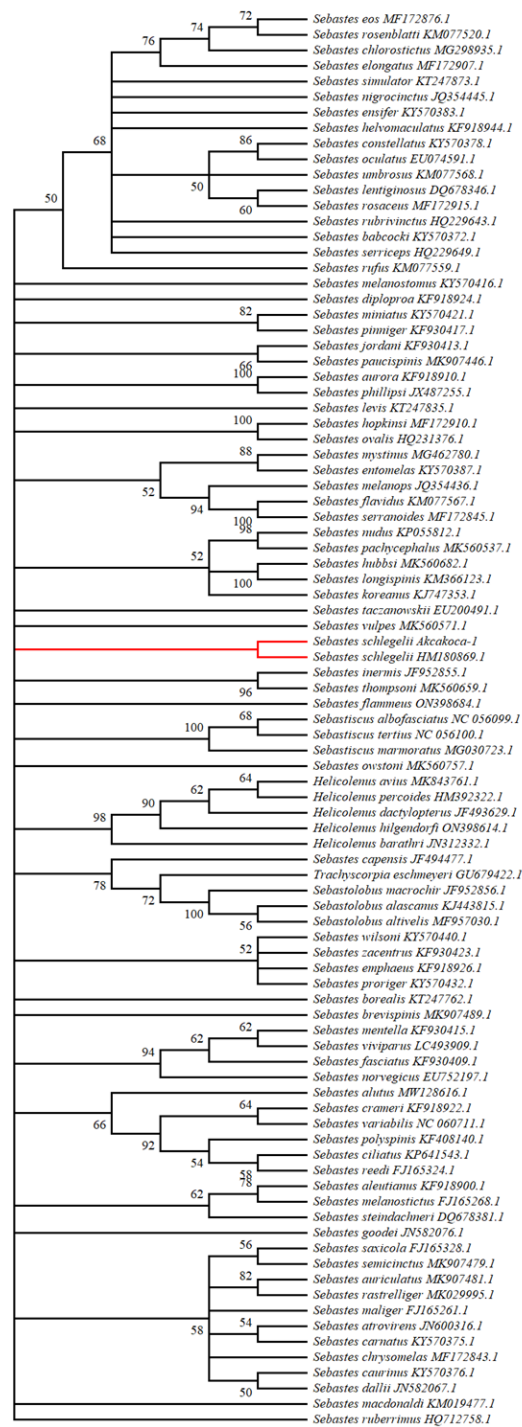


Figure 5. Maximum Parsimony tree analyses of *S. schlegelii* and other Sebastinae species distributed in the World. The red branch of the tree shows that the species we captured matches the record in the GenBank database.

Neighbour-joining and Maximum Parsimony analyses demonstrated that the captured species is *Sebastes schlegelii*, revealing the genetic confirmation of this record on the Black Sea coast of Türkiye.

Discussion

In this study, we first reported on the Korean rockfish *Sebastes schlegelii* from the Black Sea coast of Türkiye with both morphologic and genetic evidence. *S. schlegelii* is characterised by 5 spines on the preoperculum and 2 spines on the operculum. Genetic and morphological analyses confirmed that this species is *S. schlegelii*. This species is thought to have been transported to the Black Sea from other seas of the world, probably via ballast waters or aquarium escape. The most important reason for this is that the species has not been detected elsewhere in the Mediterranean. The species was only reported from the Black Sea Crimean Coast by Karpova et al. (2021).

In recent years, the occurrence of Atlanto-Mediterranean species in the Black Sea has been reported several times in various studies (Yağlıoğlu et al., 2014; Lipej et al., 2017; Yağlıoğlu & Turan, 2021). The migration of Lessepsian fish to the Turkish coast of the Black Sea was also reported for the first time by Turan et al. (2017). The changing ecological structure of the Black Sea, due to factors such as the increase in water temperature related to global climate change and variations in the influx of freshwater from closed seas like the Black Sea over the years, is considered the main reason for the entry of Mediterranean species into the Black Sea (Ben Rais Lasram et al., 2010; Turan et al., 2018). Turan et al., (2016) previously stated that there is a tendency of increasing temperatures in the Black Sea due to global climate change, and this may lead to an increase in the number of Mediterranean-Atlantic and Lessepsian fish species in the Black Sea.

The abundance and distribution of *S. schlegelii* should be monitored and tracked to understand its relationship with the native fauna of the Black Sea. Additionally, the potential impact of global climate change on the Black Sea environment and water quality parameters may accelerate or facilitate the Mediterraneanization process of the Black Sea. Therefore, further scientific research and support are crucial to comprehend the settlement process of species transported to and established in the Black Sea. Additionally, although we do not have samples on hand, based on photographs and videos received from fishermen engaged in recreational fishing along the Amasra and Samsun coasts, it is evident that the species is spreading along the Black Sea coast. It is believed that in the near future, this species may emerge as an economically important species in the Black Sea.

Acknowledgements

Thanks to fisherman Hüseyin Demircioğlu (Taşçı Hüseyin) and Hasan Tiryaki who contributed to the delivery of the grouper to us and its preservation under suitable conditions until it can be examined. We would like to express our gratitude to Ege Veterinary Clinic (Aykut Ekinci) for their X-ray services. We extend our gratitude to Volkan Demircioğlu and Cem Yavuziğit for their

assistance in providing us with photographs of the individuals caught in other provinces along the Black Sea coast of Türkiye.

Conflict of Interest

The authors declare that they have no competing interests.

Author Contributions

C.T. performed all the experiments and drafted the main manuscript text. D.Y., and S.A.D.. C.T. D.Y., and S.A.D.. performed genetic analysis. C.T., D.Y., and S.A.D. contributed morphological analysis and drafting of the manuscript. All authors reviewed and approved the final version of the manuscript.

References

- Ben Rais Lasram, F., Guilhaumon, F., Albouy, C., Somot, S., Thuiller, W., & Mouillot, D. (2010). The Mediterranean Sea as a 'cul-de-sac' for endemic fishes facing climate change. *Global Change Biology*, 16(12), 3233-3245. <https://doi.org/10.1111/j.1365-2486.2010.02224.x>.
- Doğdu, S. A., & Turan, C. (2016). Environmental DNA for detection of endangered grouper species (*Epinephelus* spp.). *Natural and Engineering Sciences*, 1(3), 42-48. <https://doi.org/10.28978/nesciences.286311>
- Fricke, R., Eschmeyer, W. N. & R. van der Laan (eds) 2023. Eschmeyer's Catalog of Fishes: Genera, Species. (<http://researcharchive.calacademy.org/research/ichthyology/catalog/fishcatmain.asp>). Electronic version accessed 20/08/2023.
- Hall, T., Biosciences, I., & Carlsbad, C. J. G. B. B. (2011). BioEdit: an important software for molecular biology. *GERF Bull Biosci*, 2(1), 60-61.
- Hyde, J. R., & Vetter, R. D. (2007). The origin, evolution, and diversification of rockfishes of the genus *Sebastes* (Cuvier). *Molecular phylogenetics and evolution*, 44(2), 790-811. <https://doi.org/10.1016/j.ympev.2006.12.026>.
- Kai, Y., & Soes, D. M. (2009). A record of *Sebastes schlegelii* Hilgendorf, 1880 from Dutch coastal waters. *Aquatic Invasions*, 4(2), 417-419.
- Kai, Y., Muto, N., Noda, T., Orr, J. W., & Nakabo, T. (2013). First record of the rockfish *Sebastes melanops* from the Western North Pacific, with comments on its synonymy (Osteichthyes: Scorpaenoidei: Sebastidae). *Species Diversity*, 18(2), 175-182. <https://doi.org/10.12782/sd.18.2.175>.
- Karpova, E. P., Tamoykin, I. Y., & Kuleshov, V. S. (2021). Findings of the Korean Rockfish *Sebastes schlegelii* Hilgendorf, 1880 in the Black Sea. *Russian Journal of Marine Biology*, 47, 29-34. <https://doi.org/10.1134/S106307402101003X>.
- Kumar, S., Stecher, G., Li, M., Knyaz, C., & Tamura, K. (2018). MEGA X: molecular evolutionary genetics analysis across computing platforms. *Molecular Biology and Evolution*, 35(6), 1547. <https://doi.org/10.1093/molbev/msy096>.

- Lipej, L., Acevedo, I., Akel, E. H. K., Anastasopoulou, A., Angelidis, A., Azzurro, E., ... & Zava, B. (2017). "New Mediterranean Biodiversity Records"(March 2017). *Mediterranean Marine Science*, 18(1), 179-201. <https://doi.org/10.12681/mms.2068>.
- Pusanov, I. I. (1967). Mediterraneanization of the Black Sea fauna and prospects of its strengthening. *Zoological J*, 46(9), 1287.
- Sanger, F., Nicklen, S. and Coulson, A. R. (1977). DNA sequencing with chain-terminating inhibitors. *Proceedings of the National Academy of Sciences*, 74(12): 5463-5467. <https://doi.org/10.1073/pnas.74.12.5463>.
- Turan, C., & Gürlek, M. (2016). Climate change and biodiversity effects in Turkish Seas. *Natural and Engineering Sciences*, 1(2), 15-24. <https://doi.org/10.28978/nesciences.286240>.
- Turan, C., Dural, M., Oksuz, A., & Öztürk, B. (2009). Levels of heavy metals in some commercial fish species captured from the Black Sea and Mediterranean coast of Turkey. *Bulletin of Environmental Contamination and Toxicology*, 82, 601-604. <https://doi.org/10.1007/s00128-008-9624-1>.
- Turan, C., Gürlek, M., Özeren, A., & Doğdu, S. A. (2017). First Indo-Pacific fish species from the Black Sea coast of Turkey: Shrimp scad *Alepes djedaba* (Forsskål, 1775)(Carangidae). *Natural and Engineering Sciences*, 2(3), 149-157. <https://doi.org/10.28978/nesciences.358911>.
- Turan, C., Gürlek, M., Başusta, N., Uyan, A., Doğdu, S. A., & Karan, S. (2018). A checklist of the non-indigenous fishes in Turkish marine waters. *Natural and Engineering Sciences*, 3(3), 333-358. <https://doi.org/10.28978/nesciences.468995>.
- Yağlıoğlu, D., & Turan, C. (2021). Occurrence of Dusky Grouper *Epinephelus marginatus* (Lowe, 1834) from the Black Sea: Is it the Mediterraneanization Process of the Black Sea?. *Natural and Engineering Sciences*, 6(3), 133-137. <https://doi.org/10.28978/nesciences.1036841>.
- Yağlıoğlu, D., Turan, C., & Öğreden, T. (2014). First record of blue crab *Callinectes sapidus* (Rathbun 1896)(Crustacea, Brachyura, Portunidae) from the Turkish Black Sea coast. *Journal of Black Sea/Mediterranean Environment*, 20(1), 13-17.



The Relationships of Otolith Dimensions (Length-Breadth) with Weight and Total Length of Greater Forkbeard (*Phycis blennoides* (Brünnich, 1768)) Captured from northeastern Mediterranean Sea

Hülya Girgin¹ , Nuri Başusta^{2*} 

¹ Dokuz Eylül University, Faculty of Veterinary, Kiraz, İzmir, Türkiye.

² Firat University, Faculty of Fisheries, 23119, Elazığ, Türkiye.

Abstract

The greater forkbeard, *Phycis blennoides* is captured by commercial trawler, has minor commercial value in Türkiye. This study is the first knowledge on otolith biometry-fish size relationships of *Phycis blennoides* living in the northeastern Mediterranean Sea. A total of 202 the greater forkbeard individuals were caught by commercial bottom trawl at a depth of 200 to 400 m in the northeastern Mediterranean. Minimum-maximum total length and weight of obtained fish specimens were found as 16.9-38.7 cm and 31.06-415.0 g for females and 16.3-38.3 cm and 27.14-504.08 g for males respectively. The difference of the total length and weight between the females and males of *P. blennoides* was statistically insignificant ($P>0.05$). The determination coefficient value showed that there were a moderate relationships between total length-right and left otolith lengths, total length-right and left otolith breadths.

Keywords:

Greater forkbeard, *Phycis blennoides*, otolith biometry, Iskenderun Bay

Article history:

Received 30 March 2023, Accepted 07 September 2023, Available online 15 December 2023

Introduction

The greater forkbeard (*Phycis blennoides*) is a demersal fish species found along the continental shelf and the slope, on the bottoms from 60 to 800 m depth (Farjallah et al., 2006). *Phycis blennoides* is captured in small numbers by bottom trawl and they have minor commercial value in Türkiye. The Greater forkbeard is distribute in the Mediterranean, Adriatic Sea, Aegean and

*Corresponding Author: Nuri BAŞUSTA, E-mail: nbasusta@firat.edu.tr

Black Seas throughout the Atlantic Ocean from Iceland to Maritania and in the Faroe Islands, Madeira and the Azores (Golani et al., 2006). The shape and size of otoliths used to determine the age of fish also provide information about the size of fish in palaeontological samples (Bostanci et al., 2012; Bařusta et al., 2013). Knowledge on the relationship between otolith biometry and total fish length is useful as fish size can be estimated from otolith morphometry measured from otoliths come across in predator stomachs and feeding ecology of fishes (Echeverria, 1987; Karachle et al., 2015). This knowledge is important for fish population management plans, prey–predator relationship studies and paleobiological research. By using the relationship between otolith biometry and total fish length, it is possible to determine fish length from otolith size or vice versa. Although various length-weight relationships of *P. blennoides* have been reported from the Aegean Sea and northeastern Mediterranean Sea, there is no detailed otolith biometry study on the greater forkbeard from the northeastern Mediterranean Sea (Filiz & Bilge, 2004; Stergiou & Moutopoulos, 2001; Girgin & Bařusta, 2021).

This research provides preliminary information on the otolith biometry-total fish size relationships of *P. blennoides* inhabiting off the Iskenderun Bay.

Materials and Methods

Phycis blennoides specimens were caught by bottom trawl at a depth of 200 to 400 m in the northeastern Mediterranean Sea (36° 13' 242" N-35° 31' 328" E, 36° 12' 927" N- 35° 14' 566" E). Trawling duration was 3 hours with 2.5 knots speed. *Phycis blennoides* specimens were transferred to the fish biology laboratory of Faculty of Fisheries, Firat University. *P. blennoides* individuals were measured for total length to the nearest 0.1 cm, weight (W) was weighted to the nearest 0.1 g in the laboratory. The sexes were determined by macroscopic observation of the gonads and then both right and left sagittal otoliths were removed from each fish and soaked in 10% KOH solution for approximately 5 minutes and stored dry in a small ziplock bag for further applications. Right and left otolith weights (OW), otolith lengths (OL), otolith breadths (OB) were taken from each specimen to the nearest 0.001 mm and 0.0001g respectively and otoliths were examined under a binocular stereomicroscope (Leica S8APO) combined to a computer (Figure 1). Differences between females and males were tested by using One-way ANOVA.

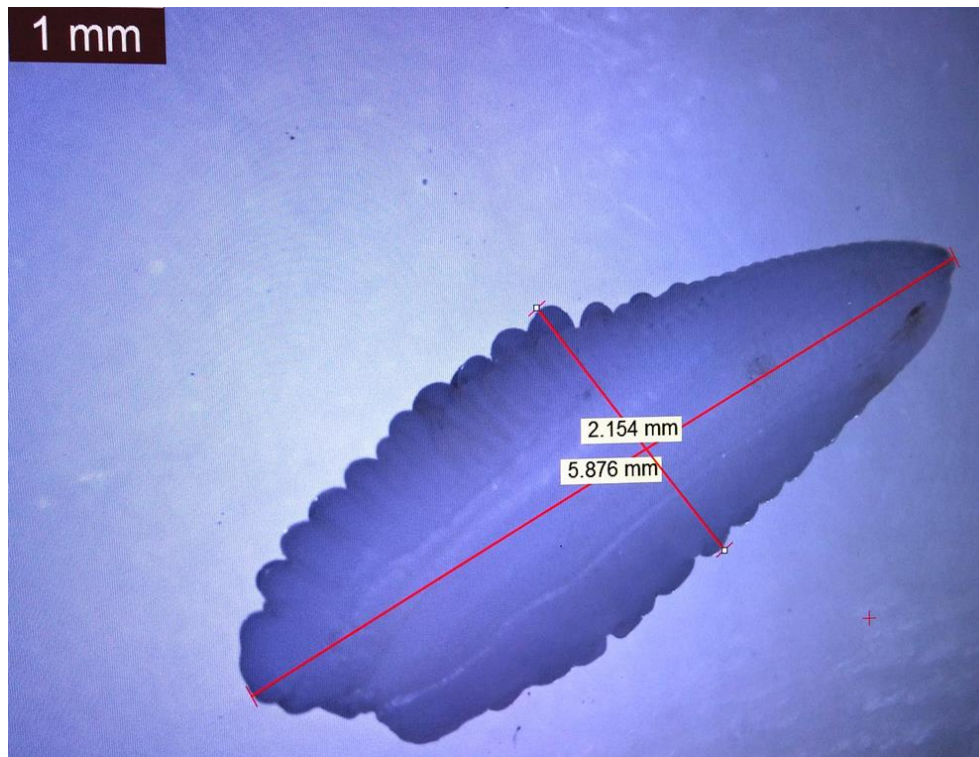


Figure 1. Otolith length and width measurements of the greater forkbeard.

The relationships of otolith biometry-total fish length were examined by using the following formula:

$$y = a + bx$$

where: x: total fish length, y: otolith length or otolith breadth, a: intercept value, b: coefficient value. Regression analyses were done by using Excel software for determining the relationships between total fish length and otolith length, breadth and weight (Dehghani et al., 2016).

Results and Discussion

A total of 202 greater forkbeard specimens (159 male and 43 female) were obtained. Minimum-maximum total length and mass of collected fish specimens were determined as 16.9-38.7 cm and 31.06-415.0 g for females and 16.3-38.3 cm and 27.14-504.08 g for males respectively. According to statistical analyses, there was no significant differences between values of male and female ($P > 0.05$; Student's t-test).

The distributions between the otolith weight, length and breadth of the *P. blennoides* population according to gender was given in Figure 2, Figure 3 and Figure 4. Accordingly, it was determined that the right and left otolith weights of female individuals were between 0.011 (g) and 0.012 (g), while the right and left otolith weights of male individuals were between 0.010 (g) and

0.011 (g). Likewise, the right and left otolith lengths of female individuals are between 11.0 - 11.5 (mm), the right otolith length of male individuals is 10.5 - 11.0 (mm), and the right and left otolith breadths of female individuals are 2.2- 4.3 (mm) in female individuals while the otolith breadths of male individuals are between 2.1 - 4.2 (mm). It is seen that the otolith weights, lengths and widths of female individuals are higher than those of male individuals.

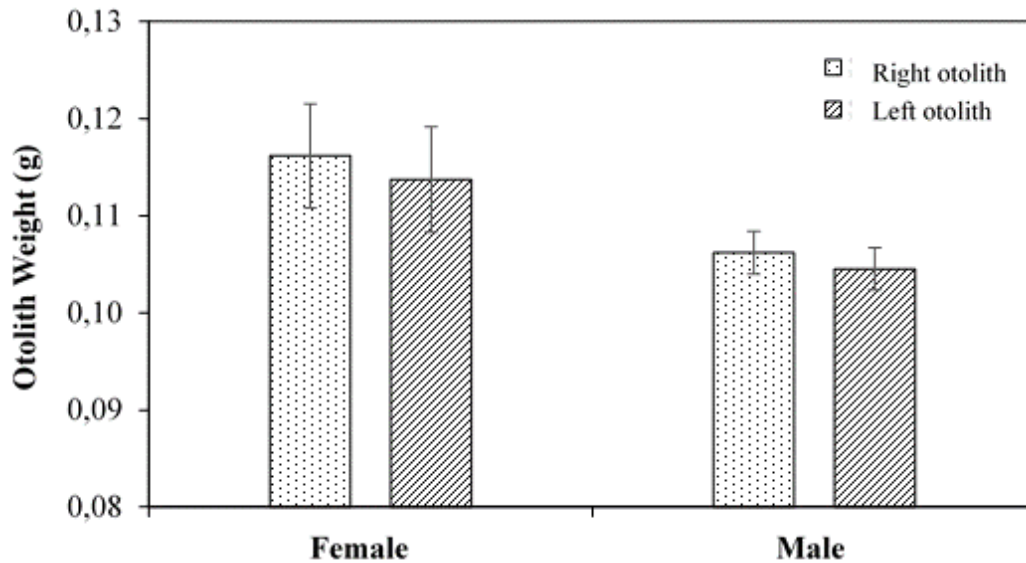


Figure 2. Right and left otolith weights according to sex in *Phycis blennoides*.

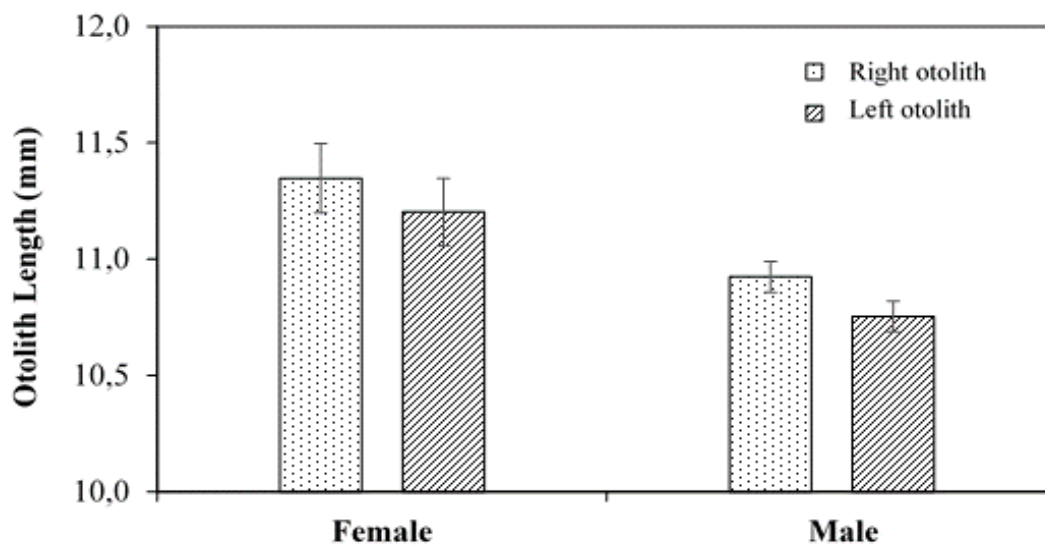


Figure 3. Right and left otolith lengths according to sex in *Phycis blennoides*.

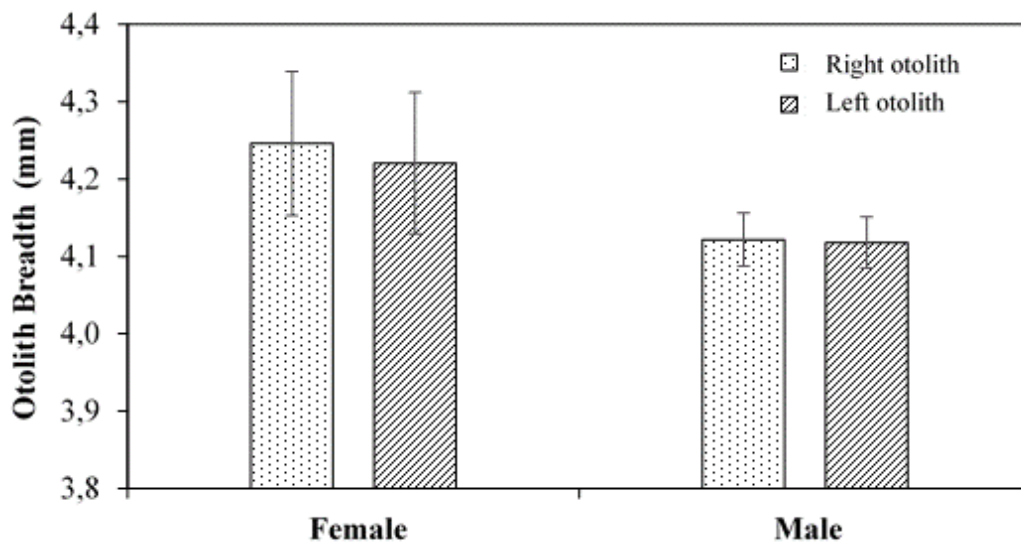


Figure 4. Right and left otolith breadths according to sex in *Phycis blennoides*.

In present study, the relationships of total length of fish with right otolith length and left otolith weight are shown in Figure 6. Both relationships were linear with equations; $y=0.0037x+0.0124$ ($R^2=0.217$) and $y=0.0036x+0.135$ ($R^2=0.203$), respectively.

According to the coefficient value of determination (R^2), both relationships show that positive and weak level. The relationships of total fish length with right otolith length and left otolith length are shown in Figure 7. Both relationships were linear with equations: $y=0.16x+6.8582$ ($R^2=0.4214$) and $y=0.1587x+6.7271$ ($R^2=0.4241$), respectively. To the coefficient of determination (R^2), it can be said that both relationships are positive and moderate level.

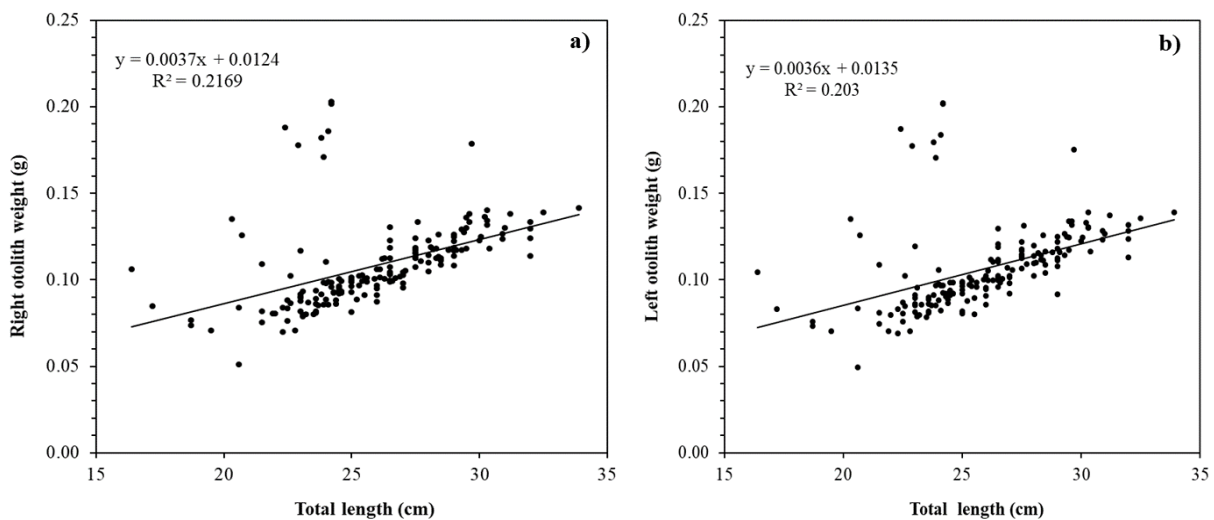


Figure 5. Relationships between total length-otolith weights of *Phycis blennoides* (a: Right otolith, b: Left otolith weights).

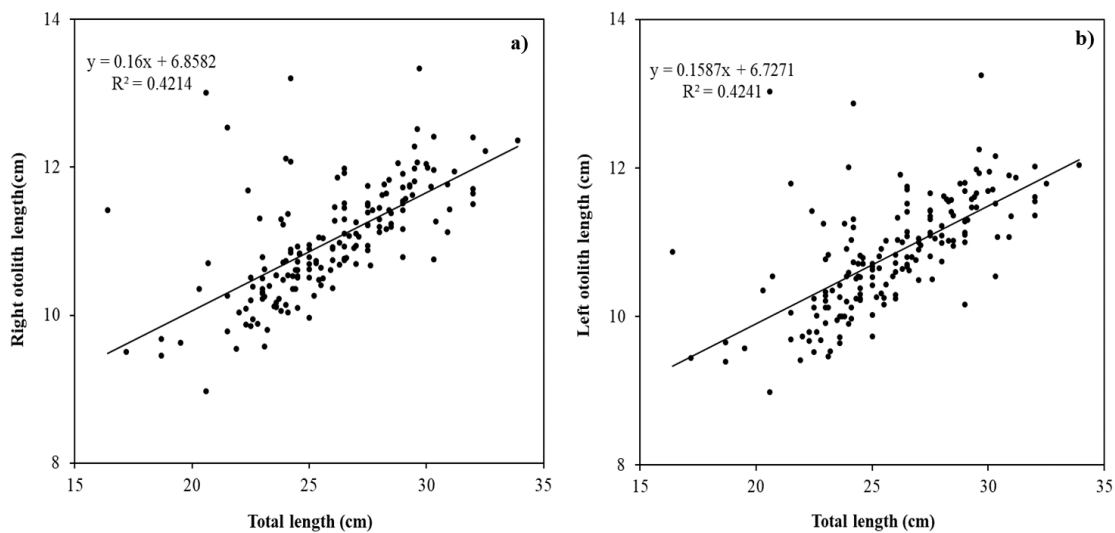


Figure 6. Relationships between total length-otolith lengths of *Phycis blennoides* (a: right otolith lengths, b: left otolith lengths).

The relationships of total fish length with right otolith breadth and left otolith breadth are shown in Figure 7. Both relationships were linear with equations: $y=0.0735x+2.2407$ ($R^2=0.3349$) and $y=0.0656x+2.4393$ ($R^2=0.2827$), respectively. According to the coefficient of determination (R^2), It is seen that both relationships are positive and weak.

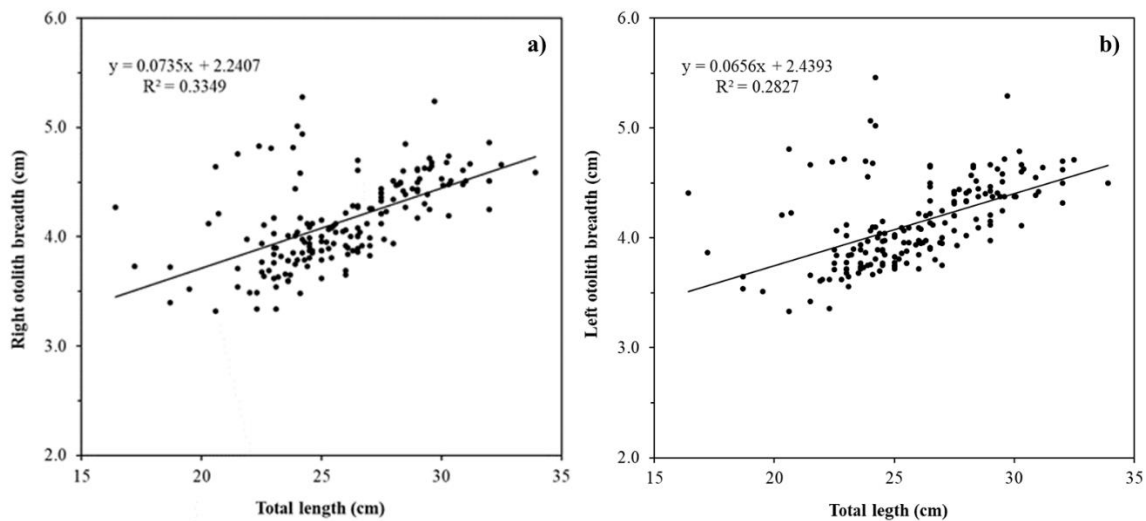


Figure 7. Relationships between total length-otolith breadth of *Phycis blennoides* (a: right otolith breadth, b: left otolith breadth).

There was no significant difference in right otolith and left otolith values ($P > 0.05$). Therefore, in future studies on this species, only the right or left otolith can be used instead of both sagittal otolith. Otolith biometry studies shows that otoliths can be used in stomach content research

and fish size in archaeological samples. Brander (1974) suggest that otolith mass has a linear relationship with the age of the fish. According to Harkönen (1986), there is a high correlation between total fish length and otolith length, and this is generally seen as a linear relationship. This study provides first information on the otolith biometry of the greater forkbeard in the northeastern Mediterranean Sea.

Acknowledgements

This study is a part of the Ph.D. Thesis prepared by Hülya Girgin at Fırat University, Institute of Science, Department of Basic Fisheries Sciences and also it was presented as an oral presentation at the International Science Symposium (ISS2017).

Conflict of Interest

The authors declare that they have no competing interests.

Author Contributions

N.B. and H.G performed all the experiments and drafted the main manuscript text. All authors reviewed and approved the final version of the manuscript.

References

- Basusta, A., Özer, E. İ., & Girgin, H. (2013). Relationship between fish length and otolith dimensions in the population of *Lepidotrigla dieuzeidei* (Blanc & Hureau, 1973) from Mediterranean. *Aquaculture Studies*, 13(3), 003-009.
- Bostanci, D., Yilmaz, S., Polat, N., & Kontas, S. (2012). The otolith biometry characteristics of black scorpionfish, *Scorpaena porcus* L., 1758. *The Black Sea Journal of Science*, 2, 59-68.
- Brander, K. (1974). The effects of age-reading errors on the statistical reliability of marine fishery modelling. *In International Symposium on the Ageing of Fish. Reading (UK)*. 19 Jul 1973..
- Dehghani, M., Kamrani, E., Salarpouri, A. & Sharifian, S., (2016). Otolith dimensions (length, width), otolith weight and fish length of *Sardinella sindensis* (Day, 1878), as index for environmental studies, Persian Gulf, Iran. *Marine Biodiversity Records*, 9(44), 1-6. <https://doi.org/10.1186/s41200-016-0039-0>
- Echeverria, W. (1987). Relationship of otolith length to total length in rockfishes from northern and central California. *Fishery Bulletin*, 85(2), 383-387.
- Farjallah, S., Slimane, B. B., Blel, H., Amor, N., & Said, K. (2006). Anisakid parasites of two forkbeards (*Phycis blennoides* and *Phycis phycis*) from the eastern Mediterranean coasts in Tunisia. *Parasitology Research*, 100, 11-17. <https://doi.org/10.1007/s00436-006-0227-7>.
- Filiz, H. and Bilge, G., (2004). Length-weight relationships of 24 fish species from the North Aegean Sea, Turkey. *Journal of Applied Ichthyology*, 20, 431-432. <https://doi.org/10.1111/j.1439-0426.2004.00582.x>

- Girgin, H., Bařusta, N., (2021). Kuzeydoęu Akdenizde Yakalanan Bıyıklı Mezgitin (*Phycis blennoides* (Brünnich, 1768)) Boy-Aęırlık İliřkileri. *Ecological Life Sciences*, 16(4), 151-156, <https://doi.org/10.12739/NWSA.2021.16.4.5A0158>.
- Golani, D., Ozturk, B., Basusta, N., (2006). Fishes of the Eastern Mediterranean. Turkish Marine Research Foundation, Istanbul, Turkey. Pub. Number, 24, 259p.
- Härkönen, T.,(1986). Guide to the otoliths of the bony fishes of the Northeast Atlantic. Danbiu ApS. Biological Consultants,. Henningsens Alle 58. DK-2900, Hellerup, Denmark. ISBN 87- 982290-2-8.
- Karachle, P.K., Bařusta, A., Bařusta, N., Bostancı, D., Buz, K., Girgin, H., Chater, I., Kokokiris, L., Kontař, S., Ktari, M.-H., Maravelias, C.T., Minos, G., Özer, E.I., Romdhani, A., Tiralongo, F., Tibullo, D., Tserpes, G., & Vasilakopoulos, P. (2015). New fisheries-related data from the Mediterranean Sea (April, 2015). *Mediterranean Marine Science*, 16, 285-293. <https://doi.org/10.1186/s41200-016-0039-0>
- Stergiou, K.I. and Moutopoulos, D.K., (2001). A review of length–weight relationships of fishes from Greek marine waters. *Aquaculture and Fisheries Professionals* (NTAFP), 24(1-2), 23–39.



Occurrence of *Homola barbata* (Fabricius, 1793) (Decapoda, Brachyura) in Finike Bay (Türkiye, Eastern Mediterranean Sea)

Cengiz Koçak ^{1*} , Coşkun Menderes Aydın ² , Aydın Ünlüoğlu ³ 

¹ Department of Hydrobiology, Fisheries Faculty, Ege University, TR 35100, Bornova-İzmir, Türkiye.

² Mediterranean Fisheries Research, Production and Training Institute, Antalya, Türkiye.

³ Dokuz Eylül University, Institute of Marine Sciences and Technology, Baku Bulv., 32 İnciraltı, TR 35340 İzmir, Türkiye.

Abstract

Bottom trawl samplings in Finike Bay revealed the existence of a brachyuran crab species, *Homola barbata* (Fabricius, 1793). *H. barbata* has been recorded only fourth time in Turkish waters, up to now. The existence of this rare species is recorded herein for the first time from the Finike Bay. It is the westernmost record of *H. barbata* on the Mediterranean coast of Türkiye. A distribution map of *H. barbata* in the eastern Mediterranean Sea is also presented, together with photographs of it.

Keywords:

Brachyura, decapoda, Homola barbata, Finike Bay, Türkiye, eastern Mediterranean Sea

Article history:

Received 30 June 2023, Accepted 01 September 2023, Available online 15 December 2023

Introduction

Homole crab *Homola barbata* (Fabricius, 1793) is a marine species belonging to the Homolidae family. These crabs live in the Mediterranean Sea and on both sides of the Atlantic Ocean. The western Atlantic range of *Homola barbata* extends from the United States (Massachusetts and Virginia to South Florida) to the Gulf of Mexico and the West Indies and along the coasts of Central and South America to Rio Grande do Sul, Brazil. *Homola barbata* is found in the eastern Atlantic in Portugal and Western Africa, including the Canary and Madeira Islands (Holthuis & Gottlieb,

*Corresponding Author: Cengiz KOÇAK, E-mail: kocakcengiz@gmail.com

1958; Palomares & Pauly, 2022). *H. barbata* inhabits depths from 10 to 682 m (Manning & Holthuis, 1981) on a variety of substrates such as mud, muddy sand, sandy and muddy detritus, coralline algae, calcareous algae, slightly sandy mud with funiculines, alcyonarians in mud, and reddish gravel with shell debris (Palomares & Pauly, 2022).

H. barbata is the only known species in the genus *Homola* in the Mediterranean Sea (cf. Guinot & Richer de Forges, 1995). *H. barbata* is one of the twelve species of the *Homola* genus occurring in the Atlantic, Pacific, and Mediterranean Seas (Ng & Richer de Forges, 2016), which are: *H. milkolk* Ng & Richer de Forges, 2016, *H. poupini* Richer de Forges & Ng, 2007, *H. ranunculus* Guinot & Richer de Forges, 1995, *H. minima* Guinot & Richer de Forges, 1995, *H. eldredgei* Guinot & Richer de Forges, 1995, *H. coriolisi* Guinot & Richer de Forges, 1995, *H. dickinsoni* Eldredge, 1980, *H. mieensis* Sakai, 1979, *H. ikedai* Sakai, 1979, *H. orientalis* Henderson, 1888, *H. vigil* A. Milne-Edwards, 1880, and *H. barbata* (Fabricius, 1793). In the eastern Mediterranean Sea, the species was reported from Greece, Cyprus, Lebanon, Israel, Egypt, Syria, and Türkiye (Figure 1; Table 1). Until now, *H. barbata* was already reported between 49.4 and 630 m from various localities in the eastern Mediterranean Sea.

In this study, the existence of this rare species is recorded herein for the first time from the Finike Bay. *H. barbata* has been recorded only fourth time in Turkish waters, up to now. It is the westernmost record of *H. barbata* on the Mediterranean coast of Türkiye.

Materials and Methods

One female *H. barbata* specimen was collected at a depth of 260-275 m with a bottom trawl survey carried out by the research vessel R/V Akdeniz Araştırma 1 at a site in Finike Bay (36°14'74"N, 30°15'23"E-36°14'53"N, 30°16'72"E) in July 2015 (Figure 1). An experimental trawl net with a cod-end mesh size of 20 mm was used in the trawling operations which were conducted according to the International Bottom Trawl Survey in the Mediterranean (MEDITS) protocol (Anonymous, 2016; 2017).

The specimen was preserved in 70% ethanol. CL (Carapace length) and CW (Carapace width) were measured with digital calipers to the nearest 0.01 mm. Manning & Holthuis (1981) and Falciai & Minervini (1996) were used for the species determination.

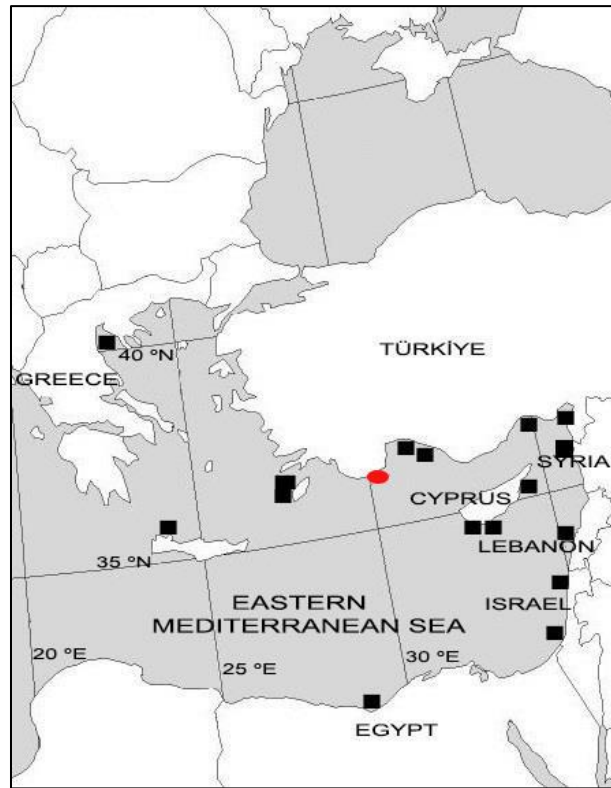


Figure 1. Previously established occurrence of *Homola barbata* (Fabricius, 1793) in the eastern Mediterranean Sea (filled rectangle) and the sampling area (red filled circle) recorded in this paper.

Results

Family: Homolidae De Haan, 1839

Genus: *Homola* Leach, 1815

Species: *Homola barbata* (Fabricius, 1793) (Figures 2-3)

Material examined: One ♀, Finike Bay (Mediterranean coast of Türkiye), 36°14'74"N 30°15'23"E to 36°14'53"N 30°16'72"E, 260-275 m, muddy bottom, bottom trawl, 23.07.2015.

Measurements (mm): CL, 31.4; CW, 22.1.

Remarks: The specimen agrees well with the description of Manning & Holthuis (1981) and that of Falciai & Minervini (1996). We only noticed that the CL of the present specimen (31.4 mm) is larger than those in Manning & Holthuis' (1981) samples (16 to 28 mm) and smaller than those in Falciai & Minervini's (1986) sample (41 mm).

Worldwide Distribution: Mediterranean Sea and on both sides of the Atlantic Ocean. (Holthuis & Gottlieb, 1958; Bertini et al. 2004; Palomares & Pauly, 2022).



Figure 2. *Homola barbata* (Fabricius, 1793), ♀, from Finike Bay (dorsal view).

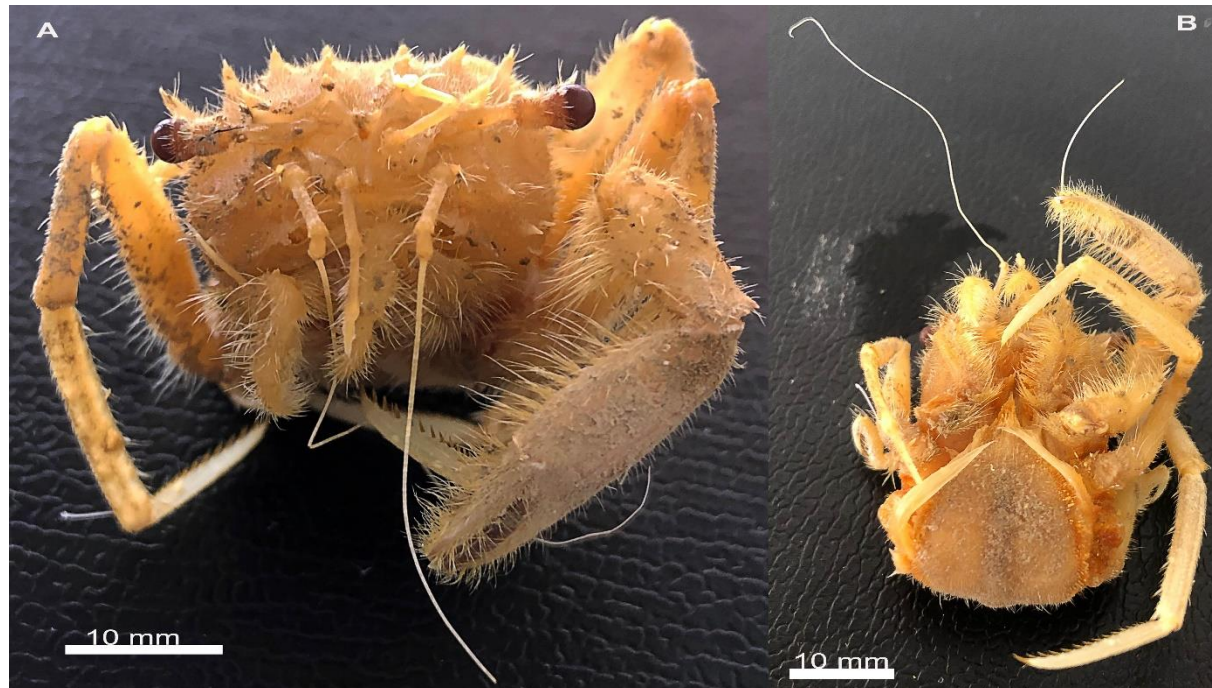


Figure 3. *Homola barbata* (Fabricius, 1793), ♀, from Finike Bay (A: Anterior view; B: Ventral view).

Discussion

In the eastern Mediterranean Sea, *H. barbata* was recorded from Greece (Lucas, 1853; Raulin, 1870; Kevrekidis & Galil, 2003; Kampouris et al., 2018), Cyprus (Hadjichristophorou, 1997; Kocataş et al., 2001), Syria (Ammar & Hmaesha, 2023), Lebanon (Shiber, 1981), Israel (Holthuis & Gottlieb, 1958), Egypt (Ramadan & Dovidar, 1972), and Türkiye (Karhan, 2015; Deval et al., 2017; Gönülal & Dalyan, 2017; Patania & Mutlu, 2021) (Figure 1; Table 1).

In the checklist of decapod crustaceans in Turkish seas given in the study of Kocataş & Katağan (2003), it was stated that *H. barbata* was reported from the Aegean and Mediterranean coasts of Türkiye in previous studies. However, there is no information about these records in the study. Later, in the updated checklist given by Ateş et al. (2010), this species was also shown among the species recorded from the Aegean and Mediterranean coasts of Türkiye, but again no information was given about the records in the study. In the last checklist of the Turkish seas, which includes Arthropoda species, it was stated that the species was previously reported from the Turkish Aegean and Mediterranean coasts, and its first record was given in the study of Kocataş & Katağan (2003) (Bakır et al., 2014). However, no record of *H. barbata* from Turkish seas has been found in the literature.

Up to now, *H. barbata* has already recorded between 49.4 and 630 m from the eastern Mediterranean Sea. The specimen herein reported was collected at a depth of 260-275 m in the region (Table 1).

Table 1. Data on *Homola barbata* (Fabricius, 1793) in the eastern Mediterranean Sea (N= number of individuals; CL (mm)= Carapace length).

Reference	Sampling Date	Occurrence depth (m)	Sampling gear	Habitat	N	CL (mm)
Lucas (1853), Raulin (1870); Crete Island, Greece (as <i>H. spinifrons</i>)	-	-	-	-	-	-
Holthuis & Gottlieb, (1958); Israel	05.05.1953	146	-	-	1	17.5
					2♀	15-35
Ramadan & Dovidar (1972); Egypt	06.1969	171-180	Trawl	silty, clayey	2♂	-
Shiber (1981); Lebanon	-	-	-	-	1	33
Hadjichristophorou et al. (1997); Cyprus	1972-1993	100	Dredge	-	-	-
Kocataş et al. (2001); Cyprus	05.1997-07.1998	62-145	Trawl	-	-	-
Kevredikis & Galil, 2003; Rhodos Island, Greece	27.5.1998	49.4-69.5	Trawl	-	-	-
	21.11.1999	68-95	Trawl	-	-	-
Karhan (2015); Türkiye	04.06.2009	68-78	Trawl	Mud;coralligen	2♀;2♂	17.3-26
	05.10.2012	70	Trawl	Muddy sand	1♀	17
	19.03.2009	126-140	Trawl	Mud	1♂	15.8
	17.06.2009	58-61	Trawl	Sandy mud	1♀	21.8
Deval et al. (2017); Türkiye	2010-2011	300	Trawl	-	2	-
Gönülal & Dalyan (2017); Türkiye	2014-2015	100-200; 200-300	Trawl	-	-	-
Kampouris et al. (2018); Greece	-	69.5-72	Tangle nets	hard bottom	-	-
Patania & Mutlu (2021); Türkiye	2014-2015	75	Trawl	less vegetation and a non-vegetated soft bottom	-	-
Ammar & Hmaesha (2023); Syria	23.02.2021	630	Trawl	-	-	-
Present study; Türkiye	23.07.2015	260-275	Trawl	mud	1♀	31.4

H. barbata has been reported only a fourth time from the Turkish waters up to date. The existence of this rare species is confirmed for the first time from the Finike Bay, and the fifth time

from Turkish waters in the present study. This constitutes the westernmost report of *H. barbata* in the Mediterranean coast of Türkiye.

Acknowledgements

We are very grateful to our colleagues from the Mediterranean Fisheries Research, Production and Training Institute (AKSAM), as well as the captain and crew of R/V Akdeniz Araştırma 1, for their assistance in sampling. Dr Sencer Akalın (Ege University, İzmir) deserves special thanks for his valuable contributions to the field. *H. barbata* specimen was provided from the project of TAGEM/HAYSUD/2015/A11/P-02/2 “Estimation of Sizes of Demersal Fish Stocks along the Mediterranean Coast of Türkiye”. Our gratitude also goes to the administration of AKSAM for their tremendous support in the project which was funded by the General Directorate of Agricultural Research and Policies of the Ministry of Food, Agriculture and Livestock.

Conflict of Interest

The authors declare that they have no known competing financial interests or personal relationships that could have appeared to influence the work reported in this paper.

Author Contributions

CK; Identified the specimen, wrote the first draft, literature: CMA, AÜ; Methodology, collected the material, reviewed and edited the first draft. All authors approved the final draft.

Funding Source

This study was supported by the General Directorate of Agricultural Research and Policies of the Ministry of Food, Agriculture, and Livestock. Project No: TAGEM/HAYSUD/2015/A11/P-02/2.

Ethical Approval Statements

Local Ethics Committee Approval was not obtained because experimental animals were not used in this study.

Data Availability Statement

The data used in the present study are available upon request from the corresponding author.

References








- Ammar, I. A. & Hmaesha, Y. B. (2022). New Records of Rare Species of Marine Invertebrates in the Eastern Mediterranean, Syria. *The Scientific Journal of King Faisal University: Basic and Applied Sciences*, 23(2), 48–53. <https://doi.org/10.37575/b/sci/220044>.
- Anonymous (2016). MEDITS-handbook version n. 8, MEDITS working group. 177 pp.
- Anonymous (2017): MEDITS-handbook version n. 9, MEDITS working group. 106 pp.
- Ateş, A.S., A. Kocataş, T. Katağan & Özcan, T. (2010). An updated list of decapod crustaceans on the Turkish coast with new record of the Mediterranean shrimp, *Processa acutirostris*

- Nouvel and Holthuis 1957 (Caridea, Processidae). *North-Western Journal of Zoology*, 6(2), 209-217.
- Bakır, A.K., T. Katağan, H. V. Aker, T. Özcan, M. Sezgin, A. S. Ateş, C. Koçak & Kırkım, F. (2014). The marine arthropods of Turkey. *Turkish Journal of Zoology*, 38, 765-831. <https://doi.org/10.3906/zoo-1405-48>.
- Bertini, G., A. Fransozo. & Melo, G.A.S. (2004). Biodiversity of brachyuran crabs (Crustacea: Decapoda) from non-consolidated sublittoral bottom on the northern coast of São Paulo State, Brazil. *Biodiversity and Conservation*, 13, 2185–2207. <https://doi.org/10.1023/B:BIOC.0000047900.96123.34>.
- Deval, M. C., S. Yılmaz. & Kapisir, K. (2017). Spatio Temporal Variations in Decapod Crustacean Assemblages of Bathyal Ground in the Antalya Bay (Eastern Mediterranean). *Turkish Journal of Fisheries and Aquatic Sciences*, 17, 967-979. https://doi.org/10.4194/1303-2712-v17_5_12.
- Falciai, L. & Minervini, R. (1996). Guide des homards, crabes, langoustes, crevettes et autres Crustacés Décapodes d'Europe. Delachaux et Niestlé SA, Paris.
- Gönülal, O. & Dalyan. C (2017). Bathymetric distribution of macroinvertebrates in the Northeastern Levantine Sea and the Northeastern Aegean Sea based on bottom-trawl surveys. *Oceanological and Hydrobiological Studies*, 46(4), 405-413. <https://doi.org/10.1515/ohs-2017-0040>.
- Guinot, D. & Richer De Forges, B., (1995). Crustacea Decapoda Brachyura : Révision de là famille des Homolidae de Haan, 1839. *Mémoires du Muséum national d'histoire naturelle*, 163, 283-517.
- Hadjichristophorou, M., Argyrou, M., Demetropoulos, A. & Bianchi, T. S. (1997). A species list of the sublittoral soft-bottom macrobenthos of Cyprus. *Acta Adriatica*, 38(1), 3-32.
- Holthuis, L. B. & Gottlieb, E. (1958). An annotated list of the decapod Crustacea of the Mediterranean coast of Israel, with an appendix listing the Decapoda of the Eastern Mediterranean. *Bulletin of the Research Council of Israel*, 7B, 1-126.
- Karhan, S.Ü. (2015). Turkish Seas Littoral Crabs (Crustacea, Decapoda, Brachyura): Systematic, Distribution and Habitat Preferences. *PhD Thesis*. University of İstanbul, İstanbul, p 324.
- Kampouris, T. E., Milenkova, D. & Batjakas, I. E. (2018). On the Finding of the Rare Crab *Paragalene longicrura* (Nardo, 1868) (Crustacea, Decapoda, Brachyura, Progeronidae) from Thermaikos Gulf, Northwest Aegean Sea, Greece. *Fishes*, 3(30). <https://doi.org/10.3390/fishes3030030>.
- Kevrekidis, K., & Galil, B. (2003). Decapoda and Stomatopoda (Crustacea) of Rodos island (Greece) and the Erythrean expansion NW of the Levantine Sea. *Mediterranean Marine Science*, 4(1), 57–66. <https://doi.org/10.12681/mms.241>.
- Kocataş, A. & Katağan, T. (2003). The Decapod Crustacean fauna of the Turkish Seas. *Zoology in the Middle East*, 29, 63-74. <https://doi.org/10.1080/09397140.2003.10637971>.

- Kocataş, A., T. Katağan & Benli, H. A. (2001). Contribution to the Knowledge of the Crustacean fauna of Cyprus. *Israel Journal of Zoology*, 47, 147-160. <https://doi.org/10.1560/YQL8-4PBT-12W2-82HV>.
- Lucas, H. (1853). Crustacea. Essai sur les animaux articulés qui habitent l'île de Crète. *Revue et Magasin de Zoologie Pure et Appliquée*, 2(5), 461-468.
- Manning, R. B. & Holthuis, L. M. (1981). West African Brachyuran Crabs (Crustacea: Decapoda). *Smithsonian Contributions to Zoology*, 306, 1-379.
- Ng, P. K. L. & Richer de Forges, B. (2016). A new species of *Homola* Leach, 1816 (Crustacea: Brachyura: Homolidae) from Palau, Western Pacific, with notes on *H. mieensis* Sakai, 1979. *Crustacean Research*, 45, 1–13. https://doi.org/10.18353/crustacea.45.0_1.
- Palomares, M. L. D. & Pauly, D. (2022). SeaLifeBase. World Wide Web electronic publication. www.sealifebase.se/summary/Homola-barbata.html
- Patania, A. & Mutlu, E. (2021). Spatiotemporal and ecological distribution of megabenthic crustaceans on the shelfshelf break of Antalya Gulf, the eastern Mediterranean Sea. *Mediterranean Marine Science*, 22 (3), 446–465. <https://doi.org/10.12681/mms.26142>.
- Ramadan, S.E. & Dowidar, N. M. (1972). Brachyura (Decapoda, Crustacea) from the Mediterranean waters of Egypt. *Thalassia Jugoslavica*, 8(1), 127-139.
- Raulin, V. (1870). Description physique de l'île de Crète (Fin), Actes de la Société linnéenne de Bordeaux, 24(3-4), 353-770.
- Shiber, J.G. (1981). Brachyura from Lebanese waters, *Bulletin of Marine Science*, 31(4), 864-875.



Two New Records of Eunicidae (Annelida, Errantia) Along the Makran Coast of Pakistan, Northern Arabian Sea

Qadeer Mohammad Ali ¹ , Quratulan Ahmed ^{1*} , Shumaila Mubarak ¹ ,
Ateeqa Baloch ¹ , Levent Bat ² , Hafsa Qazi ¹ , Iqra Shaikh ¹ 

¹ The Marine Reference Collection and Resource Centre, 75270, University of Karachi, Pakistan.

² Sinop University, Fisheries Faculty, Department of Hydrobiology, 57000, Sinop, Türkiye.

Abstract

The Makran coast of Pakistan in the Northern Arabian Sea is a region of high biodiversity yet remains relatively under-studied in terms of polychaete fauna. In this study, we presented detailed morphological and taxonomical analyses of two newly discovered species of Eunicidae polychaetes, *Eunice indica* and *Lysidice ninetta*, collected during low tide from the intertidal zone of two stations along the Makran coast: Shamal Bandar, Pasni dated 31st January 2022 and Taak Beach, Ormara, dated 31st January 2022. Before our study, only 12 species of Eunicidae were known to occur in Pakistan. The identification and description of *E. indica* and *L. ninetta* provide important information about the distribution and taxonomy of Eunicid polychaetes on the Makran coast. These findings emphasize the need for further investigations and highlight the potential for discovering additional species within the region.

Keywords:

Eunicid polychaetes, polychaeta, eunice, lysidice, balochistan, Indian Ocean

Article history:

Received 12 May 2023, Accepted 08 September 2023, Available online 15 December 2023

Introduction

Eunicidae is one of the largest Polychaetae families. Currently, it includes 460 species and 33 genera that have been described (11 of which have been taxonomically identified) (Read & Fauchald, 2021). Polychaeta species belonging to the family Eunicidae (Berthold, 1827) inhabit

*Corresponding Author: Quratulan AHMED, E-mail: quratulanahmed_ku@yahoo.com

diverse marine environments worldwide (Read & Fauchald, 2021), but reveal higher species variety in warm waters (Fauchald, 1992).

They live in both hard and soft substrates such as reefs, rocks, or sand (Rouse & Pleijel, 2001), but a larger variety of species can originate in the latter, where they live in the rock clefts and other biogenic edifices (Fauchald, 1992), primarily as free-living animals and only sporadically in undying tubes (Carrera-Parra, 2009).

Eunicids have well-developed and complicated jaw apparatus and are primarily carnivores predated on different invertebrates, or omnivores (Jumars et al., 2015); scavenging and herbivorous and other specialized feeding behaviours are also documented (Rouse & Pleijel, 2001).

According to Hartmann-Schröder & Zibrowius (1998), certain species have been described as correlating with other stalkless invertebrates, primarily soft corals, and sponges, while others are experts at boring seagrass fronds (Gambi et al., 2003). Eunicids operate as relating to ecology destructors of coral blocks and play a significant part in the bioerosion processes; they are recognized for drilling the calcareous skeleton of hard corals using their intricate and incredibly hard jaw apparatus (Hutchings, 1986). This family differs from closely related groups in the order Eunicida due to the existence of five prostomial appendages (three antennae and two lateral palps) without annuli at the base and asymmetric maxillae (right maxilla III is lacking) (Zanol et al., 2021).

The specific characteristics of the maxillae, prostomial appendages, peristomial cirri, branchiae, and forms of chaetae can be used to classify these 11 valid taxa. The only genus with three prostomial appendages is *Lysidice* (Lamarck, 1818), whereas all other genera have five appendages. Recent taxonomic investigations have subdivided the most representative and speciose taxa in the family, *Marphysa quatrefages*, 1866, and *Eunice* Cuvier, 1817, based on specific morphological traits and genetic links (Zanolet et al., 2010; 2014; Molina-Acevedo & Carrera-Parra, 2017; Molina-Acevedo, 2018).

Family Eunicidae is widely distributed in the Indian Ocean. Previous reports of eunicid worms from the Indian and Arabian seas were made by Fauvel (1953), Day (1967), Misra & Chakraborty (1983), Wehe & Fiege (2002), Selim (2009), Al-Omari (2011), Sivaleela & Venkataraman (2012), Veeramuthu et al. (2012), Bonyadi-Naeini et al. (2018), Al-Kandari et al. (2019), Sekar et al. (2019), Sivadas & Carvalho (2020). Studies on Eunicid polychaetas from Pakistan have only been conducted by Aziz (1938), Mustaqim (2000), and Mushtaq & Mustaqim (2006), even though the ecology, and taxonomy. Ali et al. (2023) reported the distribution of polychaetae worms from several stations of the Makran coast, there was little information available on the polychaeta fauna of the Makran coast. So, before our study only 12 species of Eunicidae belonging to 5 genera (*Leodice*, *Eunice*, *Marphysa*, *lysidice*, and *Palola*) were known to occur in Pakistan (Kazmi, 2022).

Hence, we have found two new records of the family Eunicidae species from the Makran coast. In this work, we assessed the specific parapodia, chaetae, branchia, and maxillae morphological and taxonomic characteristics of the recently identified species. The current article makes yet another addition to the expansion of Eunicidae species.

Materials and Methods

Worms were collected during low tide from the intertidal zone of 2 stations along the Makran coast i.e. Shamal Bandar, Pasni ($25^{\circ}14'11''\text{N}$, $63^{\circ}04'38''\text{E}$) on dated 31 January 2022 (-0.013, 3:35pm) and Taak Beach, Ormara ($25^{\circ}14'46''\text{N}$, $64^{\circ}28'35''\text{E}$) dated 2 February 2022 (-0.01, 5:10 pm). Water temperature ($^{\circ}\text{C}$), salinity ($\%$), and pH were measured simultaneously. The collected specimens were preserved in 5% formaldehyde and then cleaned, organized, and kept in 70% alcohol for further analysis. Photographs and measurements of the specimens were taken. Samples were dissected and studied under the stereo-zoom microscope (Wild 181300, Switzerland) at 10x50 magnification for identification. Parapodia temporary mounts were made, and they were examined using an upright microscope. With the use of several drawing tube microscopes, the desired parts were shown (Nikon LABOPHOT-2) at 10x4, and 10x10 magnifications. Using the available literature, the specimens were recognized up to the species level (Fauvel, 1953; Day, 1967; Miura, 1986; Martin, 1987; Fauchald 1992). Study area map developed by Mr. Abrar Ali, Marine Reference Collection and Resource Centre, University of Karachi (Figure 1). Specimens *Eunice indica* (MRC&RC-UOK-POL-EUN-05) and *Lysidice ninetta* (MRC&RC-UOK-POL-EUN-27) were deposited in repository museum of Marine Reference Collection and Resource Centre University of Karachi.

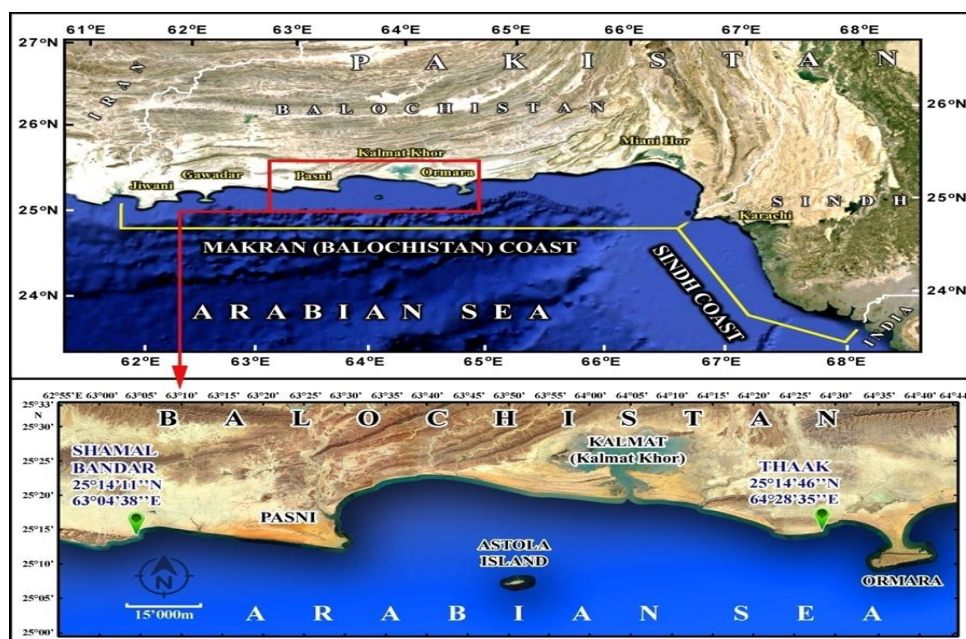


Fig. 1. Map showing the collection sites Shamal Bandar, Pasni and Taak Beach, Ormara.

Results

The physicochemical parameters water temperature (25°C), salinity (37‰), and pH (8.2) were recorded from Shamal Bandar, Pasni, dated 31 January 2022 and temperature (23°C), salinity (38‰), and pH (8.2) were recorded from Taak Beach, Ormara dated 2 February 2022 (-0.01, 5:10 pm).

In this study, we present a comprehensive examination of the morphological and taxonomical characteristics of two Eunicidae polychaetes *Eunice indica* and *Lysidice ninetta* described for the first time in the Makran Coast of Balochistan.

Eunice indica (Kinberg, 1865) (Figure 2 and Figure 3)

Systematic

Order: Eunicida

Family: Eunicidae (Berthold, 1827)

Genus: *Eunice* (Cuvier, 1817)

Species: *Eunice indica* (Kinberg, 1865)

Type locality: Bangka Island (Indonesia)

Habitat: Rocky shores, found under rocks

Material Examined: 2 specimens, Shamal Bandar, Pasni (25°14'11''N, 63°04'38''E), intertidal rocky shore, 31-01, 2022, collectors, Dr. Qadeer Mohammad Ali, and Ms. Hafsa Qazi, catalog no: MRC&RC-UOK-POL-EUN-05.

Description: The length of preserved specimens was 11.7-12.3 cm, with 76-83 chaetigers (Figure 2A), fresh color of the specimens was reddish brown, the prostomium shorten and alienated into two lobes and smaller than the peristomium, about as broad as peristomium. The peristomium is reddish brown. Prostomium faintly jagged anteriorly, with 2 eyes and 5 small occipital antennae. Prostomial antennae and peristomal tentacles are extended, flat, or unevenly furrowed. Middle three antennae expand to setigers 7-8 and external pair to setiger 1 (Figure 3A). Mandibles calcified on the frontal rim. Maxillary formula: Mx. I = 1 + 1; Mx. II = (9-1) + (8-11); Mx. III = (8-11) + 0; Mx. IV = (7-10) + 13 (Figure 3B-C). The first branchia occurs for eternity at chaetiger. The first branchia particularly filament; all other branchia pectinates; rise to a maximum of 10 to 15 filaments and originate only on the frontal third of the body (Figure 3D-E). The aciculum is almost straight yellow and blunt. Acicular chaetae yellow, numerous (4-5), boldly tridentate, and occurs as a transverse series parapodium. Each pectinate seta has five to six inner teeth and lateral asymmetrical extensions. Compound falcigers bidentate with long pointed guard striated one margin (Figure 3F-G). The pygidium has two long dorsal and two short ventral anal cirri. Sexes unknown. Distribution: Japan, New Caledonia, Gambier Islands, Indonesia, India, Indian Ocean, Persian Gulf and Red Sea.

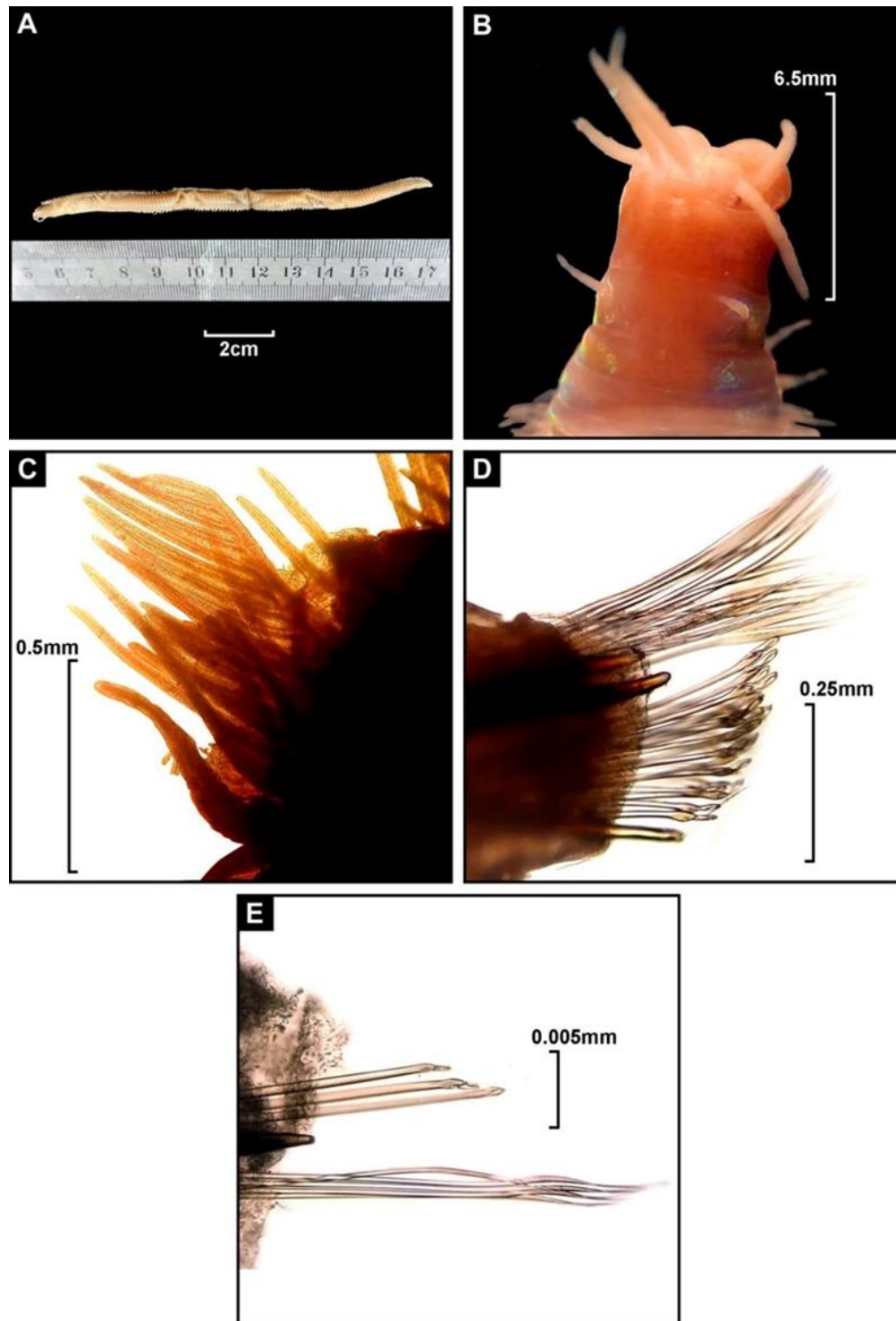


Figure 2. A: *Eunice indica*, B: Anterior end, dorsal view, C- D: Parapodia, E: Compound falciger (Size, 832x741 198 KB 300dpi 24 bit).

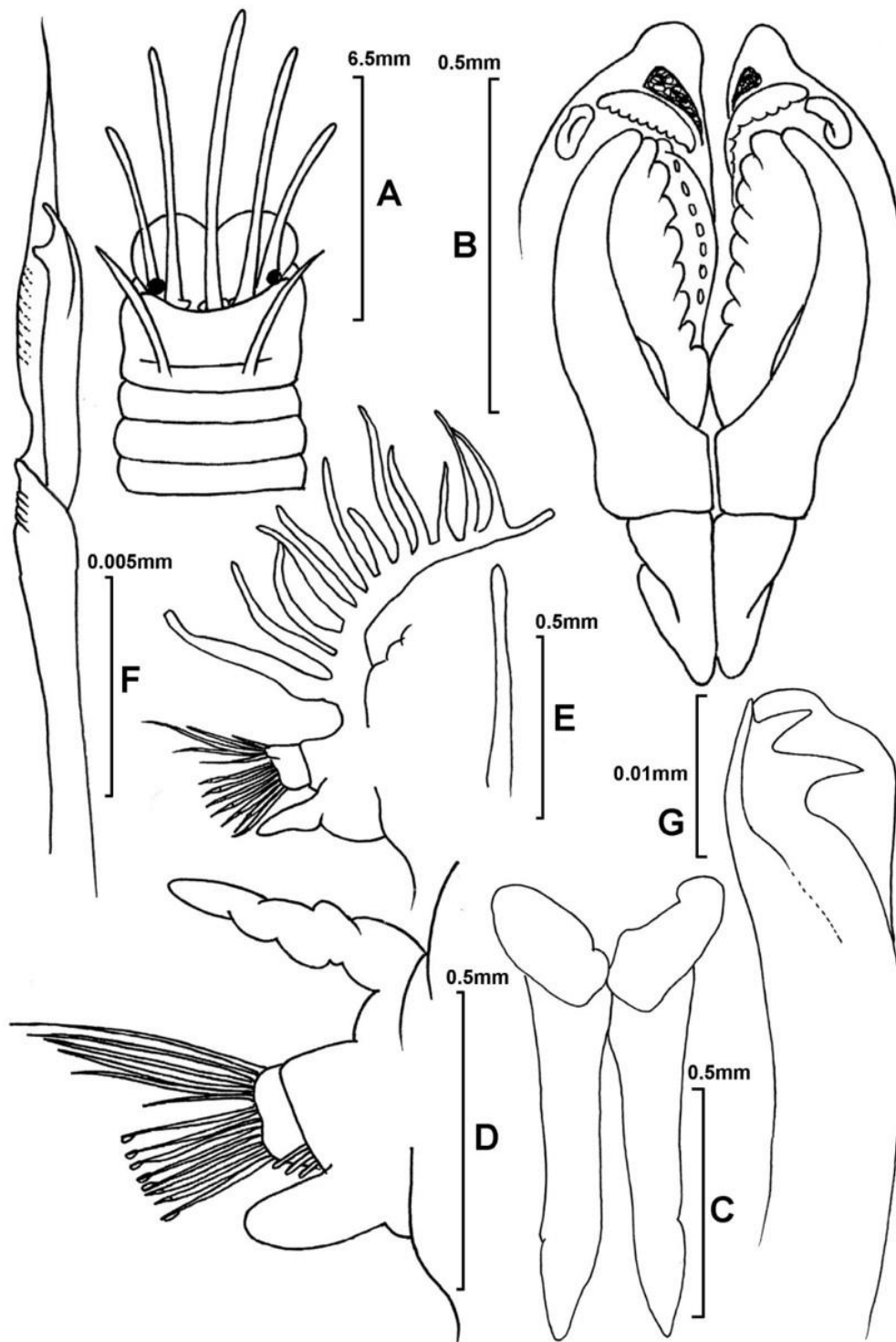


Figure 3. *Eunice indica*, A: Anterior end, dorsal view, B: Maxillae, C: Mandibles, D– E: Parapodia, F: Compound falciger, G: subacicular hook.

Lysidice cf. ninetta* Audouin & H Milne Edwards, 1833 (Figure 4 and Figure 5)**Systematic******Order:*** Eunicida***Family:*** Eunicidae (Berthold, 1827)***Genus:*** *Lysidice* (Lamarck, 1818)***Species:*** *Lysidice cf. ninetta* Audouin & H Milne Edwards, 1833***Type locality:*** France***Habitat:*** Rocky shores, found under rocks***Distribution:*** Red Sea, Indo-West Pacific, North Atlantic, North Carolina, Mediterranean Sea, Angola, India.***Material examined:*** 2 specimens, Taak Beach, Ormara (25°14'46''N, 64°28'35''E), intertidal rocky shore, 2-02-2022, collectors, Dr. Quratulan Ahmed, Ms. Shumaila Mubarak and Mr. Kashif Jameel, catalogue no: MRC&RC-UOK-POL-EUN-27.***Description:*** Length of preserved specimens 3.5-3.8 cm, with 84-88 chaetigers, generally more or less completely colourless or light brown in preservation, with still traces of white spots and white bar on setiger 2 and 5 (Figure 4A). The frontal edge of the prostomium bilobed. Three occipital antennae, sub-equal in length and the same length as the prostomium. Eyes large, black, and typically elliptical (Figure 5A). Mandibles are weighty and scratch-like, H-shaped with two black horny plates on their outside. The maxillary carriers are long and relatively narrow. Maxillary formula: Mx. I = 1 + 1; Mx. II = 4 + 4; Mx. III = 4 + 0; Mx. IV = 4 + 4; Mx. V = 1+1 or are chitinised patches (Figure 5B-C). Parapodia uniramous and lack branchia. Dorsal cirri are long and cylindrical in the first few parapodia or short and conical in the posterior parapodia. The ventral cirri are also long in anterior parapodia and short with a proximal pad in posterior ones. The acicula is dark with blunt tips (Figure 5D). Dark subacicular hooks are bidentate and hooded from chaetiger 22 onwards. The compound setae are in subacicular positions and are bidentate and hooded (Figure 5E). Each pectinate chaetae has nearly symmetrical lateral extensions and more than ten inner spines. The pygidium has two extended dorsal and two small ventral anal cirri.

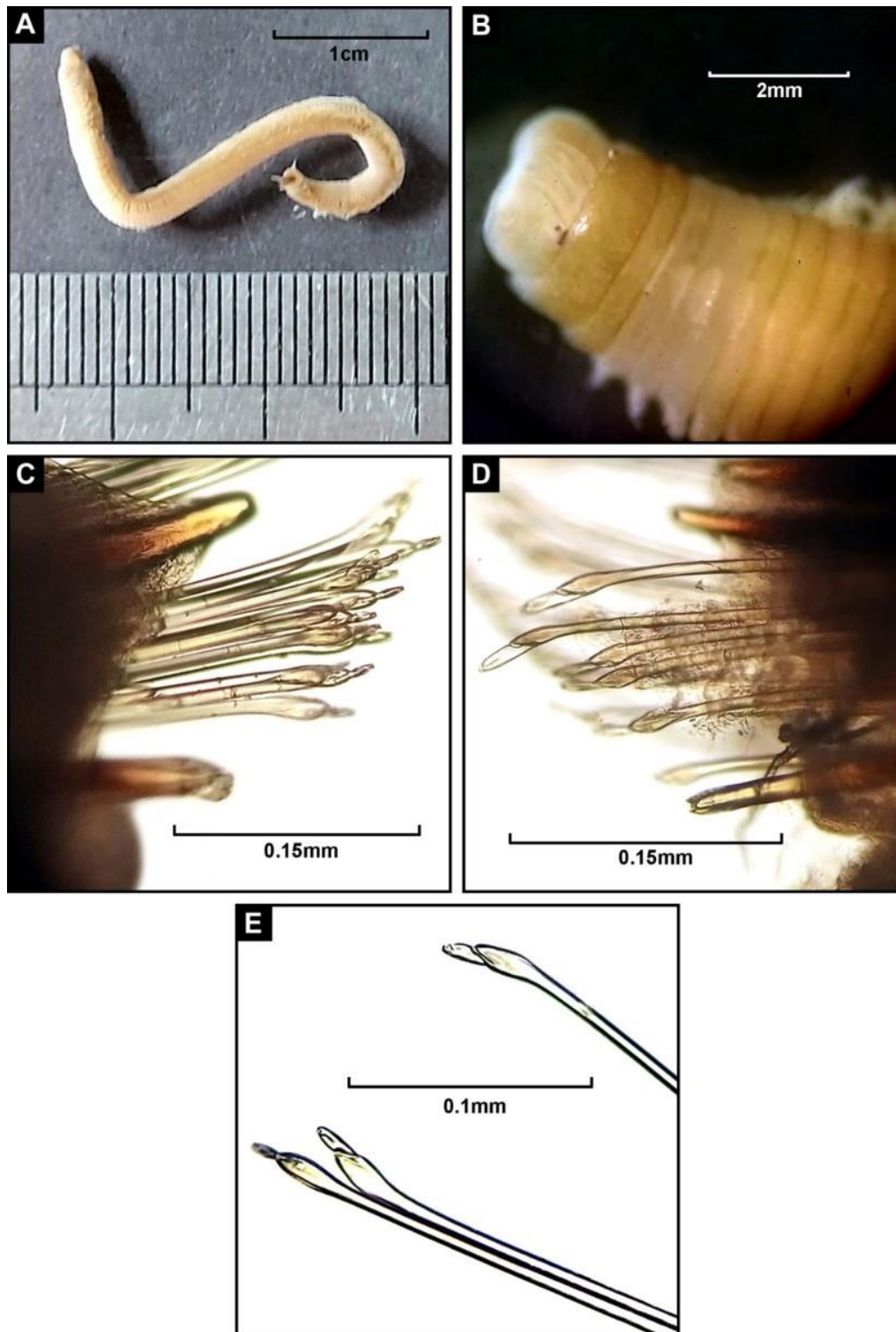


Figure 4. A: *Lysidice cf. ninetta*, B: Anterior end, dorsal view, C-D: Parapodia, E: Compound falciger.

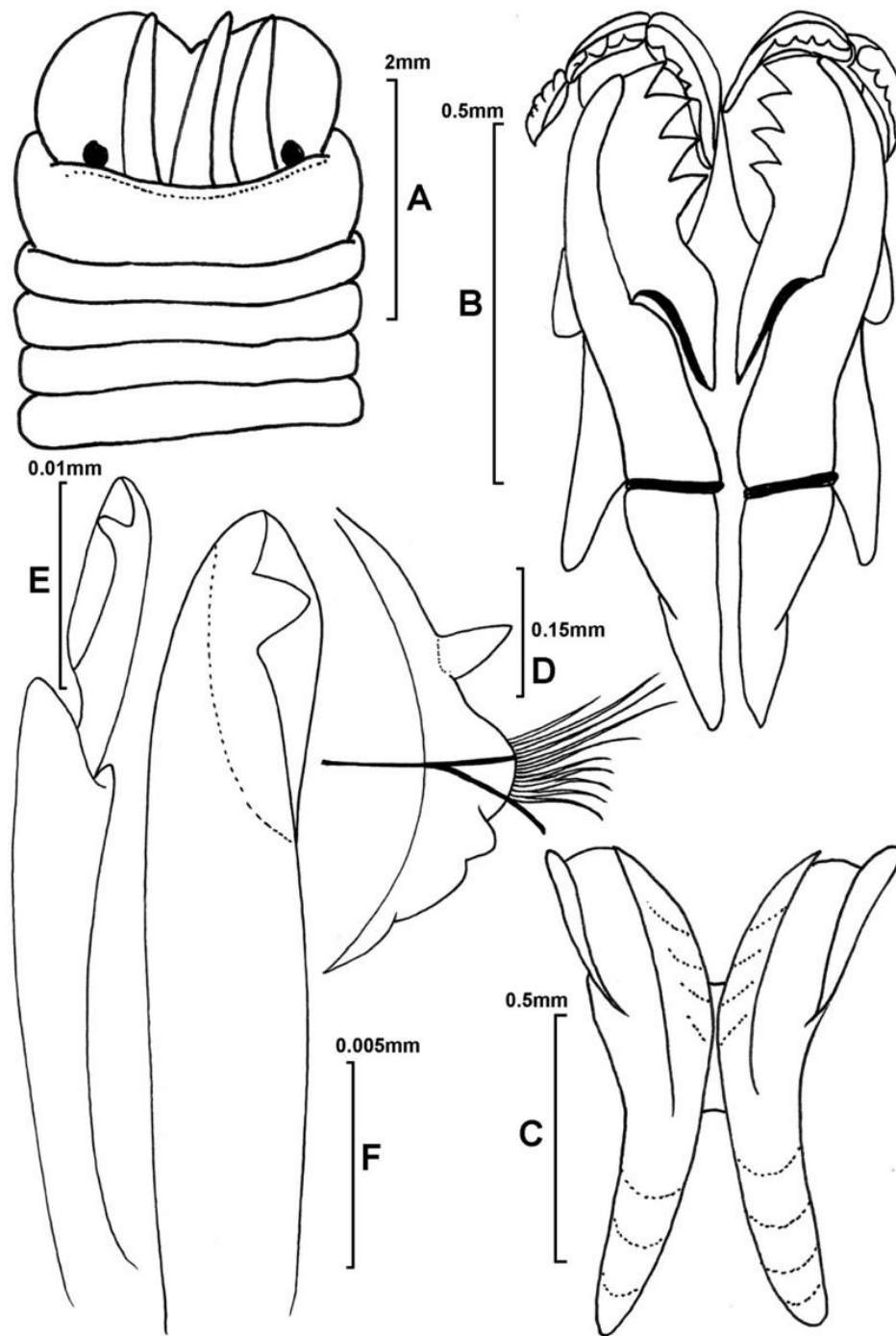


Figure 5. *Lysidice cf. ninetta*, A: Anterior end, dorsal view, B: Maxillae, C: Mandibles, D: Parapodia, E: Compound falciger, F: subacicular hook.

Discussion

Eunicida constituent is one of the most prominent, morphologically distinct polychaetes clades (Struck et al., 2006; Zanol et al., 2007). The present study indicated the first records of eunicid

polychaetes (*Eunice indica* and *Lysidice ninetta*) and their taxonomic accounts, from two rocky shores of Makran coast, Pakistan, which are particularly recorded from the Indian Ocean and Arabian Sea.

According to Fauchald, *Eunice indica* has been widely reported from the Indian Ocean and western Pacific Ocean; several similar species have been reported from this area. From Pakistan only two species of genus *Eunice* were reported e.g. *Eunice australis* and *Eunice manorae* (Aziz, 1938). The distribution of *E. indica* proper must be considered unsettled and the type locality of *E. indica* is the Bangka Island (Indonesia). The studied specimens fit well with the descriptions for *E. indica* Fauchald, (1992) description based on the holotype by Kinberg (1865), about prostomial lobes that are frontally rounded, and dorsally flattened; the shape of the antennae which are long, smooth, or irregularly crumpled (Day, 1967; Miura, 1986); other characters such as the occurrence of branchia from setiger 3, increasing to maximum of 10 filaments (Fauvel, 1953; Day, 1967). Similar to *E. tentaculata* and *E. vittata*, *E. indica* possesses several subacicular hooks in most setigers. However, *E. tentaculata* differs by the first branchia on six setiger and *Eunice indica* and *E. vittata* both have the first branchia on three setiger (Fauchald, 1992). *Eunice indica* can be distinguished from *E. vittata* by the guards on the composite falciger. *E. indica* has the acerous guards on the compound falcigers while *E. vittata* has distantly dulled guards, and concerning aciculae and subacicular hooks, aciculum is almost straight yellow and blunt, acicular chaetae yellow, boldly tridentate and occurs as a transverse series parapodium and compound falcigers bidentate with long pointed guard, agreed with earlier descriptions of (Fauvel, 1953; Day, 1967; Miura, 1986; Fauchald, 1992; Fernando & Rajasekaran, 2007; Veeramuthu et al., 2012). The holotype of *E. indica* lacks jaws but Day, (1967) gave a detailed analysis of the jaw of the specimens from Cape, Mocambique, and Madagascar which are similar to our analyzed specimens. The dorsal cirri of *E. indica* are quite small compared with the other species of the genus and occasionally creased.

From Pakistan, only two species of genus *Lysidice* were reported e.g., *Lysidice collaris* (Aziz, 1938; Mustaqim, 2000) and *Lysidice natalensis* (Mustaqim, 2000). *Lysidice cf. ninetta* is a polychaete linked with various vegetated habitats (Martin, 1987) and widely distributed in Atlantic Ocean, Indo-Pacific, and the Mediterranean Sea although there aren't many features that may be used to differentiate it from other species, therefore different specimens may come from various places (Salazar-Vallejo & Carrera-Parra, 1997). *Lysidice cf. ninetta* was originally described by Audouin and Milne Edwards (1833) and the type locality of *Lysidice cf. ninetta* is France. Their description is brief, and non-informative generally based on basic morphology. The morphological accounts of *L. ninetta* by Gath (1984) incorporated some characteristics of *Lysidice collaris*, but Fauchald (1970) contemplates it as synonymous with *L. ninetta*. *Lysidice ninetta* is a warm temperate and temperate water polychaete (George & Hartmann-Schröder 1985; Cantone 1993) and its congener. *L. collaris* a tropical species (Ben-Eliahu 1972). In the Mediterranean and South Africa, these two species of *Lysidice* are clearly distinguished by both morphological (Day, 1967; Martin, 1987) and genetic outcomes based on both nuclear (ITS1) and mitochondrial (COI) data (Iannotta et al., 2007; Talia, 2001).

The studied specimens agree well with Day (1967) from South Africa and Miura (1977) from Japan's earlier account of *L. ninetta* regarding the three occipital antennae which are sub-equal in length and shorter than the prostomium and follow the maxillary formula described by (Day, 1967; Miura, 1977). The shape of the eyes is a distinguishing characteristic which is large, black, and characteristically oval (Day, 1967; Şahin & Çınar, 2009). The parapodia lack branchia, acicula is dark with blunt tips. Higher setae are limbate capillaries and comb setae and lower setae are compound falcigerous and have bidentate blades found like the descriptions of (Day, 1967; Miura, 1977; Gathof, 1984; Martin, 1987; Veeramuthu et al., 2012; Sekar et al., 2019).

Coloration variation in *L. ninetta* was described by (Gambi et al., 2003; Iannotta et al., 2009; Şahin & Çınar, 2009). Two morphotypes (Dark morph and light morph) of *L. ninetta* were described (Iannotta et al., 2009). The prostomium and first anterior segments of the dark morph were characterized by a dark brownish coloration with fine white spots whereas in the light morph, the prostomium and first segments show greatly lightening coloration and greater pale spots. Our specimens of *Lysidice cf. ninetta* are much like the light morph of (Iannotta et al., 2009) with light brown colour and traces of white spots.

These findings emphasize the need for further investigations and highlight the potential for discovering additional species within the region. Ultimately, this study enhances our understanding of the biodiversity and ecological dynamics of the Northern Arabian Sea, emphasizing the importance of preserving and conserving this unique marine ecosystem.

In conclusion, primary objective of this research endeavor was to document new records of *Eunicidae polychaetae* inhabiting previously unexplored areas along the Makran coast. As a result of this comprehensive study, a valuable compilation of data has been generated regarding the distribution and composition of polychaeta fauna within the Makran coast region, marking a significant milestone. This pioneering document not only represents the first-time disclosure of eunicid polychaetae fauna distribution on the Makran coast but also stands as a crucial resource poised to benefit forthcoming biologists and researchers in their investigations and analyses of this particular ecosystem. In essence, this study not only broadens our understanding of the hidden diversity along the Makran coast but also bequeaths a vital tool to the scientific community. As a pioneering endeavor, it paves the way for future investigations and endeavors, providing a solid foundation upon which researchers can build to unravel the complexities of polychaeta fauna and their role in the intricate web of marine life.

Acknowledgements

The authors would like to express their sincere appreciation to Prof. Dr. Güley Kurt for her invaluable assistance and guidance in the identification of specimens and diagnosis of *Eunice indica* and *Lysidice cf. ninetta*. The guidance and assistance in scientific illustrations and photography by Mr Abrar Ali, are noteworthy. The research facilities in the laboratory and field trips from the Marine Reference Collection and Resource Centre, university of Karachi acknowledged, the services of Mr. Kashif Jameel, field assistant is appreciable, who assisted in the whole field trips and sample collection.

Conflict of Interest

The authors declare that they have no known competing financial interests or personal relationships that could have appeared to influence the work reported in this paper.

Author Contributions

All authors performed all the experiments and drafted the main manuscript text.

References

- Ali, Q. M., Ahmed, Q., Kurt, G., Bat, L., Mubarak, S., Qazi, H., Baloch, A., Shaikh, I., Baloch, A., Aziz, N., Ahmed, S., Ali, A., Ahmed, I., Ghalib, A. (2023). First report on distribution of Polychaetes (Annelida: Polychaeta) along the Makran coast of Pakistan, Northern Arabian Sea. *Journal of Materials and Environmental Science*, 14 (3), 277- 292.
- Al-Kandari, M., Sattari, Z., Hussain, S., Radashevsky, V. I., Zhadan, A. (2019). Checklist of intertidal polychaetes (Annelida) of Kuwait, Northern part of the Arabian Gulf. *Regional Studies in Marine Science*, vol. 32, pp. 100872, <https://doi.org/10.1016/j.rsma.2019.100872>
- Al-Omari, N. H. A. (2011). A guide to polychaetes (Annelida) in Qatar marine sediments. Qatar University Environmental Studies Center, 98p.
- Aziz, N. D. (1938). Fauna of Karachi, 2 Polychaetes. *Memoirs of Department of Zoology, Punjab University, Lahore*, 19-52.
- Ben-Eliahu, M. N. (1972). *Littoral polychaeta* from Cyprus. *Tethys*, 4(1), 85-94.
- Bonyadi-Naeini, A., Rastegar-Pouyani, N., Rastegar-Pouyani, E., Glasby, C. J., Rahimian, H. (2018). Intertidal polychaetes from Abu Musa Island, Persian Gulf, with a new species from the *Perinereiscultrifera* species complex (Annelida: Nereididae). *Journal of the Marine Biological Association of the United Kingdom*, 98 (8), 1965-1976. <https://doi.org/10.1017/S0025315417001564>.
- Cantone, G. (1993). Censimento dei policheti dei mari italiani: Eunicidae Berthold, 1827. *Atti della Società toscana di scienze naturali residente in Pisa. Memorie. Serie B*.
- Carrera Parra, L. (2009). F. Eunicidae Berthold, 1827. *Poliquetos (Annelida: polychaeta) de México y América TropicalI*, 167-181.
- Day, J. H. (1967). A monograph on the polychaeta of southern Africa. Pt. 1.
- Fauchald, K. (1992). *A review of the genus Eunice (Polychaeta: Eunicidae) based upon type material*.
- Fauvel, P. (1953). *Annelida Polychaeta. The fauna of India, including Pakistan, Ceylon, Burma, and Malaya*, pp. 1-507.
- Fernando, O. J., & Rajasekaran, R. (2007). Benthic Polychaetes of Tamil Nadu coast. In: *Conservation and Valuation of Marine Biodiversity*, pp. 67.
- Gambi, M. C., van Tussenbroek, B. I., Brearley, A. (2003). Mesofaunal borers in seagrasses: world-wide occurrence and a new record of boring polychaetes in the Mexican Caribbean. *Aquatic Botany*, 76(1), 65-77. [https://doi.org/10.1016/S0304-3770\(03\)00031-7](https://doi.org/10.1016/S0304-3770(03)00031-7).

- Gathof, J. M. (1984). Family Eunicidae Savigny, 1818. In: *Atlas of the Polychaetes of the Northern Gulf of Mexico*, Barry Victor and Associates, 1–31.
- George, J. D., (1985). In: *British Amphinomida, Spintherida and+ & Eunicida: Keys and Notes for the Identification of the Species*, Brill Archive.
- Hartmann-Schröder, G., & Zibrowius, H. (1998) *Polychaeta associated with antipatharia (Cnidaria: Anthozoa): description of Polynoidae and Eunicidae*. Mitteilungen aus dem Hamburgischen zoologischen Museum und Institute.
- Hutchings, P. A. (1986). Biological destruction of coral reefs: a review, *Coral Reefs*, 4, 239-252. <https://doi.org/10.1007/BF00298083>.
- Iannotta, M. A., Patti, F. P., Ambrosino, M., Procaccini, G., Gambi, M. C. (2007). Phylogeography of two species of *Lysidice* (Polychaeta, Eunicidae) associated to the seagrass *Posidonia oceanica* in the Mediterranean Sea. *Marine Biology*, 150, 1115-1126. <https://doi.org/10.1007/s00227-006-0405-2>.
- Iannotta, M. A., Gambi, M. C., Patti, F. P. (2009). Molecular evidence of intraspecific variability in *Lysidice ninetta* (Polychaeta: Eunicidae) in the Mediterranean Sea. *Aquatic Biology*, 6, 121-132. <https://doi.org/10.3354/ab00160>.
- Jumars, P. A., Dorgan, K. M., Lindsay S.M. (2015). Diet of worms emended: an update of polychaete feeding guilds. *Annual Review of Marine Science*, 7, 497-520. <https://doi.org/10.1146/annurev-marine-010814-020007>.
- Kazmi, Q. B. (2022). Marine Faunal Diversity of Pakistan Inventory and Taxonomic Resources. *Zoological Society of Pakistan*, pp. 721.
- Martin, D. (1987). Anélidospoliquetos asociados a las concreciones de lagascales de litoral Catalán. *Miscel·lània Zoològica*, 11, 61-75.
- Misra, A., Chakraborty, R. K. (1983). Further records of polychaetes from Gujarat coast. *Records of the Zoological Survey of India*, 81(1-2), 69-75. <https://doi.org/10.26515/rzsi/v81/i1-2/1983/161253>.
- Miura, T. (1977). *Eunicid polychaetous annelids from Japan*. II. La mer, vol. 15, no. 2, pp. 61-81.
- Miura, T. (1986). Japanese polychaetes of the genera Eunice and Euniphysa: Taxonomy and branchial distribution patterns. *Publications of the Seto Marine Biological Laboratory*, 31(3-6), 269-325.
- Molina-Acevedo, I.C. (2018). Morphological revision of the subgroup 1 Fauchald, 1970 of *Marphysa* de Quatrefages, 1865 (Eunicidae: Polychaeta). *Zootaxa*, 4480(1), 1-125. <https://doi.org/10.11646/ZOOTAXA.4480.1.1>.
- Molina-Acevedo, I.C., Carrera-Parra, L.F. (2017). Revision of *Marphysa* de Quatrefages, 1865 and some species of *Nicidion* Kinberg, 1865 with the erection of a new genus (Polychaeta: Eunicidae) from the Grand Caribbean. *Zootaxa*, 4241 (1), 1-62. <https://doi.org/10.11646/zootaxa.4241.1.1>.
- Mushtaq, S., & Mustaqim J. (2006). New records of polychaetous annelid (Order: Eunicida) from the coastal waters of Karachi. In 26th Pakistan Congress Zoology, Zoological Society of Pakistan.

- Mustaquim, J. (2000). Six new records of intertidal polychaetes from Pakistan. *Pakistan Journal of Marine Sciences*, 9, 97-106.
- Read, G. (2021). In: *World Polychaeta Database. Eunicidae Berthold, World Register of Marine Species*. Available online.
- Rouse, G., & Pleijel, F. (2001). *Polychaetes*. Oxford University Press.
- Salazar-Vallejo, S. I., & Carrera-Parra, L. F. (1997). Eunícidos (Polychaeta) del caribe mexicano con claves para las especies del Gran Caribe: Fauchaldius, Lysidice, Marphysa, Nematoneis y Palola. *Revista de Biología Tropical*, 45(4), 1481-1498.
- Sekar, V., Rajasekaran R., Balakrishnan S., & Raguraman R. (2019). Taxonomical keys for morphological identification of coral-associated Polychaetes from Great Nicobar Islands. *Natural Resources Management and Biological Sciences*, 1-33.
- Selim, S.A. (2009). Polychaete fauna of the Northern part of the Suez Canal (Port-Said–Toussoum). *Egyptian Journal Aquatic Research*, 35 (1), 69-88.
- Sivadas, S.K., & Carvalho R. (2020). Marine Annelida of India: taxonomy and status evaluation and an updated checklist. *Journal of Threatened Taxa*, 12(12), 16647-16714. <https://doi.org/10.11609/jott.5357.12.12.16647-16714>.
- Sivaleela, G., & Venkataraman K. (2012). Distribution of Marine Polychaetes of India. *Records of the Zoological Survey of India*, 112(4), 113-126.
- Struck, T.H., Purschke G., & Halanych K.M. (2006). Phylogeny of Eunicida (Annelida) and exploring data congruence using a partition addition bootstrap alteration (PABA) approach. *Systematic Biology*, 55 (1), 1-20. <https://doi.org/10.1080/10635150500354910>.
- Şahin, G. K., & Çınar M. E. (2009). Eunicidae (Polychaeta) species in and around Iskenderun Bay (Levantine Sea, Eastern Mediterranean) with a new alien species for the Mediterranean Sea and a re-description of Lysidice collaris. *Turkish Journal of Zoology*, 33(3), 331-347. <https://doi.org/10.3906/zoo-0806-19>.
- Talia, M. (2001). Filogeografia comparata nell'ecosistema a Posidonia oceanica (L.) Delile: la pianta e gli organismi scavatori. M.Sc. Thesis, University Federico II, Napoli, pp. 119 (in Italian).
- Veeramuthu, S., Ramadoss, R., Subramaniyan, B., Jeyaram, S., Fernando, O.J. (2012). Abundance of the boring polychaetes of Eunicidae (Annelida) in Great Nicobar Islands. *Our Nature*, 10 (1), 76-88.
- Wehe, T., & Fiege, D. (2002). Annotated checklist of the polychaete species of the seas surrounding the Arabian Peninsula: Red Sea, Gulf of Aden, Arabian Sea, Gulf of Oman, Arabian Gulf. *Fauna of Arabia*, 19, 7-238.
- Zanol, J., Fauchald, K., Paiva, P. C. (2007). A phylogenetic analysis of the genus Eunice (Eunicidae, polychaete, Annelida). *Zoological Journal of the Linnean Society*, 150 (2), 413-434. <https://doi.org/10.1111/j.1096-3642.2007.00302.x>.
- Zanol, J., Halanych, K. M., Struck, T. H., & Fauchald, K. (2010). Phylogeny of the bristle worm family Eunicidae (Eunicida, Annelida) and the phylogenetic utility of noncongruent 16S,




COI and 18S in combined analyses. *Molecular Phylogenetics and Evolution*, 55(2), 660-676. <https://doi.org/10.1016/j.ympev.2009.12.024>

Zanol, J., Halanych, K. M., & Fauchald, K. (2014). Reconciling taxonomy and phylogeny in the bristleworm family Eunicidae (polychaete, Annelida). *Zoologica Scripta*, 43(1), 79-100. <https://doi.org/10.1111/zsc.12034>.

Zanol, J., Carrera-Parra, L. F., Steiner, T. M., Amaral, A. C. Z., Wiklund, H., Ravara, A., & Budaeva, N. (2021). The current state of Eunicida (Annelida) systematics and biodiversity. *Diversity*, 13(2), 74. <https://doi.org/10.3390/d13020074>.



The Confirmed Stranding of an Adult Female Risso's Dolphin, *Grampus griseus* (G. Cuvier, 1812), in the northeastern Mediterranean Sea

Deniz Ayas * , Nuray Çiftçi , Yekta Tanış 
Mersin University, Faculty of Fisheries, Mersin, Türkiye.

Abstract

The study aimed to report a confirmed stranding record of an adult female Risso's dolphin (*Grampus griseus*) from the northeastern Mediterranean Sea. This species is classified as "Least Concern" in the Mediterranean by the International Union for Conservation of Nature (IUCN). The individual, which was first seen alive from the Erdemli shores of Mersin Bay on 10 April 2023, was tried to push back into the water after being stranded ashore. After the individual died, the corpse was brought to Mersin University Marine Life Museum for external examination. It was determined that the individual weighed 360 kg and had a length of 330 cm. Many old and new scars were found on the individual's skin. It was understood that the newly formed deep cut marks on the head area were caused by the individual hitting the fishing nets. The study is the confirmed stranding of an adult female Risso's dolphin record in the northeastern Mediterranean Sea.

Keywords:

Grampus griseus, Risso's dolphin, northeastern Mediterranean Sea, Mersin Bay, external examination

Article history:

Received 20 June 2023, Accepted 30 September 2023, Available online 15 December 2023

Introduction

Grampus griseus (Georges Cuvier, 1812) is the only dolphin species belonging to the genus *Grampus* from the Delphinidae family of the class Mammalia. Based on genetic similarity to the species, close relatives of this species have been reported to be pygmy killer whales (*Feresa attenuata*), mellow-headed whales (*Peponocephala electra*), false killer whales (*Pseudorca crassidens*) and pilot whales (*Globicephala spp.*) (Hartman, 2018).

*Corresponding Author: Deniz AYAS, E-mail: ayasdeniz@mersin.edu.tr

Risso's dolphins have blunt, square heads and lack the beak typical of other delphinids. The dorsal fin is long and crescent-shaped, and the other fins are long, pointed, and curved. The front part of the body is solid and tapers towards the tail. Adults range in length from 2.6 to 4 m, with an average body weight of around 400 kg (Jefferson et al., 1993; Stewart et al., 2002; Pawloski et al., 2003).

G. griseus is a cosmopolitan species with a wide distribution from the open tropical waters of the Pacific, Indian, and Atlantic Oceans to the temperate open waters. This pelagic species prefers to live on steep slopes with a 400-1200 m depth, usually on the edges of continental shelves or in seamounts and submarine canyons. Deep-water mesopelagic cephalopods such as octopus and cuttlefish, fish, krill, and crustaceans form their food; therefore, they dive into deep waters for feeding (Leatherwood et al., 1980; Cockcroft et al., 1993; Baird, 2009; Riccialdelli et al., 2012; Jefferson et al., 2013; Jefferson et al., 2015). The feeding of Risso's dolphins from the deep waters of the open seas is essential in transporting nutrients from the depths to the surface waters.

It has been reported that the species migrates seasonally for wintering. It has been reported that populations off the coast of Northern Scotland migrate to the Mediterranean during winter and populations off California to Mexican waters in winter (Culik, 2010). The most important feature distinguishing Risso's dolphins from other Cetaceans is their long migration, and it is emphasized that this may be related to feeding preference (Notarbartolo di Sciara et al., 1993).

Risso's dolphins are a cetacean species that move between open seas and coastal areas, which distinguishes them from other cetacean species, and they have no predators. However, like other Cetacean species, the cause of death of this species in the Mediterranean Sea is entirely due to anthropogenic activities (Pace et al., 2015). Although many factors cause Cetacean deaths, such as habitat loss, mechanical and chemical pollution, genetic drift, noise, and ship collision, fishing is the primary cause of death of the species due to its direct and indirect effects. Bycatch, driftnets, trammel and bottom nets, longlines, trawlers, international commercial whaling, entanglement, and drowning cause direct injuries and deaths of Cetacean species (Pace et al., 2015), while excessive and unconscious hunting, depletion of food sources or its destruction cause indirect effects (Karpouzli & Leaper, 2004).

Because Risso's dolphins have an anatomically wide echolocation range, noise pollution events such as maritime traffic, military activities, seismic surveys, and construction at sea can damage their sophisticated hearing system, causing permanent or temporary hearing loss (NRC, 2005; Southall et al., 2007; Weilgart, 2007; Pace et al., 2015). It has been reported that this leads to behavioral disorders due to the loss of their ability to communicate and find their prey (Richardson et al., 1995).

Deep-sea systems are accumulation areas of pollutants such as metal, organochlorine compounds (O.C.s)- polychlorinated biphenyls (PCBs), dichlorodiphenyltrichloroethane (DDT),

hexachlorobenzene (HCB), and dioxins, polycyclic aromatic hydrocarbons (PAHs) added to the marine ecosystem due to terrestrial discharges (Jakimska et al., 2011; Louvado et al., 2015; Pace et al., 2015; Jepson et al., 2016; Welty et al., 2018). Long-lived predators, especially marine mammals, are vulnerable to the effects of pollutants, many of which are persistent bioaccumulative and Toxic-PBTs that accumulate in the deep sea.

The Mediterranean is under the pressure of pollution because it is an inland sea under the influence of anthropogenic activities in coastal countries. Organobromine compounds (Polybrominated Diphenyl Ethers, PBDEs) used as flame retardants from O.C. compounds have been found at high levels in top predators (NRCC, 1983). PAHs are toxic hydrocarbons that are transported to the deep waters of the Mediterranean as a result of anthropogenic effects. There are concerns regarding the genotoxicity of PAHs for cetaceans (Tanabe & Tatsukawa, 1992; Kot-Wasik et al., 2004). The western Mediterranean and the southwestern Mediterranean Iberian Peninsula have been reported as PCB hotspots, and it has been reported that the decrease in the population of Cetacean species in these areas may be due to the decrease in the reproductive success of the PCB-affected individuals (Jepson et al., 2016). It was reported that mass mortality of marine mammal species in the Mediterranean Sea is influenced by increasing concentrations of metals, PAHs, and OCs (Muir & Howard, 2006; Pace et al., 2015). Another source of pollution in the marine ecosystem is marine litter. This garbage consists of materials such as plastic, metal, glass, rubber, and fabric. While ghost nets cause suffocation and death of sea creatures, death records have been reported in sea creatures due to obstruction in the digestive system due to the ingestion of plastic materials or toxic effects caused by plastic materials (Cheshire et al., 2009).

Commercial and tourist maritime traffic poses a significant threat to cetaceans directly through ship collisions and noise pollution and also indirectly through chemical pollution (Campana et al., 2015). Ship collisions can cause direct injury and mortality of many cetacean species, and the intensity of marine traffic causes stress and behavioral changes (Jahoda et al., 2003; Aguilar Soto et al., 2006; Tyack et al., 2011; Castellote et al., 2012; Papale et al., 2012; La Manna et al., 2013; Pirota et al., 2015; Turan et al., 2023).

Risso's dolphins have an important ecological role in the transportation of nutrients from offshore to coastal areas due to their connections with the high seas. Risso's dolphins are reported to be distributed in the Mediterranean Sea from the Alboran Sea to the Aegean Sea (Luna et al., 2022). In the Turkish Seas, Risso's dolphins were reported to be seen in Fethiye (May 1995), Alanya (August 1998), Gökova (2006), Edremit (February 2007), Saros Gulf-Gallipoli (April 2011), Bodrum (May 2011), off the Mediterranean coast of Turkey (2012) (Okuş et al., 2006; Öztürk et al., 2011; Dede et al., 2013). The stranding records of Risso's dolphins off the Turkish coasts were reported as 2 individuals in the North Aegean between 1997 and 2011 (Öztürk et al., 2011), 2 individuals off Ölüdeniz in the South Aegean between 1999 and 2000 (Öztürk et al., 2007), 1 individual caught in a fishing net in the Mediterranean Sea (Öztürk et al., 2007; 2011 see Dede et

al., 2013), 1 individual in the Marmara Sea (Dede et al., 2013) and 1 individual in İskenderun Bay (Yucel et al., 2022).

In these cases, the exact cause of death of stranded individuals was not specified. A few individuals of Risso's dolphins stranded in the Mediterranean Sea have also been reported to be in good enough condition for necropsy (Luna et al., 2022). This study is a record of an adult female Risso's dolphin confirmed stranded in the northeastern Mediterranean Sea.

Materials and Methods

On April 10, 2023, a 330 cm length 360 kg weight female *Grampus griseus* (G. Cuvier, 1812) individual was stranded on the Erdemli coast of Mersin Bay at the coordinates 36°31'03.3"N, 34°12'26.9"E. The map of the sea area where the stranded individual is presented in Figure 1. External examination was performed, and findings were documented with photographs (Figure 2-6). The stranded individual was moved to the Mersin University Marine Life Museum. After the external examinations, the individual was given the museum catalog number (MEUMC-23-11-001) and registered in the museum. Photographs of *Grampus griseus* individual are shown in Figures 2, 4, 5 and 6. The sexual maturity level of *Grampus griseus* was determined according to the characteristics of the skin stages determined by Hartman et al. (2015).

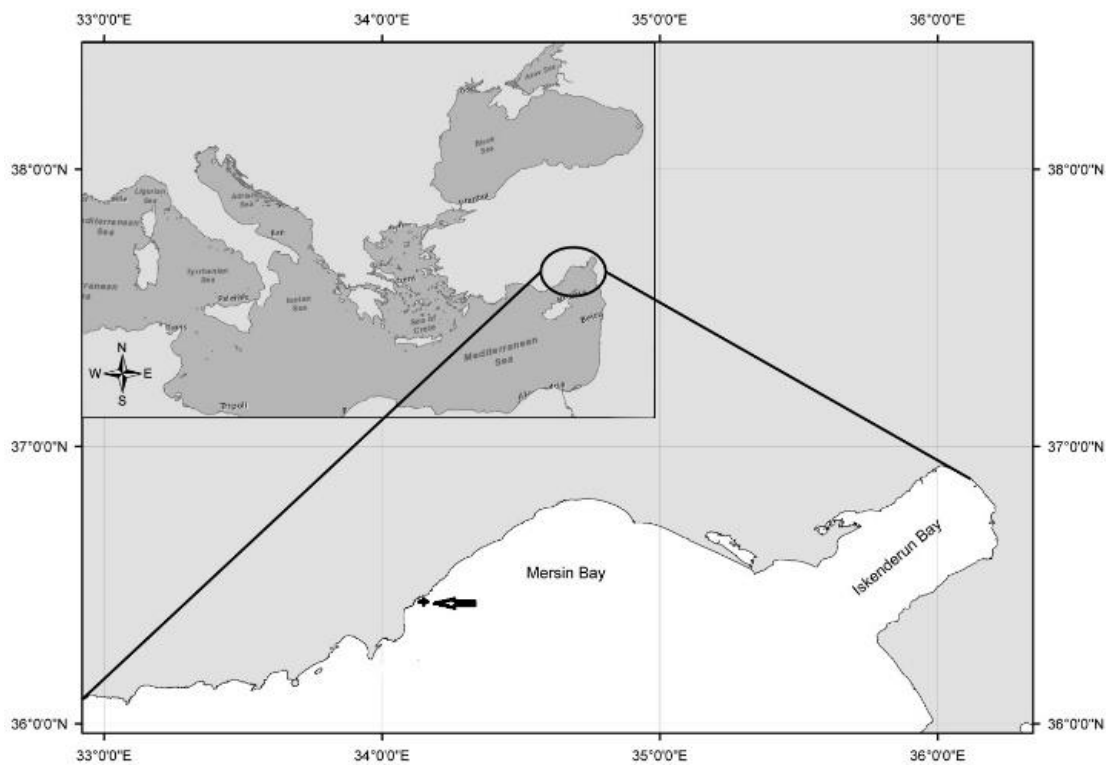


Figure 1. The location of the stranded Risso's dolphin.

Results

On April 10, 2023, the Mersin University Marine Life Museum team was informed that a Risso's dolphin individual was swimming close to the shore on the Erdemli coast of Mersin Bay. The team observed the individual in the sea for 3 hours. After the individual was stranded, it was tried to be pushed back into the water. After the stranded *G. griseus* individual was brought to the museum, it was determined that it was a female individual with a length of 330 cm and a weight of 360 kg. No skin lesions, soft tissue loss on the head, bone fractures or bleeding were found on the body surface. Only newly formed deep cuts were observed on the head of the individual.

Hartman et al. (2015) determined the sexual maturity level of *Grampus griseus* individuals according to the characteristics of the skin stages. The base skin appearance of the examined individual was black. There were many isolated scars on the dorsal fin and saddle area. There were very few isolated scars on the anterior dorsal area. There were overlapping scars on the head. According to the skin stages identified by Hartman, the individual was determined to be an adult.

Discussion

An external examination of the body revealed moderate skin scarification, the basic exterior appearance was brown to black, and numerous scars on the head. According to the characteristics of the skin stages of *Grampus griseus*, it was determined to be an adult individual (Hartman et al., 2016). Newly formed deep incisions were observed on the head of the individual. It was concluded that these marks were caused by the individual getting caught in fishing nets. The individual may have suffered from noise pollution as well as fishing activities and may have died as a result. This is because the echolocation system, which enables these species to find their place, direction, and prey, may be damaged due to high noise. It has been determined that no NAVTEX and NAVAREAIII were announced in the eastern Mediterranean on or before April 10, 2023 (Anonymous, 2023). Therefore, no military shooting training or seismic search was carried out in the region. Therefore, as the cause of death, it was evaluated that the damage to the head area due to entanglement in the nets may have initiated a process that may have caused the individual to strand.



Figure 2. The image of the Risso's dolphin before stranding.



Figure 3. The image of the Risso's dolphin before stranding.



Figure 4. Efforts to push the individual of the Risso dolphin back into the water after being stranded ashore.



Figure 5. The female Risso's dolphin stranded in Mersin Coastline (Erdemli).



Figure 6. Deep incisions in the head of the Risso's dolphin individual.

Risso's dolphins are one of 10 non-endemic but resident cetacean species in the Mediterranean (Pace et al., 2015). Its distribution throughout the Mediterranean basin from west to east has been reported (Öztürk et al., 2011; Luna et al., 2022). These Risso's dolphins, which are distributed on the slopes extending from about 500 m to 1500 m off the continental slopes, are mostly found on the edge slopes rich in plankton and fish, which are nutrient-upwelling areas. Luna et al. (2022) reported that *G. griseus* could find prey both in open sea waters and possibly in benthic regions in the continental slope, which they reached with long deep dives. They thus could feed on a wide variety of cephalopod species (Baumgartner, 1997). This indicates that Risso dolphins have an important ecological role, providing nutrient transport from the open sea to coastal areas.

Risso's dolphins have been reported to be seen in Fethiye (May 1995), Alanya (August 1998), Gökova (2006), Edremit (February 2007), Saros Gulf-Gelibolu (April 2011), Bodrum (May 2011), off the Mediterranean Sea (2012) (Okuş et al., 2006; Öztürk et al., 2011; Dede et al., 2013). The stranding records of Risso's dolphins off the coasts of Turkey include 2 individuals in the North Aegean between 1997-2011 (Öztürk et al., 2011), 2 individuals off Ölüdeniz in the South Aegean between 1999-2000 (Öztürk et al., 2007), 1 individual caught in fishing nets in the Mediterranean Sea (Öztürk et al., 2007; 2011; Dede et al., 2013), 1 individual in the Sea of Marmara (Dede et al., 2013) and 1 individual in the Gulf of İskenderun (Yucel et al., 2022). This study constitutes the confirmed record of *G. griseus* from the Northeastern Mediterranean.

This study contributes to updating the records and death records of Risso's dolphins living in deep seas in the Turkish Seas. Risso's dolphins have critical ecological roles, such as maintaining

the natural balance of the populations of these species by consuming the vertebrate and invertebrate species that make up their food, as well as the interaction between deep and surface waters and the transport of some nutrients in the open sea to coastal areas. Therefore, it is imperative to protect this species to maintain ecological balance.

Acknowledgements

We thank the Coast Guard and local government teams for their support. This study was supported by the Research Fund of Mersin University with Project Numbers 2021-1-AP5-4306 and 2021-2-AP5-4485.

Conflict of Interest

There is no conflict of interest between the authors

Author Contributions

The contributions of the authors to the article should be stated.

References

- Aguilar Soto, N., Johnson, M., Madsen, P.T., Tyack, P.L., Bocconcelli, A., & Fabrizio Borsani, J. (2006). Does intense ship noise disrupt foraging in deep-diving Cuvier's beaked whale (*Ziphius cavirostris*). *Marine Mammal Science*, 22, 690-699. <https://doi.org/10.1111/j.1748-7692.2006.00044.x>.
- Anonymous (2023). Seyir Hidrografi ve Oşinografi Dairesi Başkanlığı-2023 Yılı (shodb.gov.tr)
- Baird, R. (2009). *Risso's dolphin, Grampus griseus*. pp. 975–976. In: Encyclopedia of Marine Mammals 2nd edition, Academic Press.
- Cheshire, A.C., Adler, E., Barbière, J., Cohen, Y., Evans, S., Jarayabhand, S., Jeftic, L., Jung, R-T., Kinsey, S., Kusui, E.T., Lavine, I., Manyara, P., Oosterbaan, L., Pereira, M.A., Sheavly, S., Tkalin, A., Varadarajan, S., Wenneker, B., & Westphalen, G. (2009). UNEP/IOC Guidelines on Survey and Monitoring of Marine Litter. *UNEP Regional Seas Reports and Studies*, 186; IOC Technical Series No. 83.
- Campana, I., Crosti, R., Angeletti, D., Carosso, L., David, L., Di-Meglio, N., Moulins, A., Rosso, M., Tepsich, P., & Arcangeli, A. (2015). Cetacean response to summer maritime traffic in the Western Mediterranean Sea. *Marine Environmental Research*, 109, 1-8. <https://doi.org/10.1016/j.marenvres.2015.05.009>.
- Castellote, M., Clark, C.W., & Lammers, M. (2012). Acoustic and behavioural changes by fin whales (*Balaenoptera physalus*) in response to shipping and airgun noise. *Biological Conservation*, 147, 115-122. <https://doi.org/10.1016/j.biocon.2011.12.021>.
- Cockroft, V.G., Haschick, S.L., & Klages, N.T.W. (1993). The diet of Risso's dolphin, *Grampus griseus* (Cuvier, 1812), from the east coast of South Africa. *Zeitschrift für Säugetierkunde*, 58, 286-293.
- Culik, B. (2010). *Grampus griseus* (On-line). CMS (Convention on Migratory Species). http://www.cms.int/reports/small_cetaceans/data/g_griseus/g_griseus.htm.

- Dede, A., Tonay, A.M., Bayar, H., & Öztürk, A.A., (2013). First stranding record of a Risso's Dolphin (*Grampus griseus*) in the Marmara Sea, Turkey. *Journal of the Black Sea/Mediterranean Environment*, 19(1), 121-126.
- Hartman, K.L. (2018). *Risso's dolphin: Grampus griseus*. pp. 824-827. In: Encyclopedia of Marine Mammals Academic Press.
- Hartman, K.L., Wittich, A., Cai, J.J., Van Der Meulen, F.H. & Azevedo, J.M.N. (2015). Estimating the age of Risso's dolphins (*Grampus griseus*) based on skin appearance. *Journal of Mammalogy*, 97(2), 490-502. <https://doi.org/10.1093/jmammal/gyv193>.
- Jakimska, A., Konieczka, P., Skóra, K., & Namieśnik, J. (2011). Bioaccumulation of metals in tissues of marine animals, Part II: metal concentrations in animal tissues. *Polish Journal of Environmental Studies*, 20(5), 1127-1146.
- Jahoda, M., Lafortuna, C.L., Biassoni, N., Almirante, C., Azzellino, A., Panigada, S., Zanardelli, M., & Notarbartolo Di Sciara, G. (2003). Mediterranean fin whale's (*Balaenoptera physalus*) response to small vessels and biopsy sampling assessed through passive tracking and timing of respiration. *Marine Mammal Science*, 19, 96-110. <https://doi.org/10.1111/j.1748-7692.2003.tb01095.x>.
- Jefferson, T., Leatherwood, S., & Webber, M. (1993). *Marine Mammals of the World*. Rome: United Nations Environment Programme.
- Jefferson T.A., Webber, M.A., & Pitman, R.L. (2015). *Marine Mammals of the World: A Comprehensive Guide to Their Identification*, 2nd ed. Elsevier, San Diego, CA
- Jefferson, T.A., Weir, C.R., Anderson, R.C., Ballance, L.T., Kenney, R.D., & Kiszka, J.J. (2013). Global distribution of Risso's dolphin, *Grampus griseus*: a review and critical evaluation. *Mammal Review*, 44, 5668. <https://doi.org/10.1111/mam.12008>.
- Jepson, P. D., Deaville, R., Barber, J. L., Aguilar, À., Borrell, A., Murphy, S., Barry, J., Brownlow, A., Barnett, J., Berrow, S., Cunningham, A.A., Davison, N.J., ten Doeschate, M., Esteban, R., Ferreira, M., Foote, A.D., Genov, T., Giménez, J., Loveridge, J., Llavona, Á., Martin, V., Maxwell, D.L., Papachlimitzou, A., Penrose, R., Perkins, M.W., Smith, B., de Stephanis, R., Tregenza, N., Verborgh, P., Fernandez, A., & Law, R. J. (2016). PCB pollution continues to impact populations of orcas and other dolphins in European waters. *Scientific Reports*, 6(1), 18573. <https://doi.org/10.1038/srep18573>.
- Karpouzli, E., & Leaper, R. (2004). Opportunistic observations of interactions between sperm whales and deep-water trawlers based on sightings from fisheries observers in the northwest Atlantic. *Aquatic Conservation: Marine and Freshwater Ecosystems*, 14, 95-103. <https://doi.org/10.1002/aqc.595>.
- Kot-Wasik, A., Dabrowska, D., & Namiesnik, J. (2004). Photodegradation and biodegradation study of benzopyrene in different liquid media. *Journal of Photochemistry and Photobiology A: Chemistry*, 168, 109-115. 185. <https://doi.org/10.1016/j.jphotochem.2004.05.023>.
- La Manna, G., Manghi, M., Pavan, G., Lo Mascolo, F., & Sara, G. (2013). Behavioural strategy of common bottlenose dolphins (*Tursiops truncatus*) in response to different kinds of boats in

- the waters of Lampedusa Island (Italy). *Aquatic Conservation: Marine and Freshwater Ecosystems*, 23, 745-757. <https://doi.org/10.1002/aqc.2355>.
- Leatherwood, S., Perrin, W. F., Kirby, V. L., Hubbs, C. L., & Dahlheim, M. (1980). Distribution and movements of Risso's dolphin, *Grampus griseus*, in the eastern North Pacific. *Fishery Bulletin*, 77(4), 951-963.
- Louvado, A., Gomes, N. C. M., Simões, M. M., Almeida, A., Cleary, D. F., & Cunha, A. (2015). Polycyclic aromatic hydrocarbons in deep sea sediments: Microbe-pollutant interactions in a remote environment. *Science of the Total Environment*, 526, 312-328. <https://doi.org/10.1016/j.scitotenv.2015.04.048>.
- Luna, A., Sánchez, P., Chicote, C., & Gazo, M. (2022). Cephalopods in the diet of Risso's dolphin (*Grampus griseus*) from the Mediterranean Sea: A review. *Marine Mammal Science*, 38(2), 725-741. <https://doi.org/10.1111/mms.12869>.
- Muir, D.C., & Howard, P.H. (2006). Are there other persistent organic pollutants? A challenge for environmental chemists. *Environmental Science & Technology*, 40, 7157-7166. <https://doi.org/10.1021/es061677a>.
- NRC (2005). *Marine mammal populations and ocean noise: Determining when noise causes biologically significant effects*. The National Academies Press, Washington, DC.
- NRCC (1983) Polycyclic aromatic hydrocarbons in the aquatic environment: formation, sources, fate and effects on aquatic biota. NRC Associate Committee on Scientific Criteria for Environmental Quality, Publication No. NRCC 18981, Ottawa, Ontario.
- Notarbartolo di Sciara, G., Venturino, M.C., Zanardelli, M., Bearzi, G., Borsani, F. J., & Cavalloni, B. (1993). Cetaceans in the central Mediterranean Sea: Distribution and sighting frequencies. *Italian Journal of Zoology*, 60(1), 131-138. <https://doi.org/10.1080/11250009309355800>.
- Okuş, E., Yükses, A., Yokeş, M. B., Yılmaz, I. N., Aslan-Yılmaz, A., Karhan, S. Ü., Demirel, N., Demir, V., Zeki, S., Taş, S., Sur, H. I., Altiok, H., Müftüoğlu, E., Balkis, N., Aksu, A., Gazioglu, C. (2006) *Marine biological diversity assessment of Gökova specially protected area, Final Report. Istanbul University, Institute of Marine Sciences and Management, Istanbul, Turkey*. Authority for Specially Protected Areas, Ministry of Environment and Forestry of Turkey (in Turkish).
- Öztürk, B., Salman, A., Öztürk A. A., & Tonay A. (2007). Cephalopod Remains in the Diet of Striped Dolphins (*Stenella coeruleoalba*) and Risso's Dolphins (*Grampus griseus*) in the Eastern Mediterranean. *Vie Et Milieu - Life and Environment*, 57(1/2), 53-59.
- Öztürk, A. A., Tonay, A. M., & Dede, A. (2011). Strandings of the beaked whales, Risso's dolphins, and a minke whale on the Turkish coast of the Eastern Mediterranean Sea. *Journal of Black Sea/Mediterranean Environment*, 17(3), 269-274.
- Pace, D. S., Tizzi, R., & Mussi, B. (2015). Cetaceans value and conservation in the Mediterranean Sea. *Journal of Biodiversity & Endangered Species*, S1:S1.004. <https://doi.org/10.4172/2332-2543.S1.004>.

- Papale, E., Azzolin, M., & Giacoma, C. (2012). Vessel traffic affects bottlenose dolphin (*Tursiops truncatus*) behaviour in waters surrounding Lampedusa Island, south Italy. *Journal of the Marine Biological Association of the UK*, 92, 1877-1885. <https://doi.org/10.1017/S002531541100083X>.
- Pawloski, J., Nachtigall, P. Au, W., Philips, J., & Roitblat, H. (2003). Echolocation in Risso's dolphin, *Grampus griseus*. *The Journal of the Acoustical Society of America*, 113(1), 605-616.
- Pirotta, E., Merchant, N.D., Thompson, P.M., Barton, T.R., & Lusseau, D. (2015). Quantifying the effect of boat disturbance on bottlenose dolphin foraging activity. *Biological Conservation*, 181, 82-89. <https://doi.org/10.1016/j.biocon.2014.11.003>.
- Riccialdelli, L., Newsome, S. D., Goodall, R. N. P., Fogel, M. L., & Bastida, R. (2012). Insight into niche separation of Risso's dolphin (*Grampus griseus*) in the Southwestern South Atlantic via $\delta^{13}\text{C}$ and $\delta^{15}\text{N}$ values. *Marine Mammal Science*, 28(4), 503-515. <https://doi.org/10.1111/j.1748-7692.2011.00554.x>.
- Richardson, W.J., Greene, C.R. Jr., Malme, C.I., & Homson, D.H. (1995). *Marine Mammals and Noise*. Academic Press, New York.
- Southall, B. L., Bowles, A. E., Ellison, W. T., Finneran, J. J., Gentry, R. L., Greene, C. R., Jr., Kastak, D., Ketten, D. R., Miller, J. H., Nachtigall, P. E., Richardson, W. J., Thomas, J. A., & Tyack, P. L. (2007). Marine Mammal Noise Exposure Criteria: Initial scientific recommendations, *Aquatic Mammals*, 33, 411-521. <https://doi.org/10.1080/09524622.2008.9753846>.
- Stewart, B., Clapham, P., Powell, J., & Reeves, R. (2002). *National Audobon's Guide to Marine Mammals of the World*. New York: Alfred A. Knopf.
- Tanabe, S., & Tatsukawa, R. (1992). *Chemical modernization and vulnerability of cetaceans: increasing toxic threat of organochlorine contaminants*. In: Persistent Pollutants in Marine Ecosystems, 161-177., Pergamon Press Ltd, Oxford.
- Turan, C., Dođdu, S. A., & Uysal, İ. (2023). Mapping stranded whales in turkish marine waters. *Annales: Series Historia Naturalis*, 33,1, 127-136.
- Tyack, P.L., Zimmer, W.M., Moretti, D., Southall, B.L., Claridge, D.E., Durban, J.W., Clark, C.W., D'Amico, A., DiMarzio, N., Jarvis, S., McCarthy, E., Morrissey, E., Ward, J., & Boyd, IL. (2011). Beaked whales respond to simulated and actual navy sonar. *PLoS One* 6: e17009.
- Yucel, N., Kilic, E., Turan, C., & Demirhan, S.A. (2022). Microplastic occurrence in the gastrointestinal tract of a Risso's dolphin *Grampus griseus* in the northeastern Mediterranean Sea. *Aquatic Sciences and Engineering*, 37(4), 235-239. <https://doi.org/10.26650/ASE20221131876>.
- Weilgart, L. (2007). A brief review on known effects of noise on marine mammals. *International Journal of Comparative Psychology*, 2, 157-168.
- Welty, C.J., Sousa, M.L., Dunnivant, F.M., & Yancey, P.H. (2018). High-density element concentrations in fish from subtidal to hadal zones of the Pacific Ocean. *Heliyon*, 4(10): e00840. <https://doi.org/10.1016/j.heliyon.2018. e00840>.



DNA Damage in Fish Due to Pesticide Pollution

Ayşegül Ergenler* , Funda Turan 

Faculty of Marine Science and Technology, Iskenderun Technical University, 31200 Iskenderun, Hatay, Türkiye.

Abstract

Toxic contaminants, including pesticides, microplastics, and heavy metals, have a significant impact on aquatic life and other aquatic species. These pollutants come from anthropogenic sources such as crop growing, industrial operations, effluent, residential wastewater, and leaching, as well as environmental events like storms, floods, and seismic processes. Pesticides, particularly pesticides, have been shown to have detrimental effects on aquatic ecology, causing decreased growth, restricted larvae and embryo development, and dysfunction in primary organs like the gill, liver, kidney, and gonad. Genotoxicity from pesticide exposure raises safety concerns, as prolonged exposure can lead to oxidative stress, mutagenicity, and cellular apoptosis. Pesticide exposure can lead to elevated levels, even without measurable concentrations in biological matrices. The toxicity of pesticides directly affects aquatic life, leading to high mortality rates or the complete elimination of species that serve as their food source. To maintain the well-being of aquatic organisms, particularly fish, and protect aquatic ecosystems, it is crucial to investigate safe, acceptable, and efficient alternatives to pesticides. In this study, we focus on the hematological, biochemical, and histopathological changes induced by pesticide exposure and highlight strategies for mitigating the adverse impacts of pesticides on fish. Further investigation is needed to determine species suitability for toxicity detection, an essential aspect of monitoring aquatic environments for agricultural pesticides.

Keywords:

Pesticide, aquatic organism, genotoxicity

Article history:

Received 12 May 2023, Accepted 25 August 2023, Available online 15 December 2023

*Corresponding Author: Ayşegül ERGENLER, E-mail: aergenler@gmail.com

Introduction

Pesticides are used globally to control and eliminate pests, including germs, fungi, plants, slugs, vermin, rats, and parasites. These products are classified according to the species they are meant to target and are sold in different formats such as fluids, accumulated pellets, substances, polymeric segments, covered pellet tablets, and encapsulating components. However, with the increasing use of pesticides to increase agricultural production, concerns about environmental pollution and dangerous effects on non-target organisms are also increasing (Wang et al., 2021).

Pesticides may be transmitted from the intended medium to other environmental mediums, such as water, the atmosphere, and soil, via numerous mechanisms of transfer, involving a process known as volatilization, and discharge. The effects of pesticide compounds on aquatic ecosystems have been the subject of various studies due to their ability to infiltrate the aquatic environment in various ways. Some pesticides can cause oxidative stress, which is strongly linked to the growth and development of aquatic species. Pesticide exposure may lead to musculoskeletal deformities, spinal curvature, and abnormal growth during the development of fish embryos (Li et al., 2018; Ergenler & Turan, 2022)

Many environmental variables and pesticides, resulting from an imbalance between cellular oxidative and anti-oxidative stress processes, may induce oxidative stress. Antioxidant enzymes and non-enzymatic antioxidants work by absorbing reactive oxygen species (ROS) and safeguarding cells from damage caused by oxidative stress. Oxidative stress amplifies the inflammatory response and impairs cellular responses to infections and toxic substances, which may lead to detrimental aggravation (Jia et al., 2020; Teng et al., 2022)

Fish are immediately exposed to pesticides and mutagens that are discharged into the environment because of agricultural run-off. Fishes demonstrate greater susceptibility to several pollutants and toxins in comparison to invertebrates (Stanley et al., 2016). Additionally, fish have become valuable biological markers of contamination because they inhabit various trophic stages in aquatic ecosystems and have different degrees of tolerance. The toxicants or pollutants can build up in the bodies of fish via the process of bioaccumulation, which may pose potential dangers to human health. Prior research has shown that exposure to butachlor may cause the development of pericardial edema (PE) and yolk sac edema (YSE) in zebrafish embryos, with the severity of these effects depending on the concentration of butachlor. Zebrafish embryos have been observed to have morphological defects as a result of exposure to chlorpyrifos, pendimethalin, glyphosate, pyriproxyfen, glyphosate, pyraoxystrobin, ziram, and penconazole. Fish biomarkers serve as potential indicators of pollution, facilitating the timely identification of contamination in the aquatic environment (Mazur et al., 2023). Various scientific research on ecological management has focused on using more sensitive tests to identify genotoxicity in diverse samples. Micronucleus assays (MN) and single-cell gel electrophoresis (comet test) are very sensitive, fast, and often used techniques for identifying the mutagenic and clastogenic impacts of xenobiotics in

both prokaryotes and eukaryotes (Turan & Ergenler, 2022a;b; Turan & Ergenler, 2023; Sherif et al., 2023).

Therefore, fish biomarkers may serve as signals of pollution, facilitating the timely identification of pollution in the aquatic environment. Biomarkers are indicators of alterations in biological systems resulting from exposure to harmful substances, offering distinct insights into the well-being of ecosystems and the impact of environmental pollution. Several scientific research on environmental monitoring has focused on the implementation of more sensitive tests to identify genotoxicity in various substances. The micronucleus assays (MN) and single-cell gel electrophoresis, also known as comet assay, are highly sensitive, fast, and often used techniques for identifying the mutagenic and clastogenic impacts of contaminants in both bacterial cells and eukaryotic (Ergenler & Turan, 2022a; Turan & Ergenler, 2023). The objective of this review was to assess the impact of DNA breakage caused by pesticides on aquatic species.

Pesticide-Induced Biochemical Changes/ Oxidative Stress In Fish

The unrestricted use of pesticides in aquatic ecosystems and agriculture presents a substantial danger to human well-being. The presence of insecticides, herbicides, and fungicides in marine and terrestrial environments results in various health problems among numerous animal species. The unforeseen repercussions underscore the need for enhanced oversight and management to mitigate their detrimental impact on the environment and organisms. The use of pesticides in agriculture often results in the dissemination of pollutants into nearby soils, leading to pollution that may infiltrate groundwater and drinking water sources. These compounds pose a significant threat to fish, since they may impede their metabolism and lead to mortality. Ensuring animals get top-notch feed is essential for maximizing their performance and enhancing their general health and well-being. The growing need for animal proteins has resulted in the escalation of livestock farming and the use of commercial feeds. The use of pesticides is considered necessary for achieving high yields of feeds and fodders, however, it might result in detrimental effects on the fish population (Sherif et al., 2023).

Pesticide-Induced Behavioural Changes in Fish

Pesticides have been seen to induce several behavioral changes in different fish species, including reduced activity levels and impaired swimming abilities. These alterations make the fish more vulnerable to predation, hinder their feeding capabilities, and compromise their capacity to retain positions and defend territories (Prashanth et al., 2011). Pesticides have been shown to disrupt the schooling behavior of fish by causing them to exhibit hanging, unpredictable, and irregular movements, as well as disrupted swimming. The disruption of schooling behavior also makes the fish more vulnerable and prone to predation. Due to the presence of pesticides, fish experience stress, and a weakened immune system, making them more prone to illnesses, secondary infections, and pathogens (Nwani et al., 2010; Satyavardhan, 2013). *Catla catla* exposed to methyl parathion caused enhanced opercula movements, sudden jerky movements, loss of balance, changes in body

color, frequent surfacing, and increased mucus production (Ilavazhahan et al., 2010). *Labeo rohita* exposed to cypermethrin caused rapid, unpredictable, and erratic swimming movements, loss of balance, increased sensitivity, and sinking to the bottom of the water (Chanu et al., 2023). Pesticides can alter the migratory behavior of migratory fish, as suggested by Nagaraju et al. (2017). This alteration disrupts their life cycle, specifically affecting the capacity of salmonid fish to transition from freshwater to saltwater. However, this occurrence is prompting further studies to concentrate specific attention on the important time of transition that takes place in estuaries. Research has shown that adult salmon modify their migratory route to avoid pollutants and polluted regions during their migration, leading to a delay in their spawning (Satyavardhan, 2013). *Tor putitora* exposed to cypermethrin caused many observable effects in jumping, such as increased surface activity and increased air swallowing, loss of balance, sudden swimming movements, weakness, immobility, upright postures, and internal bleeding (Ullah et al., 2015). Moreover, the application of sodium cyanide resulted in specific alterations in behavior, including increased excitability, rapid and unpredictable movements, and impaired swimming abilities in *Oreochromis mossambicus*, *Catla catla*, *Cirrhinus mrigala*, *Labeo rohita*, and *Cyprinus carpio* (David et al., 2019).

Genotoxicity

The majority of pesticides are genotoxic, meaning they can cause DNA damage, increase the occurrence of tumors, and have negative effects on the health and reproduction of aquatic species. These effects may ultimately diminish the productivity of aquaculture. In the study conducted by Bhatnagar et al. (2016) on the emergence of nuclear abnormalities in the blood cells of *C. mrigala*, the micronucleus (MN) test was used and it was observed that micronucleus production was associated with chlorpyrifos exposure. The research revealed the presence of nuclear abnormalities such as cracked eggs and large-sized micronuclei, as well as changes in cell shape. These findings provide strong evidence for the effect of chlorpyrifos on the nucleus. Palanikumar et al. (2014) suggested that micronuclei test findings were a correlation between high doses of chlorpyrifos and the increase in the occurrence of abnormalities in *C. chanos*. In the study by Turan & Ergenler (2022) in which they used the comet test to investigate the genotoxic effects of different doses of abamectin on *C. carpio*, a significant increase in DNA strand breaks, which could cause genetic damage, was observed in *C. carpio* exposed to abamectin. Turan & Ergenler (2022) and Ergenler & Turan (2023) conducted studies showing significant increases in the formation of micronuclei and DNA strand breaks in *C. carpio* after exposure to acetamiprid and thiamethoxamine, and evidence was presented for the genotoxic effects of pesticides on fish.

In conclusion, the use of pesticides for diverse objectives might lead to possible risks to water quality and all aquatic life. The present review research indicates that pesticides affect fish species. Bioaccumulation is a mechanism via which pesticides may accumulate in aquatic organisms, particularly fish species. The proliferation of pesticides resulted in the emergence of

several illnesses in fish species, subsequently leading to a diverse array of health issues. To preserve a healthy ecosystem, it is advisable to minimize the use of pesticides.

Acknowledgements

The authors duly thank the Scientific and Technological Research Council of Turkey (TUBITAK/2250 and TUBITAK BİÇABA program for A. ERGENLER).

Conflict of Interest

The authors declare that they have no competing interests.

Author Contributions

All authors' contributions are equal for the preparation of research in the manuscript.

References

- Bhatnagar, A., Yadav, A. S., & Cheema, N. (2016). Genotoxic effects of chlorpyrifos in freshwater fish *Cirrhinus mrigala* using micronucleus assay. *Advances in Biology*, 2016. <http://dx.doi.org/10.1155/2016/9276963>.
- Chanu, K. R., Mangang, Y. A., Debbarma, S., & Pandey, P. K. (2023). Effect of glyphosate-based herbicide roundup on hemato-biochemistry of *Labeo rohita* (Hamilton, 1822) and susceptibility to *Aeromonas hydrophila* infection. *Environmental Science and Pollution Research*, 1-14. <https://doi.org/10.1007/s11356-023-29967-8>.
- David, E., Eleazu, C., Igweibor, N., Ugwu, C., Enwefa, G., & Nwigboji, N. (2019). Comparative study on the nutrients, heavy metals and pesticide composition of some locally produced and marketed rice varieties in Nigeria. *Food Chemistry*, 278, 617-624. <https://doi.org/10.1016/j.foodchem.2018.11.100>.
- Ergenler, A., & Turan, F. (2022). Assessment of the genotoxic effect of thiamethoxam in *Cyprinus carpio* by the micronucleus and Comet assays. *Journal of the Black Sea/Mediterranean Environment*, 28(1), 66-77.
- Ilavazhahan, M., Tamil, S. R., & Jayaraj, S. S. (2010). Determination of LC50 of the bacterial pathogen, pesticide and heavy metal for the fingerling of freshwater fish *Catla catla*, *Global Journal of Environmental Research* 4(2), 76-82.
- Jia, M., E, Z., Zhai, F., & Bing, X. (2020). Rapid multi-residue detection methods for pesticides and veterinary drugs. *Molecules*, 25(16), 3590. <https://doi.org/10.3390/molecules25163590>.
- Li, H., Yu, S., Cao, F., Wang, C., Zheng, M., Li, X., & Qiu, L. (2018). Developmental toxicity and potential mechanisms of pyraoxystrobin to zebrafish (*Danio rerio*). *Ecotoxicology and Environmental Safety*, 151, 1-9. <https://doi.org/10.1016/j.ecoenv.2017.12.061>.
- Liang, Y., Li, J., Lin, Q., Huang, P., Zhang, L., Wu, W., & Ma, Y. (2017). Research progress on signaling pathway-associated oxidative stress in endothelial cells. *Oxidative Medicine and Cellular Longevity*, 7156941 | <https://doi.org/10.1155/2017/7156941>.

- Mazur, I., Baran, P. A., Kasprzak, P. M., Tszedel, M., & Błońska, D. (2023). Development of a Method of Analysing TNT and its Derivatives in the Trichoptera Larvae of the Genus *Hydropsyche angustipennis*, Curtis 1834, Selected as a Bioaccumulation Indicator for the Detection of Aquatic Environment Pollution with Explosive Residues. *Problemy Mechatroniki: uzbrojenie, lotnictwo, inżynieria bezpieczeństwa*, 14 (3) : 77-94. <https://doi.org/10.5604/01.3001.0053.8821>.
- Nagaraju, Y., Triveni, S., Reddy, R. S., & Vidyasagar, B. (2017). Screening of Potassium Releasing Rhizospheric Isolates for Agrochemicals Compatibility. *International Journal of Current Microbiology and Applied Sciences*, 6(11), 372-378. <https://doi.org/10.20546/ijcmas.2017.611.042>
- Nwani, C. D., Ugwu, D. O., Okeke, O. C., Onyishi, G. C., Ekeh, F. N., Atama, C., & Eneje, L. O. (2013). Toxicity of the chlorpyrifos-based pesticide Termifos®: effects on behaviour and biochemical and haematological parameters of African catfish *Clarias gariepinus*. *African Journal of Aquatic Science*, 38(3), 255-262. <https://doi.org/10.2989/16085914.2013.780153>.
- Prashanth, M. S. (2011). Histopathological changes observed in the kidney of freshwater fish, *Cirrhinus mrigala* (Hamilton) exposed to cypermethrin. *Recent Research in Science and Technology*, 3(2), 59-65.
- Prathiksha, J., Narasimhamurthy, R. K., Dsouza, H. S., & Mumbreakar, K. D. (2023). Organophosphate pesticide-induced toxicity through DNA damage and DNA repair mechanisms. *Molecular Biology Reports*, 1-15. <https://doi.org/10.1007/s11033-023-08424-2>.
- Satyavardhan, K. (2013). A comparative toxicity evaluation and behavioral observations of fresh water fishes to Fenvalerate™. *Middle East Journal of Scientific Research*, 13(2), 133-136.
- Sherif, M., Makame, K. R., Östlundh, L., Paulo, M. S., Nemmar, A., Ali, B. R., ... & Adam, B. (2023). Genotoxicity of occupational pesticide exposures among agricultural workers in arab countries: a systematic review and meta-analysis. *Toxics*, 11(8), 663. <https://doi.org/10.3390/toxics11080663>.
- Stanley, J., Preetha, G., Stanley, J., & Preetha, G. (2016). Pesticide toxicity to fishes: exposure, toxicity and risk assessment methodologies. *Pesticide Toxicity to Non-target Organisms: Exposure, Toxicity and Risk Assessment Methodologies*, 411-497.
- Teng, Y., Chen, X., Jin, Y., Yu, Z., & Guo, X. (2022). Influencing factors of and driving strategies for vegetable farmers' green pesticide application behavior. *Frontiers in Public Health*, 10, 907788. <https://doi.org/10.3389/fpubh.2022.907788>.
- Turan, F., & Ergenler, A. (2022). Investigation of the Genotoxic Effect of Acetamiprid in *Cyprinus carpio* Using the Micronucleus Analysis and the Comet Assay. *Turkish Journal of Maritime and Marine Sciences*, 8(2), 80-89. <https://doi.org/10.52998/trjmms.1037906>.
- Turan, F., & Ergenler, A. (2023). The Genotoxic Damage in *Cyprinus carpio* Exposed to Abamectin. *Natural and Engineering Sciences*, 8(2), 119-128. <https://doi.org/10.28978/nesciences.1338147>.

- Turan, F., Karan, S., & Ergenler, A. (2020). Effect of heavy metals on toxicogenetic damage of European eels *Anguilla anguilla*. *Environmental Science and Pollution Research*, 27, 38047-38055. <https://doi.org/10.1007/s11356-020-09749-2>.
- Ullah, S., & Zorriehzakra, M. J. (2015). Ecotoxicology: a review of pesticides induced toxicity in fish. *Advances in Animal and Veterinary Sciences*, 3(1), 40-57.
- Wang, X., Li, X., Wang, Y., Qin, Y., Yan, B., & Martyniuk, C. J. (2021). A comprehensive review of strobilurin fungicide toxicity in aquatic species: emphasis on mode of action from the zebrafish model. *Environmental Pollution*, 275, 116671. <https://doi.org/10.1016/j.envpol.2021.116671>.



Glucose-Sensitive Biosensor Design by Zinc Ferrite ($ZnFe_2O_4$) Nanoparticle-Modified Poly (o-toluidine) Film

Ali Tuncay Ozyilmaz * , Esiye Irem Bayram 

The University of Mustafa Kemal, Science and Arts Faculty, Chemistry Department, 31040 Hatay-Türkiye.

Abstract

Glucose oxidase (GOD) immobilized poly(o-toluidine) (POT) coated Pt electrode was designed for glucose-sensitive biosensor. Since POT film structure affects enzyme activity, parameters of enzyme immobilization and POT synthesis conditions were optimized. Optimal monomer concentration for POT film synthesis was determined as 40 mM and the scanning rate was determined as 50 mV/s. As for the immobilization process results, GOD, glutaraldehyde (GAL) and chitosan (Chi) concentrations were decided as 2 mg/ml 0.10%, and 0.5% for the Pt/POT electrode. Zinc ferrite nanoparticle ($ZnFe_2O_4$ NP) was immobilized together with POT film in the presence of GOD enzyme. It was revealed that $ZnFe_2O_4$ NP increased the current responses and stability of the Pt/POT electrode.

Keywords:

Poly (o-toluidine), glucose oxidase, amperometric biosensor, zinc ferrite nanoparticle, conductive polymer

Article history:

Received 22 June 2023, Accepted 03 September 2023, Available online 15 December 2023

Introduction

Glucose oxidase (GOD)-based enzyme electrodes are commonly used in biosensor design for glucose determination (Uang et al., 2003; Guo et al., 2011; Salimi et al., 2011; Khun et al., 2012; Zhang et al., 2013). An enzyme-containing biosensor is formed as a result of the immobilization of the protein molecule onto the substrate surface. This is necessary for the creation of glucose biosensor. In order to obtain the GOD biosensor, there are various strategies on immobilization

*Corresponding Author: Ali Tuncay OZYILMAZ, E-mail: atuncay@mku.edu.tr

techniques, such as incorporation or entrapment into the polymer structure during electropolymerization synthesis (Eftekhari 2004; Yu et al., 2005; Ozyilmaz et al., 2011), application to the electrode surface with gel substrate (Pauliukaite et al., 2006; Hui et al., 2005; Huang et al. 2011; Haighi et al., 2012 ; Wang et al., 2013), crosslinking with glutaraldehyde (Ghica et al., 2009), by covalent bonding (Shervedani et al., 2007; Abu-Rabeah et al., 2009), or adsorbed/ on solid surface (Jiang et al., 2012; Salimi et al., 2011 ; De Jesus et al., 2013;). Chitosan, known as a natural cationic polymer, attracts the attention of researchers due to its good adhesion, permeability and its film-forming ability. Therefore, chitosan is added to the gel structure for enzyme immobilization to glutaraldehyde or other reagents (Li et al., 2012). However, the structurally low conductivity of chitosan negatively affects the performance of enzyme-based biosensors such as GOD. (Zhang et al 2013). Research is being carried out to solve this problem caused by chitosan by adding components such as nanoparticles and nanocomposites to its structure (Li et al 2012; Chen et al., 2011; Khun et al., 2012; Wang et al., 2013), ionic liquid (Zhang et al 2013) or modifying the interface between chitosan and the substrate surface via conductive polymers (Chen et al., 2011), by Prussian Blue (Zhan et al., 2013), by nanoparticles (Guo et al., 2011; Chen et al., 2011,). Various conductive polymers were utilized to obtain glucose biosensor like polyaniline (PANI) (Ozyilmaz et al., 2023; Ozdemir et al 2010), polypyrrole (Raicopol et al 2013; Ozyilmaz et al., 2011; Ozyilmaz et al., 2018), poly(o-anisidine) (POA) (Ozyilmaz et al., 2017; Savale et. al 2009). Recent studies have determined that dimensionally reduced nanostructured metal oxides have unique advantages in immobilizing enzymes. At the same time, their large surface area shows that they have high sensitivity due to their desired microstructure and contribution to the electron transfer between active sites of enzyme and electrode. ZnO is among the most used nanoparticles for this purpose (Jung and Lim 2013; Wang et al., 2011).

This study discusses the design of glucose biosensor electrodes using poly (o-toluidine) (POT), a conductive polymer. The effect of POT synthesis parameters and zinc ferrite ($ZnFe_2O_4$) nanoparticle concentration on the structure of biosensor was determined by obtaining current response at different glucose concentrations. Also, kinetic parameters and operational stability of enzyme electrode were obtained.

Material and Methods

Aspergillus niger origin GOD (EC 1.1.3.4, ...U/mg), o-toluidine (OT), chitosan (Chi), zinc ferrite nanoparticles ($ZnFe_2O_4$ NP, <100 nm), glucose anhydrous, glutaraldehyde (GAL) were purchased from Sigma. OT was used after distillation, stored in dark. All other reagents were of analytical grade and used without further purification. Electrochemical analyzers, Chi606 was used to synthesis polymer film and measuring current values and Chi660b was used to impedance studies. All electrochemical experiments were performed in a single compartment cell with three electrode configurations. The reference electrode was an Ag/AgCl (3M KCl) electrode and counter electrode was a platinum plate with surface area of 0.25 cm².

Preparation of Enzyme Electrode

Preparation of the enzyme electrode was carried out in three steps. Firstly, POT films were obtained on the Pt surface. Secondly, the obtained Pt/POT was placed in chitosan and GOD containing solution for 3 seconds and this electrode was dried for 2 hours in an open environment. Finally, the Pt/POT/GOD-Chi electrode was kept in glutaraldehyde solution for 10 seconds to ensure cross-linking between GOD amine groups and Chi to prevent the escape of the GOD component. The formation of the Pt/POT-GOD electrode by ZnFe₂O₄ nanoparticle was carried out with adding the nanoparticles to Chi+GOD containing solution and homogenizing it using a sonicator. When not in use, the electrode was stored at 4°C.

Polymer Film Synthesis

Poly(o-toluidine) was synthesized on Pt electrode in neutral medium of 0.20 M sodium oxalate solution (NaOX) and o-toluidine as monomer. The POT films were obtained by optimize the parameters of synthesis as scan rate, segment number and monomer concentration after comprehensive preliminary studies. POT homopolymer films were obtained by applying cyclic voltammetry technique in NaOX + o-toluidine monomer solution, at the potential range of 0.2 to 2.0 V. Structure, conductivity and porosity of polymer films play an important role in response current of enzyme electrodes. So, electro polymerization parameters were determined in detail of scan rate, segment number and monomer concentration.

Biochemical Characterization of Enzyme Electrodes

For all electrodes obtained in the study, current values were obtained depending on glucose concentrations between 0.1 to 3.0 mM at constant potential. The glucose solution was constantly stirred during measurements. The current value gets using glucose free buffer solution was subtracted from that of glucose + buffer solution. Net current value as μA was accepted as current response. Optimal pH values for each electrode were determined by using glucose solution prepared with buffer solutions at different pHs. KM and I_{max} values were calculated from the Lineweaver-Burk Graph obtained from the current values read depending on different glucose concentration at optimum pH value. Reuse stability was investigated by using the electrodes 20 successive times in 5 mM glucose.

Results and Discussion

Optimization of POT Synthesis Parameters

The synthesis parameters of POT films were obtained for scan rate, segment number and monomer concentration by monitoring current response depending on glucose concentration. Monomer concentrations were changed between 0.04% - 0.07% for POT homopolymer. Since the structure of the poly(o-toluidine) film is important for the immobilization of the GOD molecule, in order to obtain a proper POT film, POT films were first synthesized on Pt electrodes at o-toluidine monomer concentrations between 40 and 70 mM. Concentration ranges used for o-toluidine monomer were

decided by preliminary studies. The concentrations of Chi, GOD and GAL and scan rate, segment number were kept constant while GOD electrodes were fabricated. Current responses were obtained at different glucose concentrations using the prepared Pt electrodes. Figure 1, given as a percentage of the maximum current value, shows the measured current values of the Pt/POT electrode depending on different glucose concentrations. In Figure 1, both highest current responses and linearity were obtained for the Pt/POT electrode with the POT film synthesized using 40 mM o-toluidine monomer.

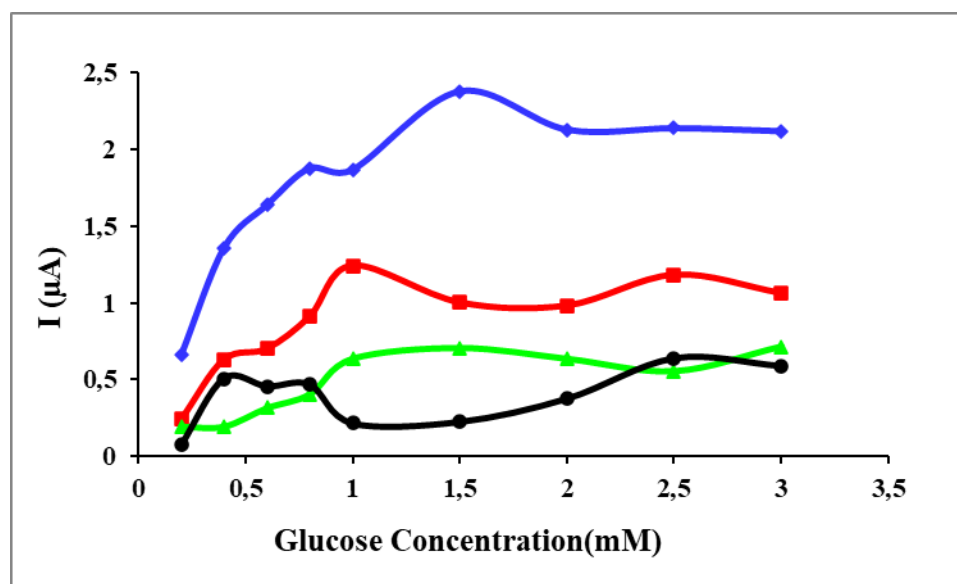


Figure 1. Current responses obtained for glucose concentration of Pt/POT-GOD electrodes fabricated by POT film synthesized for different concentrations of o-toluidine such as 40 mM (♦); 50 mM (■); 60 mM (▲) and 70 mM (●).

As the scan rate increases too much, defects and irregularities in the structure of the synthesized conductive polymer films increase. Therefore, when creating biosensor electrodes, it is important to create a more regular and densely stacked polymer film with appropriate scan rate. Since conductivity of polymer film is affected by scan rate depending on the structure of the conductive polymer, it will also affect the electron transfer rate, which is important for measurements of biosensor electrodes. For this reason, Pt electrodes were coated by POT homopolymer film applying scan rates of 100, 50 and 20 mV/s. POT homopolymer films were synthesized by applying proper scan rate at the potential range of 0.20 to 2.0 V in 0.150 M NaOX solution + the optimum monomer concentration. Therefore, to subject the POT film synthesis to the same duration, 10, 26 and 50 cycles were applied to the scan rates of 20, 50 and 100 mV/s, respectively. Figure 2 shows the current response of the Pt/POT-GOD electrodes obtained with the POT polymer film synthesized with different scan rates. As seen in Figure 2, the current values obtained by applying a scan rate of 50 mV/s for the Pt/POT-GOD electrode were the highest for all glucose concentrations. Additionally, 50 mV/s for POT synthesis was chosen as the optimal

scan rate, as Pt electrodes exhibited a more linear current response for current measurements against different glucose concentrations.

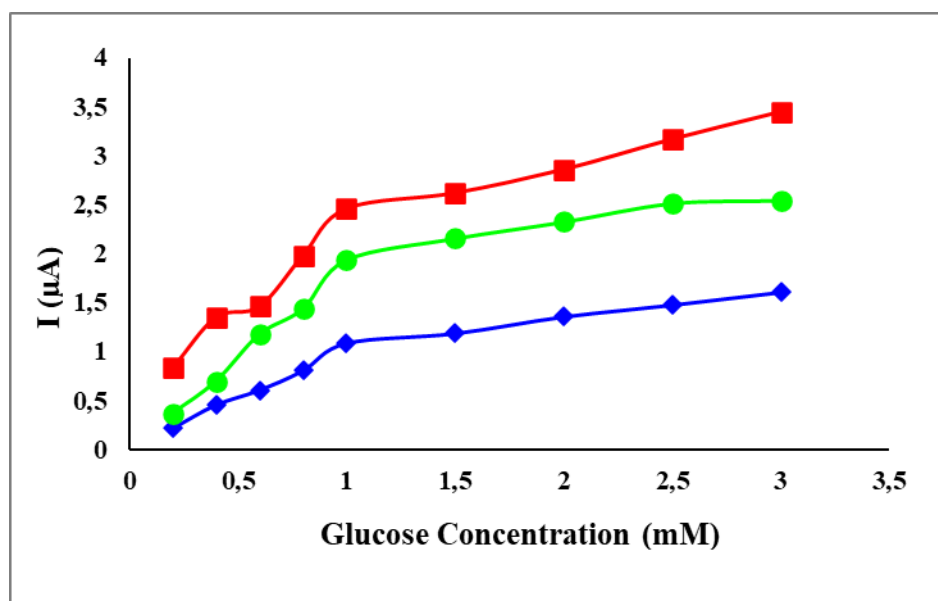


Figure 2. Current responses obtained for glucose concentration of Pt/POT-GOD electrodes fabricated by POT film synthesized for different scan rates; (\blacklozenge : 20 mV/s-2 segment, \blacksquare : 50 mV/s-4 segment, \bullet : 100 mV/s-8 segment).

POT homopolymer films were obtained on the Pt electrode by 2, 4 and 6 segment number. The synthesis of POT film was carried out by proper scan number between 0.20 to 2.0 V in 0.150 M NaOX + o-toluidine by optimal monomer concentration. Figure 3 shows the current responses of Pt/POT-GOD electrodes were obtained applying different segment number. In Figure 3, the current responses of the electrodes fabricated by applying 2 segments were highest at low glucose concentration. On the other hand, it was determined that the current values of Pt/POT-GOD electrodes obtained by POT film synthesized by applying 4 segments increased depending on the increasing glucose concentration. At the same time, it was observed that the linearity of the curve increased.

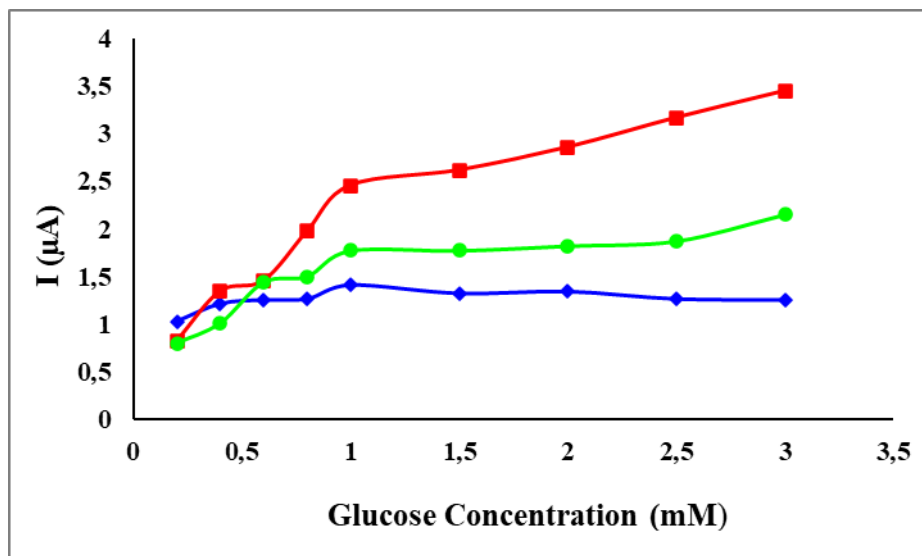


Figure 3. Current responses obtained for glucose concentration of Pt/POT-GOD electrodes fabricated by POT film synthesized for different segments (\blacklozenge : 2 segments, \blacksquare :4 segment, \bullet :6 segment).

The effect of chitosan, glucose oxidase and glutaraldehyde concentrations on enzyme immobilization conditions were studied for enzyme electrode activity and the current values obtained for 3 mM glucose were given in Figure 4 in A, B and C, respectively. The GOD-based Pt/POT electrode fabricated using 0.5% Chi solution gave the highest current response (Figure 4A). In Figure 4 (B) and (C), the highest current values were determined when Pt/POT-GOD electrodes were obtained by adding 0.10% glutaraldehyde and 2 mg/ml glucose oxidase for enzyme-based Pt/POT electrodes. So, parameters of enzyme immobilization were determined as 0.5% chitosan, 2 mg/ml glucose oxidase and 0.10% glutaraldehyde for POT based electrodes in the continue studies. Since GOD enzyme activity is affected by enzyme immobilization conditions, it is expected that hydrogen peroxide amount that will emerge and the current values obtained will also be affected.

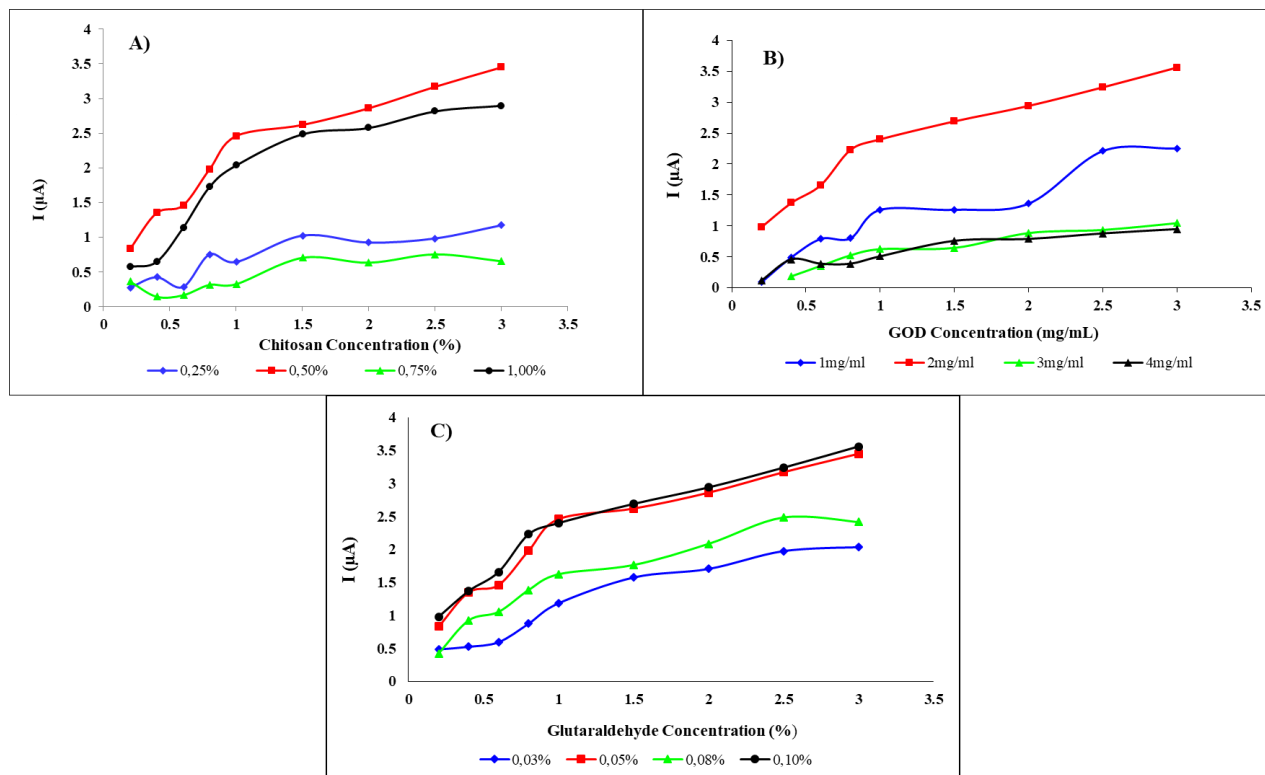


Figure 4. Current responses of POT based electrodes prepared by different immobilization conditions such as concentrations of Chi (A), GOD (B), GAL(C).

The Effect of ZnFe_2O_4 Nanoparticle Modification on Current Response

Biosensor enzyme electrode was developed by $\text{ZnFe}_2\text{O}_4\text{NP}$ using different four concentrations such as 0.1; 0.5 ; 2.0 and 4.0 mg for per ml of chitosan solution. It can be seen in Figure 5 that adding $\text{ZnFe}_2\text{O}_4\text{NP}$ to the polymer film increased the biosensor efficiency. The Pt/POT-GOD electrode obtained when 2 mg $\text{ZnFe}_2\text{O}_4\text{NP}/\text{ml}$ was added to the GOD + Chi solution showed the highest current values. The current values obtained for other amounts of nanoparticle were lower than those of $\text{ZnFe}_2\text{O}_4\text{NP}$ -free Pt/POT electrode, on the other hand, the efficiency of electrode enhanced when 2.0 mg $\text{ZnFe}_2\text{O}_4\text{NP}/\text{ml}$ was used. Nanoparticles were used to increase glucose oxidase electrode in the literature.

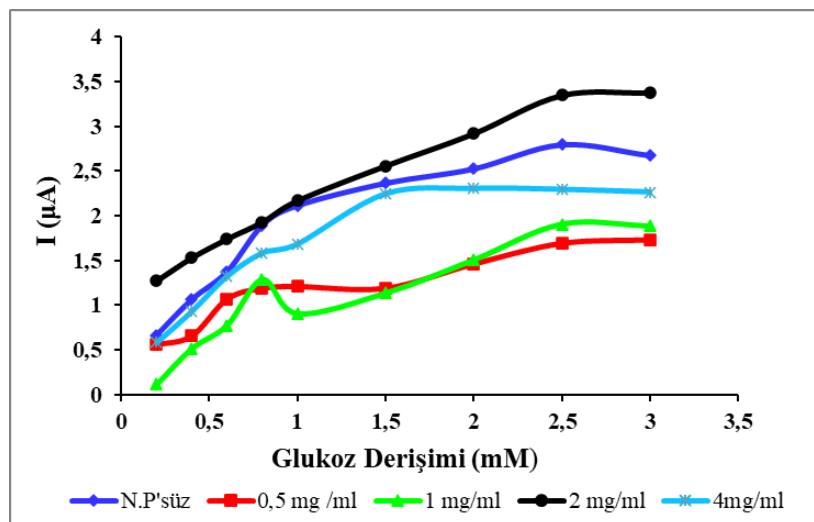


Figure 5. Current response of POT based biosensors modified with ZnFe₂O₄NP. —♦—: ZnFe₂O₄NP-free; —■—: 0.5; —▲—: 1.0; —●—: 2.0 and —*—: 4.0 mg/ml.

Biochemical Characterization of Enzyme Electrode

Kinetic parameters, operational stability and optimal pH values were also studied for biochemical characterization with the Pt/POT-GOD electrode obtained using optimal data. The current responses of the electrodes were obtained for different pH values in 3 mM glucose solution. Both Pt/POT/Chi-GOD-ZnFe₂O₄NP and Pt/POT/Chi-GOD electrodes showed the highest current responses at pH 6.0 given in Table 1. K_M and I_{max} values of both of Pt/POT-GOD electrodes given in the Table 1 were estimated by Lineweaver-Burk curve using current responses measured for glucose concentrations range from 0.10 to 10 mM. As seen in Table 1, I_{max} value of Pt/POT/Chi-GOD electrode was considerably lower than that of Pt/POT/Chi-GOD-ZnFe₂O₄NP electrode. With this result, ZnFe₂O₄NP in the enzyme-containing polymer film contributed to the increase of I_{max} value. K_M value of Pt/POT enzyme electrode that was modified by ZnFe₂O₄NP was slightly lower than that of this nanoparticle free counterpart.

Table 1. Optimal pH values and kinetic parameters of Pt/POT-GOD electrodes with and without ZnFe₂O₄NP.

	pH	K _M (mM)	I _{max} (μA)
Pt/POT/Chi-GOD/GAL	6	0.43	3.01
Pt/POT/Chi-GOD-ZnFe ₂ O ₄ /GAL	6	0.59	3.23

Operational stabilities of the Pt/POT electrode with and without ZnFe₂O₄NP were also investigated by 20 successive in the 5 mM glucose solution. The results of measurements repeated five times were similar. For all 20 cycles, obtained current values as the percentage of initial current

were calculated and Fig.6 shows the results. It was observed that the initial current activities of both Pt/POT/Chi-GOD and Pt/POT/Chi-GOD-ZnFe₂O₄NP electrodes were almost the same. At the end of 20th cycles, the current values of Pt/POT/Chi-GOD and Pt/POT/Chi-GOD-ZnFe₂O₄NP electrodes were observed to be a little of increase with 101.0% and 107.0% according to the first measured current values. This may occur due to changes in the POT film and GOD structure, which will increase enzyme activity and electron transfer. These results show that the enzyme electrodes are quite stable for reuse.

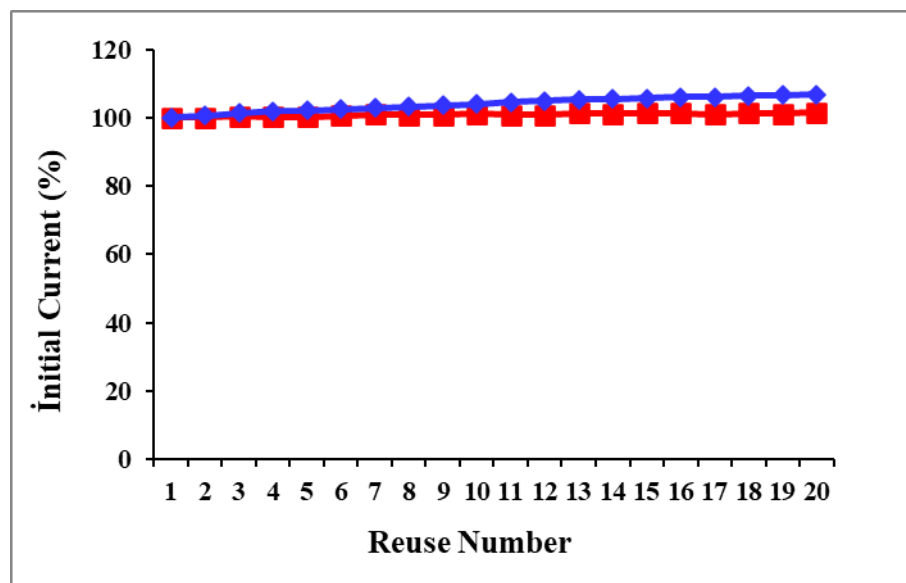


Figure 6. Operational stabilities of Pt/POT/Chi-GOD and Pt/POT/Chi-GOD-ZnFe₂O₄NP electrodes.

In conclusion, to fabricate a glucose-sensitive enzyme electrodes, double-layer POT polymer films with and without nanoparticle were synthesized on the Pt surface. The efficiency of the obtained electrodes was determined by measuring current values at different glucose concentrations. Accordingly, it has been observed that since synthesis conditions such as monomer concentration, scan rate and segment number change the surface structure of the electrodes, they also change the current responses of the biosensor electrodes. In addition, the current responses of biosensor electrodes are affected by the amounts of Chi, Gal, GOD and ZnFe₂O₄NP in the POT polymer film structure. The stability and current values were higher for Pt/POT/Chi-GOD-ZnFe₂O₄NP electrode than that of Pt/POT/Chi-GOD electrode. Therefore, it is thought that the reason for the increase in the current responses of the Zn-containing enzyme electrode is that the nanoparticle contributes to the increase in the conductivity of the polymer film and the electron transfer between the metal and enzyme interfaces. So, the necessity of determining biosensor design parameters in order to increase the efficiency of biosensor electrodes was revealed in this study.

Acknowledgements

This study was funded by Scientific Research Units of The University of Mustafa Kemal in Turkey, Project no: 8681.

Conflict of Interest

The authors declare that they have no competing interests.

Author Contributions

All authors' contributions are equal for the preparation of research in the manuscript.

References

- Abu-Rabeah, K., Marks, R.S. (2009). Impedance study of the hybrid molecule alginate–pyrrole: Demonstration as host matrix for the construction of a highly sensitive amperometric glucose biosensor. *Sensors and Actuators B*, 136, 516–522. <https://doi.org/10.1016/j.snb.2008.09.020>
- Chen, S., Fu, P., Yin, B., Yuan, R., Chai, Y., & Xiang, Y. (2011). Immobilizing Pt nanoparticles and chitosan hybrid film on polyaniline nanofibers membrane for an amperometric hydrogen peroxide biosensor. *Bioprocess and biosystems engineering*, 34(6), 711–719. <https://doi.org/10.1007/s00449-011-0520-4>.
- De Jesus, C.G., Lima, D., Santos, V., Wohnrath, K., Pessoa, C.A. (2013). Glucose biosensor based on the highly efficient immobilization of glucose oxidase on layer-by-layer films of silsesquioxane polyelectrolyte. *Sensors and Actuators B*, 186, 44–51. <https://doi.org/10.1016/j.snb.2013.05.063>.
- Eftekhari, A. (2004). Electropolymerization of aniline onto passivated substrate and its application for preparation of enzyme-modified electrode. *Synthetic Metals*, 145, 211–216. <https://doi.org/10.1016/j.synthmet.2004.05.016>.
- Ghica, M.E., & Brett, C.M.A. (2009). Poly (brilliant cresyl blue) modified glassy carbon electrodes: Electrosynthesis, characterisation and application in biosensors. *Journal of Electroanalytical Chemistry*, 629, 35–42. <https://doi.org/10.1016/j.jelechem.2009.01.019>.
- Guo, M., Fang, H., Wang, R., Yang, Z., Xu, X., J. (2011). Electrodeposition of chitosan-glucose oxidase biocomposite onto Pt–Pb nanoparticles modified stainless steel needle electrode for amperometric glucose biosensor. *Journal of Materials Science: Materials in Medicine*, 22, 1958–1992. <https://doi.org/10.1007/s10856-011-4363-y>.
- Haighi, B., Nazari, L., Sajjadi, S.M. (2012). Fabrication and Application of a Sensitive and Highly Stable Copper Hexacyanoferrate Modified Carbon Ionic Liquid Paste Electrode for Hydrogen Peroxide and Glucose Detection. *Electroanalysis*, 24, 2165–2175. <https://doi.org/10.1002/elan.201200277>.
- Huang, S., Ding, Y., Liu, Y., Su, L., Filosa Jr, R., Lei, Y. (2011) Glucose Biosensor Using Glucose Oxidase and Electrospun Mn₂O₃-Ag Nanofibers. *Electroanalysis*, 23, 1912–1920. <https://doi.org/10.1002/elan.201100221>.

- Hui, Y., Nan, L., Jhing-Zhong, X., Jun-Jie, Z., Chin. J. (2005). A Glucose Biosensor Based on Immobilization of Glucose Oxidase in Chitosan Network Matrix. *Chinese Journal of Chemistry*, 23, 275–279. <https://doi.org/10.1002/cjoc.200590275>.
- Jiang, Y., Zhang, Q., Li, F., Niu, L. (2012). Glucose oxidase and graphene bionanocomposite bridged by ionic liquid unit for glucose biosensing application. *Sensors and Actuators B*, 161, 728–733. <https://doi.org/10.1016/j.snb.2011.11.023>.
- Jung, S., & Lim, S. (2013). ZnO Nanowire-based Glucose Biosensors with Different Coupling Agents. *Applied Surface Science*, 265, 24–29. <https://doi.org/10.1016/j.apsusc.2012.10.069>.
- Khun, K., Ibupoto, Z.H., Lu, J., AlSalhi, M.S., Atif, M., Ansari, A., Willander, M. (2012). Potentiometric glucose sensor based on the glucose oxidase immobilized iron ferrite magnetic particle/chitosan composite modified gold coated glass electrode. *Sensors and Actuators B*, 173, 698–703. <https://doi.org/10.1016/j.snb.2012.07.074>.
- Li, J., Yuan, R., Chai, Y., Che, X., Li, W. (2012). Construction of an amperometric glucose biosensor based on the immobilization of glucose oxidase onto electrodeposited Pt nanoparticles-chitosan composite film. *Bioprocess and Biosystems Engineering*, 35, 1089–1095. <https://doi.org/10.1007/s00449-012-0693-5>.
- Salimi, A., & Noorbakhsh, A. (2011). Layer by layer assembly of glucose oxidase and thiourea onto glassy carbon electrode: Fabrication of glucose biosensor. *Electrochimica Acta*, 56, 6097–6105. <https://doi.org/10.1016/j.electacta.2011.04.073>.
- Ozdemir, C., Yeni, F., Odaci, D., Timur, S. (2010). Electrochemical glucose biosensing by pyranose oxidase immobilized in gold nanoparticle-polyaniline/AgCl/gelatin nanocomposite matrix. *Food Chemistry*, 119, 380–385. <https://doi.org/10.1016/j.foodchem.2009.05.087>.
- Ozyilmaz, G., Ozyilmaz, A.T., Can, F. (2011). Glucose Oxidase/polypyrrole Electrodes Synthesized in pToluenesulfonic Acid and Sodium pToluenesulfonate. *Applied Biochemistry and Microbiology*, 47, 217–225. <https://doi.org/10.1134/S0003683811020153>.
- Ozyilmaz, G., Ozyilmaz, A.T., Akyüreköglü, R.H. (2017). Poly(N-Methylpyrrole)-Chitosan layers for Glucose Oxidase Immobilization for Amperometric Glucose Biosensor Design. *Natural and Engineering Sciences*, 2, 123–134. <https://doi.org/10.28978/nesciences.354825>.
- Ozyilmaz, G., Ozyilmaz, A.T., Ağçam, S. (2018). Using Response Surface Methodology for Amperometric Glucose Biosensor Construction. *Natural and Engineering Sciences*, 3, 1–15. <https://doi.org/10.28978/nesciences.379311>.
- Pauliukaite, R., Paquim, A.M.C., Brett, A.M.O., Brett, C.M.A. (2006). Electrochemical, EIS and AFM characterisation of biosensors: Trioxysilane sol-gel encapsulated glucose oxidase with two different redox mediators. *Electrochimica Acta*, 52, 1–8. <https://doi.org/10.1016/j.electacta.2006.03.081>.

- Raicopol, M., Prună, A., Damian, C., Pilan, L. (2013). Functionalized single-walled carbon nanotubes/polypyrrole composites for amperometric glucose biosensors. *Nanoscale Research Letters*, 8, 1–8. <https://doi.org/10.1186/1556-276X-8-316>.
- Savale, P.A., Shirsat, M.D. (2009). Synthesis of Poly(o-anisidine)/H₂SO₄ Film for the Development of Glucose Biosensor. *Applied Biochemistry and Biotechnology*, 159, 299–309. <https://doi.org/10.1007/s12010-008-8135-1>.
- Shervedani, R.K., Hatefi-Mehrjardi, A. (2007). Electrochemical characterization of directly immobilized glucose oxidase on gold mercaptosuccinic anhydride self-assembled monolayer. *Sensors and Actuators B*, 126, 415–423. <https://doi.org/10.1016/j.snb.2007.03.023>.
- Uang, Y.M., Chou, T.C. (2003). Fabrication of glucose oxidase/polypyrrole biosensor by galvanostatic method in various pH aqueous solutions. *Biosensors and Bioelectronics*, 19, 141–147. [https://doi.org/10.1016/S0956-5663\(03\)00168-4](https://doi.org/10.1016/S0956-5663(03)00168-4).
- Wang, L., Gao, X., Jin, L., Wu, Q., Chen, Z., Lin, X. (2013). Amperometric glucose biosensor based on silver nanowires and glucose oxidase. *Sensors and Actuators B*, 176, 9–14. <https://doi.org/10.1016/j.snb.2012.08.077>.
- Yağız, E., Ozyilmaz G., Ozyilmaz A.T. (2023). Response Surface Methodology use in construction of polyaniline coated carbon paste electrode-based biosensor: Modification and characterization. *Biotechnology and Applied Biochemistry*, In press. <https://doi.org/10.1002/bab.2528>.
- Yu, E. H., & Sundmacher, K. (2007). Enzyme electrodes for glucose oxidation prepared by electropolymerization of pyrrole. *Process Safety and Environmental Protection*, 85(5), 489–493. <https://doi.org/10.1205/psep07031>.
- Zhang Y, Liu Y, Chu Z, Shi L, Jin W, (2013), Amperometric glucose biosensor based on direct assembly of Prussian blue film with ionic liquid-chitosan matrix assisted enzyme immobilization. *Sensors and Actuators B*, 176, 978–984. <https://doi.org/10.1016/j.snb.2012.09.080>.



Leaf Image Classification Based on Pre-trained Convolutional Neural Network Models

Yunus Camgözlü * , Yakup Kutlu 

Computer Engineering, Engineering and Natural Science Faculty, Iskenderun Technical University, Iskenderun, Türkiye.

Abstract

It is important to identify a high-performance model that can classify all leaves and even differentiate according to regional variations of the same leaf type. In this study, a leaf classification model was created using 5 different datasets with different number of images and compared with models. For this purpose, 4 different pre-trained models called VGG16, InceptionV3, MobileNet and DenseNet are used. In addition, a new model was proposed and model training was carried out using these datasets. Using the all models, inputs are transformed into feature vectors by parameter transfer method and used for classification with the nearest neighbor algorithm and support vector machine. The performance of the classifications were compared with similar studies in the literature.

Keywords:

Artificial intelligence, machine learning, deep learning, parameter transfer, pre-trained model, feature transformation

Article history:

Received 15 May 2023, Accepted 12 August 2023, Available online 15 December 2023

Introduction

Useful plants that are frequently used in daily life to raise our living standards such as pharmacy, alternative medicine, medicine. However, there are harmful plants as well as useful plants. Moreover, expert knowledge is required for its use. Misuse of plants based on hearsay information or the use of plants that are thought to be medicinal by the public even though they are poisonous cause serious problems. Moreover, it could cause people to die. It is known that many plants are used in alternative medicine in Turkey as well as all over the world. When leaf similarities are

*Corresponding Author: Yunus CAMGÖZLÜ, E-mail: yunus.camgozlu@iste.edu.tr

taken into account, if people do not have expertise, they cannot be expected to have detailed knowledge about these plants. There is a known fact that leaf characteristics provide many useful clues for taxonomy of the leaf (Jiang et al., 2013). With technological developments, it is possible to produce solutions or improve such problems. For this reason, it is aimed to develop a recognition system based on artificial intelligence applied to leaf images for this problem that requires expertise such as recognizing plants and using them correctly.

Artificial intelligence is developing gradually. Compute Unified Device Architecture (CUDA) was developed by Nvidia. Therefore, researchers started using GPU as it allowed easy processing of big data in Artificial intelligence algorithm. CUDA enables simultaneous parallel processing of neural networks using thousands of cores in GPUs (Ilievski et al., 2018). It is frequently used in different areas such as social media, e-commerce, suggestion systems, autonomous system etc. in our daily life. As a result of its use in such different areas, customized methods have been developed for different processes. One of these methods is specially trained convolutional neural network models. These models are also called feature learning because they directly calculate the parameters using input data. However, due to this feature, a large dataset is needed for the training of the convolutional neural network model. On the other hand, working with a large amount of datasets can be extremely costly due to the need for hardware. For this reason, feature transformation is performed using pre-trained models and classification is evaluated with the obtained feature set.

This method is defined as parameter transfer or transfer learning. It is a convolutional neural network (CNN), which is one of the sub-branches of deep learning and is frequently used in many areas where high performance is required (Kutlu et al., 2017). In this method, there are parameters such as multiple functions, layers and filters that may vary according to the work done. While developing a new convolutional neural network model, it is necessary to examine appropriate parameters by considering many parameters such as pooling layer parameter (Camgözlü & Kutlu, 2019), filter size, image size (Camgözlü & Kutlu, 2020), number of layers.

In literature there are many studies for leaf classification such as convolutional neural network models (Wu et al., 2007; Kadir et al., 2013; Kulkarni et al., 2013; Atabay, 2016; Barre et al., 2017), support vector machine (Hewitt and Mahmoud, 2018; Zhang et al., 2020; Tsolakidis et al., 2014; Shah et al., 2017; Tomar and Agarwal, 2016; Wang et al., 2014, 2020), nearest neighbor algorithm (Tomar & Agarwal, 2016; Wang et al., 2014). In addition, There are studies in which classification is made with different methods using feature vectors extracted from the trained convolutional neural network called pre-trained models (Lee et al., 2017; Beikmohammadi & Faez, 2018; Wang et al., 2018; Raj & Vajravelu, 2019). Different classification methods such as logistic regression (LR), support vector machine (SVM), Naive Bayesian, linear discriminant analysis (LDA), radial fundamental probabilistic neural network (RF-PNN), multilayer perceptron (MP), AdaBoost, probabilistic neural network have been used (Silva et al., 2013; Jiang et al. 2013; Padoa & Maravillas, 2015; Mostafa et al., 2020; Sujith & Neethu, 2021).

Different dataset was used in these studies. Therefore, five different leaf datasets (which are Mendeley, Swedish Leaf, Flavia, UCL, Leafsnap) were used in this study. Silva et al. (2013), Padoa & Maravillas (2015), Tomar & Agarwal (2016) have been used UCL dataset to classify leaf using LDA, Naive Bayesian and SVM respectively.

Barre et al. (2017), Beikmohammadi & Faez (2018), Shah et al. (2017), Hewitt & Mahmoud (2018), Kumar et al. (2012) have been used leafsnap dataset to develop classification model. Barre et al. (2017) used CNN models. Beikmohammadi & Faez (2018) used pretrained CNN models. Hewitt & Mahmoud (2018) used SVM models. Shah et al. (2017) used SVM and CNN models. Kumar et al. (2012) used KNN models.

Swedish Leaf dataset has been used by Hewitt & Mahmoud (2018), Zhang et al. (2020), Tsoiakidis et al. (2014), Sujith & Neethu (2021), Atabay (2016), Anubha Pearline et al. (2019) to develop classification model. SVM has been used by Hewitt & Mahmoud (2018), Zhang et al. (2020), Tsoiakidis et al. (2014). Sujith & Neethu (2021), Atabay (2016), Anubha Pearline et al. (2019) have used MLP, CNN and pre-trained model respectively.

The Flavia dataset was used by Wu et al. (2007), Kumar et al. (2012), Kulkarni et al. (2013), Kadir et al. (2013), Tsoiakidis et al. (2014), Lavania & Matey (2014), Wang et al. (2014), Atabay (2016), Shah et al. (2017), Barre et al. (2017), Lee et al. (2017), Anubha Pearline et al. (2019), Hewitt and Mahmoud (2018), Beikmohammadi & Faez (2018), Raj & Vajravelu (2019), Wang et al. (2020), Zhang et al. (2020), Mostafa et al. (2020) Sujith & Neethu (2021), with different classification models such as KNN PNN SVM CNN etc.

It is important to identify a high-performance model that can classify all leaves and even differentiate according to regional variations of the same leaf type. In this study, 5 different datasets consisting of leaf images were determined in order to create a good model and compare. Four different convolutional neural network models which are trained previously, were used. These pre-trained models are VGGNet (Simonyan & Zisserman, 2015), InceptionV3 (Szegedy et al., 2001), MobileNet (Howard et al. 2017), DenseNet (Huange et al, 2017). In addition, a new convolutional neural network training was carried out with the existing datasets. It is used on classification with nearest neighbor algorithm (KNN) and support vector machine (SVM) after feature transfer. All results are compared in detailed with the similar studies in literature.

Material and Methods

Datasets and Data Augmentation

As a result of the literature review, Many different types of gray or black images with different color spaces were found in the images. Images with many different species and with different color space were found. In addition, these data sets will be combined into a new data set to create a more general model.

- Mendeley Data Set (Chouhan et al., 2019): Mendeley dataset consists of diseased and healthy leaves. In this data set, which includes 12 species and 4404 images, those unsuitable for use were excluded from diseased leaf images.
- Swedish Leaf Dataset (Soderkvist, 2001): 1125 leaf images of 15 species in the Swedish Leaf dataset have white backgrounds.
- Flavia Dataset (Wu et al., 2007) : Leaf images in the Flavia dataset , which includes 32 species and 1907 images, have white backgrounds.
- UCL Data Set (Silva et al., 2013): In the UCL dataset , which includes 40 species and 443 images, the background colors of the leaf images differ.
- Leafsnap Data Set (Kumar et al., 2012): Images in the section called lab in the Leafsnap data set, which consists of 2 parts, were used. This dataset consists of 185 species and 23147 images.
- Combined Data Set: While all data sets were combined, similar species were reduced to a single species, thus reducing the total number of species from 283 to 270.

When the data sets used were examined, data duplication was applied using image processing techniques in order to reduce the number of images per species in each data set and to increase the training performance. After pre-processing, 5 different datasets Mendeley Swedish Leaf, Flavia, UCL , Leafsnap which have different types and amount were shown in Table 1. The samples of images from each datasets is shown in Figure 1. UCL and Mendeley datasets have colored backgrounds, while the others have white backgrounds. While the UCL dataset, which has fewer images than the others, was first subjected to mirroring and then to rotation, other datasets were only rotated. In the rotation process performed on all 4 datasets, 11 different angles of rotation were applied from 30 degrees to 330 degrees with an increase of 30 degrees, and a total of 12 different angles were obtained by including the original images as shown in Figure 2. Leafsnap dataset, which is out of these 4 datasets, was created from images that were rotated 90, 180 and 270 degrees in addition to the original images. Since the images in the datasets are in different rotations, data augmentation made limited to avoid over-learning. It was applied at different scales according to the change in the number of images for the species with many images. All datasets were converted to images with the same background by applying background color correction to non-white backgrounds in 5 different datasets..This process ensured that the combined data set had similar properties. While all data sets were combined, similar species were reduced to a single species, thus reducing the total number of species from 283 to 270. Total amount of images are 62.424.

Table 1. The database information according to species, images, data and augmentation.

Dataset	Number of species	Number of images	Number of images after data augmentation
Mendeley	12	4.149	52.624
Swedish Leaf	15	1.125	13.500
Flavia	32	1.907	22.877
UCL	40	443	10.632
Leafsnap	184	11.234	57.966

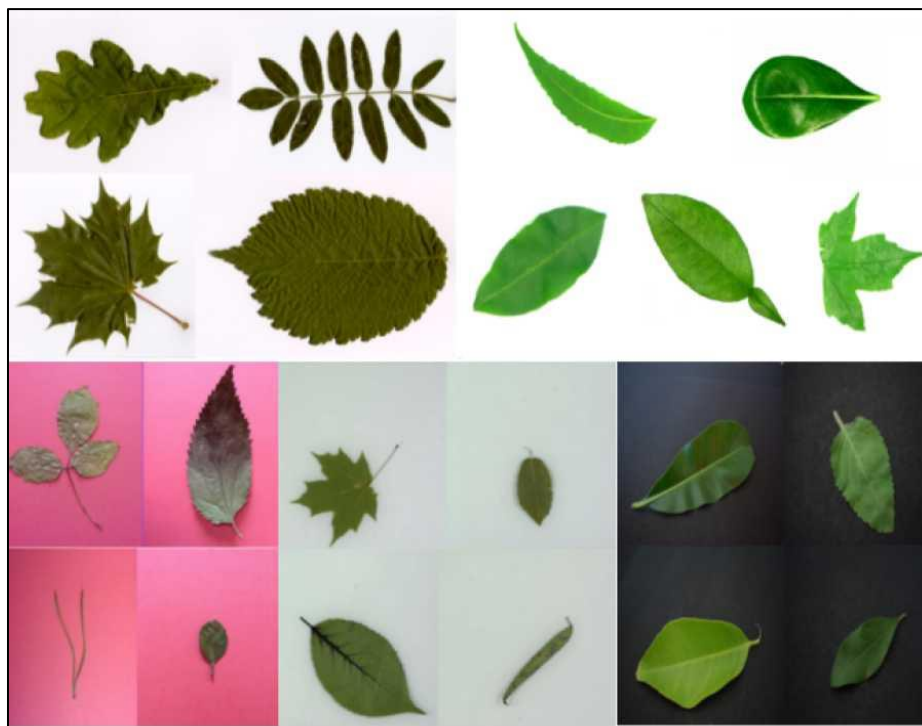


Figure 1. The samples of images from each datasets.



Figure 2. An image sample with different angles in the rotation process.

Convolutional Neural Network

Convolutional neural networks use local receptive fields, shared weights, and subsampling to extract local features and then combine them in an invariant manner (Kwolek, 2005). It performs these operations effectively with the model created as a result of the combination of different layers. In the convolutional neural network model, which consists of different numbers of convolution and pooling layers, different results can be obtained by changing the parameters such as function and filter size in these layers. The multidimensional matrix with the features obtained through the filters used transforms it into a one-dimensional vector through the plane layer and transmits it to the fully connected layer for classification. In this layer, classification is done by making predictions according to the labels. The convolutional neural network structure is shown in Figure 3 in detail, classification is made using the feature vector obtained as a result of feature learning from the leaf images taken as input data.

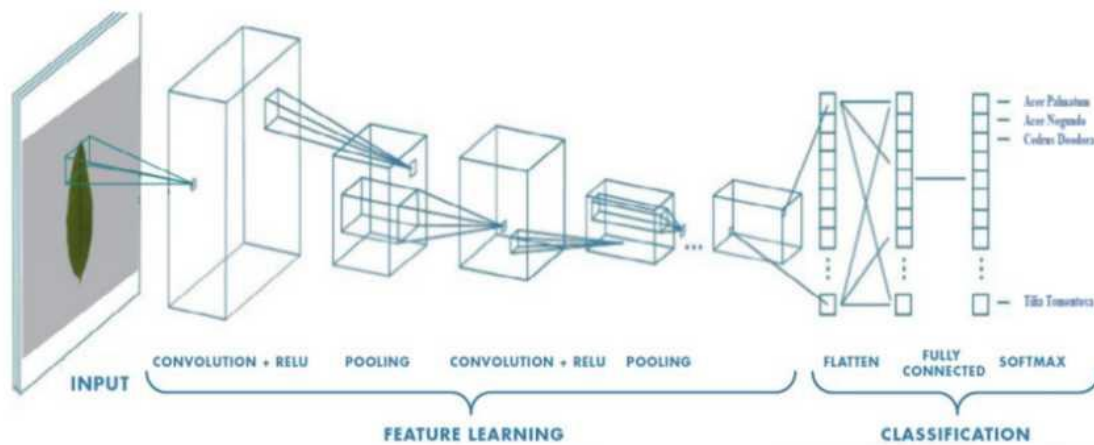


Figure 3. The CNN structure Model.

Pre-trained Models

There are many pre-trained models that are trained with high image size, number of images and processing power. The model structure is shown in Figure 4. In these examinations, 4 pre-trained models with 2 different plane layer sizes were determined. The image sizes to be used for these models are limited due to the pre-training. 128x128 color images were used, taking into account the processing power and time required for the operations to be performed after feature extraction.

In this study, VGGNet developed by Simonyan and Zisserman (2015), InceptionV3 developed by Szegedy et al. (2015), MobileNet developed by Howard et al. (2017), and finally DenseNet created by Huang et al. (2018) were preferred as pre-trained models. 128x128 was chosen as the input image size for all transfer model. The VGGNet pre-trained model is trained with a subset of ImageNet with 1000 classes and 1000 images for each class. This cluster contains 1.2 million training data, 50 000 validation data and 150 000 test data. The InceptionV3 pre-trained model was trained using the dataset in the large-scale visual recognition competition ImageNet Large Scale Visual Recognition Challenge 2012 (ILSVRC2012). The MobileNet pre-trained model is trained using ImageNet. MobileNet is based on a modern architecture that uses deeply separable convolutions to create lightweight, deep neural networks. In the DenseNet pre-trained model, each layer is connected with other layers in a feed-forward manner. The large-scale image recognition competition was trained using the dataset set in ImageNet Large Scale Visual Recognition Challenge 2012 (ILSVRC2012).

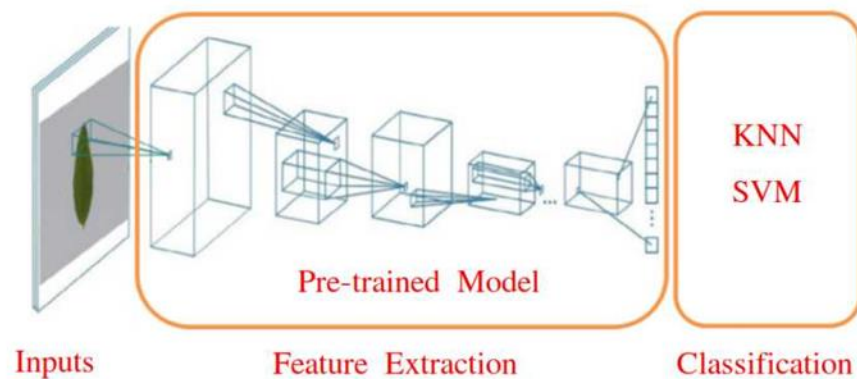


Figure 4. The classification structure using Pre-trained CNN Model.

The convolutional neural network model created in this study and the pre-trained models used in the plane layer size, initial image dimensions and the final state of the feature extraction data before the plane layer are shown in Table 2. Looking at these data, it is seen that the high image size and flattening layer size of the pre-trained models are higher than the model created. In addition, high image size and multi-layer structure are among the main reasons for the high leveling layer size.

Table 2. Parameters of models.

Model Names	Flatten Layer Sizes	Image Size	Before Flatten Layer
VGGNet (Simonyan ve Zisserman, 2015)	8 192	128 x 128 x	4 x 4 x 512
InceptionV3 (Szegedy et al., 2001)	8 192	128 x 128 x	2 x 2 x 2048
MobileNet (Howard et al. 2017)	16 384	128 x 128 x	4 x 4 x 1024
DenseNet (Huange et al, 2017)	16 384	128 x 128 x	4 x 4 x 1024
New CNN Model	1 536	90 x 75 x 1	3 x 2 x 256

Creating New CNN Model

There are many parameters in convolutional neural networks. There is no specific method for determining these parameters. For this reason, the parameters is determined experimentally. In this study, the parameters obtained in the previous studies of Camgözlü & Kutlu (2019; 2020) were used . For this purpose, appropriate parameters were used in studies where the effects of parameters such as mean pooling, filter size, image background color, image size were also examined. The model to be used in this study consists of 6 convolution layers and 3 pooling layers. As a result of the studies, the pooling layer size was determined as 3 and the pooling type was determined as average pooling, while the convolution filter size was determined as 3.

Feature Extraction

In this study, an image entered pre-trained models as inputs was transferred into an feature vector after operations such as convolution, pooling, which were done before the classification layer. Therefore, an image is converted to a new input vector depending on the model's parameters by using pre-trained models. The feature map is obtained with the transformation approach in the middle layers of the CNN models and is given as an input to the last layer called classification layer. In this study, KNN and SVM algorithms are preferred as classifiers in the classification layer.

K-Nearest Neighbors

There are many machine learning classification algorithms in the literature. One of these algorithms is the nearest neighbor algorithm (KNN). In addition to the use of different types of distance calculation functions in the KNN algorithm, which is based on the distance between two points, the parameters such as how many nearest neighbors will be made during the calculation vary. There are different methods to measure the performance of this algorithm. This feature selection method allows the removal of features that do not add new information, with which some other features highly interact with them, which might otherwise lead to redundancy and poor predictive ability (Soucy & Mineau, 2001a).

Support Vector Machine

Support Vector Machines is one of the supervised learning algorithms that can be applied to both classification and regression problems. It has an algorithm that finds a decision boundary between the two classes that are furthest from a point using training inputs. An SVM classifier creates a maximum-margin hyperplane located in a transformed input space and maximizes the distance to the nearest clean-split instances when generating instance classes.

It has the ability to classify nonlinear data by expanding the input data area, thanks to different kernel functions such as linear, polynomial, radial basis, sigmoid. The task of learning a support vector machine is typically treated as a constrained quadratic programming problem. However, in its natural state it is in fact an unconstrained empirical loss minimization, with a penalty term for the norm of the classifier being learned (Soucy & Mineau, 2001b).

Cross Validation and Performance Criteria

In classification problems, the performance of the model when new data other than the training data comes in is called generalization performance. The generalization performance of classification models in applications is measured with examples not used in training. For this purpose, cross validation is used to ensure that all examples are used both in training and in generalization performance as a test. The 10- fold cross validation visualization is given in the Figure 5.

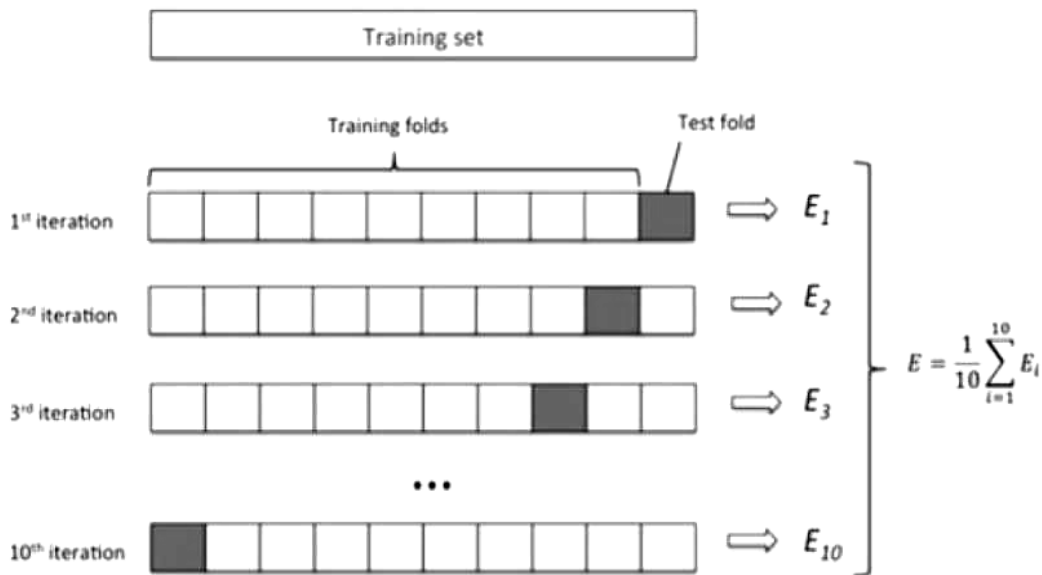


Figure 5. The 10-fold cross validation visualization (Petkov, 2018).

In K-Fold cross validation method, all dataset is separated into k subsets. While k-1 subset of these is used as train set, one of them is used as test set. Since the test dataset do not used during training, performance is obtained with test dataset. This process is repeated until the all subset is used for testing. The performance of classifier is evaluated as test performance by taking the averages separately for training and testing results.

Experimental Study

In this study, the open source tensorflow library used for CNN training was used. A computer with AMD Ryzen 5 3600x processor, Nvidia GTX 1080 graphics card and 32 gigabytes of system memory was used in these processes. In the CNN training, python was chosen from programming languages such as C++, python, and java, and the tensorflow library, which is an open-source library, was used.

In this study, five different datasets were used to determine suitable models for leaf classification. It was carried out to develop a new CNN model for leaf classification and to determine the appropriate parameters. In addition, four pre-trained models were used. The pre-trained models, which includes new trained CNN, were utilized as feature extraction (feature transformation). After feature extraction the feature vectors were used for classification in KNN and SVM. The results were evaluated together according to the number of images in the datasets, the number of species, the number of iterations and the obtained success rates. In addition, the results are compared each other's and with similar studies in literature.

While developing the new CNN model, the datasets used for training and testing were separated at a rate of 80% and 20%. The results of the new model, which includes the number of species in the datasets, the number of images, the number of iterations and accuracy rates, are given in Table 3. According to these results, it can be said that a good performance was achieved with low iteration.

Table 3. The accuracy rates of the new CNN model in classification with different datasets.

Dataset	Number of species	Number of images	Number of iterations	Train accuracy	Test accuracy
Mendeley	12	52 624	5 000	97,35	92,08
Swedish Leaf	15	13 500	10 000	98,94	90,87
Flavia	32	22 877	10 000	97,60	91,89
UCL	40	10 632	20 000	98,58	88,00
Leafsnap	184	57 966	10 000	95,50	86,78

The feature vectors obtained from the new CNN model and pre-trained models were classified with KNN, and the results are shown in Table 4. As the results, pre-trained models performed close results when the number of species were low, performed poorly in the Leafsnap

dataset with high species counts. But using high amount of images in new CNN model, it made the performance increased.

Table 4. Accuracy rates of pre-trained models using KNN classifier.

Methods	Mendeley	Swedish Leaf	Flavia	UCL	Leafsnap
New CNN + KNN	95,65	97,32	97,21	89,48	87,46
InceptionV3 + KNN	82,19	92,47	93,15	90,17	54,33
MobileNet + KNN	89,09	98,67	98,87	95,81	62,53
VGGNet + KNN	86,91	97,56	96,98	93,52	56,18
DenseNet + KNN	89,00	97,15	96,77	95,80	61,22

The feature vectors obtained from the new CNN model and pre-trained models were classified with SVM as well, and the results of 5 different datasets and 5 model are shown in Table 5. According to these results, it was seen that better results were obtained in the pre-trained models in the datasets that do not have a high number of species. Using high amount of images in new CNN model, it made the performance increased when using SVM as well.

Table 5. Accuracy rates of pre-trained models using SVM classifier.

Methods	Mendeley	Swedish	Flavia	UCL	Leafsna
New CNN + SVM	97,27	98,47	97,47	94,35	91,71
InceptionV3 + SVM	91,17	97,22	96,26	94,59	68,33
MobileNet + SVM	97,74	99,82	99,56	98,78	80,51
VGGNet + SVM	96,52	99,45	98,63	98,25	78,21
DenseNet + SVM	96,57	99,29	98,53	97,89	80,39

Finally, all data sets were combined and used as a single data set and the results were obtained. Since some species are similar in these datasets, a dataset containing a total of 270 different species was created. After data reproduction, 62424 images were created and used in classification. The feature transformation was performed with combining all data sets and classification was carried out with KNN and SVM models. The classification results are given in Table 6.

Table 6. Accuracy rates of all models using KNN and SVM classifier for Combined Dataset.

Methods	Accuracy
New CNN + KNN	81,18
InceptionV3 + KNN	68,57
MobileNet + KNN	75,31
VGGNet + KNN	70,45
DenseNet + KNN	75,55
New CNN + SVM	86,00
InceptionV3 + SVM	72,77
MobileNet + SVM	84,36
VGGNet + SVM	82,79
DenseNet + SVM	83,56

Comparison of the Classification Performances

Comparing the proposed models with other studies in the literature is a bit difficult because of the reasons such as preprocessing, methods, datasets, and the number of images in the datasets. In this respect, a comparison was made with studies using similar datasets in terms of making the comparison a little more meaningful and the consistency of the method.

Mendeley dataset is a kind of leaf disease. Therefore, there is no study in the literature that has been classified leaf images using Mendeley dataset. There are 12 different leaf species in dataset. When the results among the models are considered, it is seen that the MobileNET + SVM approach provides the best performance among the methods in the dataset. The classification performance of the Mendeley dataset is shown in Table 7.

Table 7. Comparison of classification performances for Mendeley dataset.

Methods for Feature Transformation	Mendeley Dataset		Classification Accuracy	
	Number of species	Number of images	with KNN	with SVM
new CNN			95,65	97,27
InceptionV3			82,19	91,17
MobileNet	12	52.624	89,09	97,74
VGGNet			86,91	96,52
DenseNet			89,00	96,57

The UCL dataset has been used less than other datasets due to its high number of species and low number of images. The comparison of the results of methods, which used the UCL dataset, are shown in Table 8. The best performance was obtained from MobileNET + SVM models which achieved a much higher performance.

Table 8. Comparison of classification performances of the UCL dataset with different classification methods.

Published by	Method	Number of species	Number of images	Accuracy
Padao, 2015	Naive Bayesian	30	340	74,10
Tomar, 2016	SVM	40	443	84,70
Silva, 2013	LDA	15	171	87,00
In this study	MobileNet + SVM	40	10 632	98,78

The Leafsnap dataset has highest species number between datasets. The comparison of the results of models that used the Leafsnap dataset is shown in Table 9. Results were achieved by different classification methods using this dataset. Some researchers seem to have reduced species when used this dataset. In the studies used the same number of species, the second-best performance was obtained. The method that provides the best performance in this study is obtained from new CNN + SVM model.

Table 9. Comparison of classification performances for the Leafsnap dataset.

Published by	Method	Number of species	Number of images	Accuracy
Hu, 2018	MSF-CNN	184	-	85.28
Shah, 2017	SVM	150	7 710	85,37
Barre, 2017	CNN	184	272 300	86,30
Beikmohammadi, 2018	MobileNet + LR	184	29 107	90,54
Song, 2019	ABCNN	184	-	91.43
Ganguly, 2022	BLeafNet	184	-	92.22
Hewitt, 2018	SVM	183	7 440	92,40
Shah, 2017	CNN	150	7 710	95,61
Kumar, 2012	KNN	184	29 107	96,80
In this study	New CNN + SVM	184	57 966	91,71

The comparison of the results of methods that used the Swedish Leaf dataset is shown in Table 10. there are 15 leaf species in this database. Considering the studies used the Swedish Leaf data set, it was seen that high performance has been achieved. The methods proposed in this study has seemed to be as good as the results in the literature.

Table 10. Comparison of classification performances of the Swedish Leaf dataset with different classification methods.

Published by	Method	Number of species	Number of images	Accuracy
Wang, 2017	CNN + SVM	15	1 125	97,63
Hewitt, 2018	SVM	15	1 125	97,80
Zhang, 2020	SVM	15	1 125	97,93
Tsolakidis, 2014	Linear SVM	15	750	98,13
Sujith, 2020	ANN	15	1 125	98,23
Pearline, 2019	VGG + LR	15	1 125	98,52
Atabay, 2016	CNN	15	2 250	99,11
In this study	MobileNet + SVM	15	13 500	99,82

Flavia dataset is one of the most used datasets in the literature. The comparison of the results of methods used the Flavia dataset are given in Table 11. There are many models applied in literature to classify Flavia dataset. It was seen that the results obtained from the pre-trained models were quite high in the classification of the Flavia dataset.

Table 11. Comparison of classification performances of the Flavia dataset with different classification methods.

Published by	Method	Number of	Number of	Accurac
Lavanaia, 2014	KNN	33	1 907	87,50
Wu, 2007	PNN	32	1 800	90,00
Shah, 2017	SVM	32	1 907	93,22
Kadir, 2011	PNN	32	1 600	93,75
Kulkarni, 2013	RF - PNN	32	1 600	93,82
Kumar, 2019	MP - AdaBoost	32	1 907	95,42
Pearline, 2019b	VGG+ LR	32	1 907	96,25
Hewitt, 2018	SVM	32	1 907	96,66
Tsolakidis, 2014	MobileNet + LR	32	1 600	97,18
Atabay, 2016	CNN	32	3 814	97,24
Barre, 2017	CNN	32	44 623	97,90
Sujith, 2020	GLCM+LBP+PHOG+NCA	32	1 907	98,23
Zhang, 2020	SVM	32	1 907	98,53
Wang, 2018	DPCNN + SVM	32	1 907	98,53
Ganguly, 2022	BLeafNet	32	-	98,70
Shah, 2017	CNN	32	1 907	99,28
Lee, 2017	CNN + SVM	32	2 603	99,30
Beikmohammadi,	MobileNet + LR	32	1 907	99,60
In this study	MobileNet + SVM	32	22 877	99,56

Finally, since there are no similar studies in the literature for the same combined dataset, a comparison cannot be made. Using similar approach Gajjar et al. (2022) evaluates the performance of EfficientNet model when applied to a combination of the Flavia, Folio datasets, LeafSnap, Swedish, and Middle European Woody Plants 2014, naming it the F2LSM dataset. They reported 98% of accuracy for combined dataset containing 374 different types. A study in the form of a combined data set obtained by merging all data sets was presented by Camgözlü & Kutlu (2021). They used 270 different types and 65100 images and 80% of the dataset was reserved for training and 20% for testing. 88% training accuracy and 79% test accuracy were achieved. In addition, the models used in this study were compared with each other (as shown Table 12). It is seen that the best model is performed with the new CNN model trained with leaf images and SVM. It is thought that this means that the number of samples is high and a new CNN model specially trained with leaf images provides better results.

Table 12. Comparison of classification performances of the Combined Dataset using different models.

Methods for Feature Transformation	Combined Dataset		Classification Accuracy	
	Number of species	Number of images	with KNN	with SVM
new CNN			81,18	86,00
InceptionV3			68,57	72,77
MobileNet	270	62 424	75,31	84,36
VGGNet			70,45	82,79
DenseNet			75,55	83,56

In the proposed study, the trained CNN model was used as a feature transformation tool and performances were examined with KNN and SVM classifiers. Since the obtained performances better describe the generalization performance, the 10fold Cross validation method was applied.

Classification of leaf datasets using convolutional neural networks is scarce in the literature. However, the long duration of the training and the need for high equipment in the models used in these studies make it difficult for the researchers. In the literature, there are leaf recognition models in which pre-trained models are used instead of training a new model.

In conclusion, in this study, 5 different image datasets were used. In order to achieve a generalization performance for rotation independent, amount of images were augmented by images rotated in 12 different angular positions. 4 different pre-trained models were used for feature extraction. In addition to these, training was carried out by creating a CNN model with lower parameters trained with leaf image datasets and this model was used for feature extraction as well. All developed models for leaf classification system were compared.

In general, In the results of the overall performance, a high performance has been achieved in all datasets. It is seen in detail in Tables. When the new trained CNN model is compared with the pre-trained models, it is seen that it performs close to each other's. As a result of the comparison, the increase in the number of class and images shows that the classification problem is getting bigger. Considering this situation, the new trained CNN model created for leaf classification has been achieved better result according to the results of the Leafsnap dataset, where the number of species is much higher than other datasets. The parameters of pre-trained models VGGNet model, InceptionV3, MobileNet , DenseNet and New CNN Model are 8192, 8192, 16384, 16384 and 1536 respectively. The new CNN model has achieved as good results as the pre-trained models, and sometimes even better. This shows that the model trained with own dataset could be good even if they have small parameters. As a result, it was observed that the performance of the specially trained CNN model increased. It has been seen that others can achieve good performance and the high number of data is another parameter that increases the performance of the models.

In this study, different classification methods and different data sets were used. When these results and the studies in the literature are examined, it has been determined what kind of method will be used in hardware with low processing power. As it can be seen in the comparison tables, many CNN models have been used in the literature. The common issue with them is the high hardware requirements used. But, it may not always be high hardware. In this case, instead of training deep learning models, it is possible to use their capabilities by using pre-trained models as a feature transformation. Nevertheless, it is necessary to say that training with the relevant data set is better than pre-trained models. However, in the absence of hardware, it can be used as an alternative.

Accordingly, it has been determined that the classification of the features extracted from the pre-trained models with different feature vector sizes according to the capacity of the system being processed requires both less time and less processing power. It should be taken into account that pre-trained models can be used, considering that the performance difference between the pre-trained and the trained models result is not very large. As a result, getting very good results by performing feature transformation with pre-trained models depends on the dataset. Pre-trained models don't require training, so they don't require high processing power. However, it should not be forgotten that the new CNN model requires serious hardware to perform training, especially in datasets with high samples.

Conflict of Interest

The authors declare that they have no competing interests.

Author Contributions

All authors' contributions are equal for the preparation of research in the manuscript.

References

- Anubha Pearline, S., Sathiesh Kumar, V., Harini, S. (2019). A study on plant recognition using conventional image processing and deep learning approaches. *Journal of Intelligent & Fuzzy Systems*, 36(3):1997-2004. <https://doi.org/10.3233/JIFS-169911>.
- Atabay, H. A. (2016). A convolutional neural network with a new architecture applied on leaf classification. *IIOAB J*, 7(5):226-331.
- Barre, P., Stöver, B. C., Müller, K. F., Steinhage, V. (2017). Leafnet: A Computer vision system for automatic plant species identification. *Ecological Informatics*, 40:50-56. <https://doi.org/10.1016/j.ecoinf.2017.05.005>.
- Beikmohammadi, A. & Faez, K. (2018). Leaf classification for plant recognition with deep transfer learning. In 2018 4th Iranian Conference on Signal Processing and Intelligent Systems (ICSPIS), pages 21-26. IEEE.
- Camgözlü, Y., & Kutlu, Y. (2019). Analysis of pooling effect on CNN using leaf database. *Natural and Engineering Sciences*, 4(3):115-121.

- Camgozlu, Y., & Kutlu, Y. (2020). Examining the difference between image size, background color, gray picture and color picture in leaf classification with deep learning. *International Journal of Intelligent Systems and Applications*, 3, 130-133.
- Camgözlü, Y., & Kutlu, Y. (2021). Yaprak Sınıflandırmak için Yeni Bir Evrişimli Sinir Ağı Modeli Geliştirilmesi . *Bilecik Şeyh Edebalı Üniversitesi Fen Bilimleri Dergisi* , 8 (2) , 567-574 . <https://doi.org/10.35193/bseufbd.887643>.
- Chouhan, S. S., Singh, U. P., Kaul, A., Jain, S. (2019). A data repository of leaf images: Practice towards plant conservation with plant pathology. In 2019 4th International Conference on Information Systems and Computer Networks (ISCON), pages 700-707. IEEE.
- Gajjar, V. K., Nambisan, A. K., & Kosbar, K. L. (2022). Plant Identification in a Combined-Imbalanced Leaf Dataset. *IEEE Access*, 10, 37882-37891. <https://doi.org/10.1109/ACCESS.2022.3165583>.
- Ganguly, S., Bhowal, P., Oliva, D., & Sarkar, R. (2022). BLeafNet: A Bonferroni mean operator based fusion of CNN models for plant identification using leaf image classification. *Ecological Informatics*, 69, 101585. <https://doi.org/10.1016/j.ecoinf.2022.101585>.
- Hewitt, C. & Mahmoud, M. (2018). Shape-only features for plant leaf identification. arXiv preprint *arXiv:1811.08398*. <https://doi.org/10.48550/arXiv.1811.08398>.
- Howard, A., Zhu, M., Chen, B., Kalenichenko, D., Wang, W., Weyand, T., Andretto, M. Adam, H. (2017). MobileNets: Efficient Convolutional Neural Networks for Mobile Vision Applications. *arXiv: 1704.04861*. <https://doi.org/10.48550/arXiv.1704.04861>.
- Huang, G., Liu, Z., Van Der Maaten, L., Weinberger, K. Q. (2017). Densely connected convolutional networks. In *Proceedings of the IEEE conference on computer vision and pattern recognition*. 4700-4708.
- Ilievski, A., Zdraveski, V., Gusev, M. (2018). How CUDA powers the machine learning revolution. In *2018 26th Telecommunications Forum (TELFOR2018)*. 420-425.
- Jiang, W., Özaktaş, B. B., Mantri, N., Tao, Z., Lu, H. (2013). Classification of camellia species from 3 sections using leaf anatomical data with back-propagation neural networks and support vector machines. *Turkish Journal of Botany*, 37(6):1093-1103. <https://doi.org/10.3906/bot-1210-21>.
- Kadir, A., Nugroho, L. E., Susanto, A., Santosa, P. I. (2013). Leaf classification using shape, color, and texture features. arXiv preprint *arXiv:1401.4447*. <https://doi.org/10.48550/arXiv.1401.4447>.
- Kulkarni, A., Rai, H., Jahagirdar, K., Upparamani, P. (2013). A leaf recognition technique for plant classification using RBPNN and zernike moments. *International Journal of Advanced Research in Computer and Communication Engineering*, 2(1):984-988.
- Kumar, N., Belhumeur, P. N., Biswas, A., Jacobs, D. W., Kress, W. J., Lopez, I. C., Soares, J. V. (2012). Leafsnap: A computer vision system for automatic plant species identification. In *European conference on computer vision*, 502-516.

- Kutlu, Y., Altan, G., İşçimen, B., Doğdu, S. A., Turan, C. (2017). Recognition of species of triglidae family using deep learning. *Journal of the Black Sea/Mediterranean Environment*, 23(1), 56-65.
- Kwolek, B. (2005). Face detection using convolutional neural networks and gabor filters. In *International Conference on Artificial Neural Networks*, 551-556..
- Lavania, S. & Matey, P. S. (2014). Leaf recognition using contour based edge detection and sift algorithm. In *2014 IEEE International Conference on Computational Intelligence and Computing Research*, pages 1-4.
- Lee, S. H., Chan, C. S., Mayo, S. J., Remagnino, P. (2017). How deep learning extracts and learns leaf features for plant classification. *Pattern Recognition*, 71:1-13. <https://doi.org/10.1016/j.patcog.2017.05.015>.
- Mostafa, S. I., Abd El-Latif, Y. M., Reda, N. M. (2020). Fast And Accurate System For Leaf Recognition. *International Journal of Computer Sciences and Engineering*, 8(8), 73-79. <https://doi.org/10.26438/ijcse/v8i8.7379>.
- Padao, F. R. F. & Maravillas, E. A. (2015). Using naive bayesian method for plant leaf classification based on shape and texture features. In *2015 International Conference on Humanoid, Nanotechnology, Information Technology, Communication and Control, Environment and Management (HNICEM)*, 1-5.
- Petkov, N. (2018). Automatic segmentation of indoor and outdoor scenes from visual lifelogging. In *Applications of Intelligent Systems: Proceedings of the 1st International APPIS Conference*, 310, 194.
- Raj, A. P. S. S. & Vajravelu, S. K. (2019). Ddla: dual deep learning architecture for classification of plant species. *IET Image Processing*, 13(12):2176-2182. <https://doi.org/10.1049/iet-ipr.2019.0346>.
- Shah, M. P., Singha, S., & Awate, S. P. (2017). Leaf classification using marginalized shape context and shape+ texture dual-path deep convolutional neural network. In *2017 IEEE International Conference on Image Processing (ICIP)*, 860-864.
- Silva, P. F., Marcal, A. R., Silva, R. M. (2013). Evaluation of features for leaf discrimination. In *International Conference Image Analysis and Recognition*, 197-204.
- Simonyan, K., & Zisserman, A. (2014). Very deep convolutional networks for large-scale image recognition. *arXiv*, 1409.1556. <https://doi.org/10.48550/arXiv.1409.1556>.
- Soderkvist, O. (2001). *Computer vision classification of leaves from swedish trees* (MsC thesis), Linköping University, Linköping, Sweden.
- Soucy, P. & Mineau, G. W. (2001). A simple knn algorithm for text categorization. In *Proceedings 2001 IEEE International Conference on Data Mining*, 647-648. IEEE.
- Sujith, A. & Neethu, R. (2021). Classification of plant leaf using shape and texture features. In *Inventive Communication and Computational Technologies*, 269-282.
- Szegedy, C., Vanhoucke, V., Ioffe, S., Shlens, J., Wojna, Z. (2016). Rethinking the inception architecture for computer vision. In *Proceedings of the IEEE conference on computer vision and pattern recognition*, 2818-2826.

- Tomar, D. & Agarwal, S. (2016). Leaf recognition for plant classification using direct acyclic graph based multi- class least squares twin support vector machine. *International Journal of Image and Graphics*, 16(03),1650012. <https://doi.org/10.1142/S0219467816500121>.
- Tsolakidis, D. G., Kosmopoulos, D. I., Papadourakis, G. (2014). Plant leaf recognition using zernike moments and histogram of oriented gradients. In *Hellenic Conference on Artificial Intelligence*, 406-417.
- Wang, X., Du, W., Guo, F., Hu, S. (2020). Leaf recognition based on elliptical half gabor and maximum gap local line direction pattern. *IEEE Access*, 8:39175-39183. <https://doi.org/10.1109/ACCESS.2020.2976117>.
- Wang, Z., Sun, X., Ma, Y., Zhang, H., Ma, Y., Xie, W., Zhang, Y. (2014). Plant recognition based on intersecting cortical model. In *2014 International joint conference on neural networks (IJCNN)*, 975-980.
- Wang, Z., Sun, X., Yang, Z., Zhang, Y., Zhu, Y., Ma, Y. (2018). Leaf recognition based on DPCNN and BOW. *Neural Processing Letters*, 47(1):99-115. <https://doi.org/10.1007/s11063-017-9635-1>.
- Wu, S. G., Bao, F. S., Xu, E. Y., Wang, Y.-X., Chang, Y.-F., Xiang, Q.-L. (2007). A leaf recognition algorithm for plant classification using probabilistic neural network. In *2007 IEEE International Symposium on Signal Processing and Information Technology*, 11-16. IEEE.
- Zhang, Y., Cui, J., Wang, Z., Kang, J., Min, Y. (2020). Leaf image recognition based on bag of features. *Applied Sciences*, 10(15):5177. <https://doi.org/10.3390/app10155177>.